

The Role of Rnd3 in Keratinocytes

By

SHABANA BEGUM

A thesis submitted to

The University of Birmingham

For the degree of

DOCTOR OF PHILOSOPHY

College of Life and Environmental sciences

School of Biosciences

University of Birmingham

April 2017

UNIVERSITY OF
BIRMINGHAM

University of Birmingham Research Archive

e-theses repository

This unpublished thesis/dissertation is copyright of the author and/or third parties. The intellectual property rights of the author or third parties in respect of this work are as defined by The Copyright Designs and Patents Act 1988 or as modified by any successor legislation.

Any use made of information contained in this thesis/dissertation must be in accordance with that legislation and must be properly acknowledged. Further distribution or reproduction in any format is prohibited without the permission of the copyright holder.

Abstract

The skin is continuously being shed and therefore it is vital that it is renewed. Epidermal self-renewal is dependent on a population of keratinocyte stem cells (KSC) that reside in the basal layer. During epidermal regeneration, KSC divide asymmetrically giving rise to more stem cells as well as committed progenitors. Committed progenitors exit the cell cycle before going on to differentiate to form the highly resilient cells that make up the outermost layer. It is thought that committed progenitors and KSC are differentially regulated therefore allowing for such different behaviors.

Rnd3 is an atypical GTPase that is constitutively active and has been previously shown to regulate keratinocyte differentiation. However, the identification of the molecular mechanism is currently unknown.

The work presented here shows that Rnd3 depletion enriches for keratinocytes with a number of 'stem-like' phenotypes including reduced differentiation, reduced cell size, increased adhesion to ECM proteins and a deregulation of putative stem cell markers. Furthermore, using a quantitative proteomic approach, it can be seen that Rnd3 regulated the abundance of proteins involved in regulating stem cell function.

This work proposes a function for Rnd3 in the regulation of key proteins involved in keratinocyte differentiation and self-renewal.

“Sometimes, if you stand on the bottom rail of a bridge and lean over to watch the river slipping slowly away beneath you, you will suddenly know everything there is to be known.”

— A.A. Milne

Dedicated to the love of my life, my loving Dad, my Aba.

Acknowledgements

The preparation and completion of the project would be impossible without the support from the numerous people around me. I would therefore like to thank the following people.

I would firstly like to thank the BBSRC and the Midlands Integrative Biosciences training partnership and all those involved with running course for funding this work and their support during the duration of this project.

Thanks to Anne Ridley for providing me with the Flag-Rnd3 constructs. Thanks to members of the Heath, Cunningham, Murphy, Kanhere and Tomlinson groups for their help and advice when designing and conducting experiments (and the occasional reagent). Also thanks to the members of central services for sorting out countless technical problems as well as their ability to make me laugh. To Alessandro for his support using the confocal microscope and help in analyzing microscopy images

I would like to thank Debbie, Andy, Rian, Tom, Sabah, Adil, Mai, Tijs, and Trushar for their patience with my mass spectrometry questions and for the stimulating scientific and non-scientific discussions and cups of tea.

I would like to also thank everybody on the fifth floor, past and present, who have made my experience in the lab a wonderful one.

Extra special thanks to Neil and Aditi for always making time for my discussions, and for their continual support and their unshakeable belief in me.

Finally, thanks to all of my friends and family and to my Mum for supporting and loving me through everything.

I am forever indebted to my loving Dad.

Table of Contents

Chapter 1	1
1.1 The Epidermis.....	1
1.2 The Regulation of Terminal differentiation.....	4
1.3 The regulation of intracellular adhesion during terminal differentiation.....	4
1.4 The regulation of intracellular adhesion during terminal differentiation.....	7
1.5 Transcriptional regulation of terminal differentiation	10
1.5.1 The TP63 family if transcription factors	10
1.5.2 AP-1	12
1.6 Epidermal self-renewal	14
1.7 Keratinocyte stem cell markers.....	18
1.7.1 Clonogenic markers.....	20
1.7.2 Cell size	21
1.7.3 Adhesion Markers	21
1.7.4 Cell clustering	22
1.7.5 Biochemical markers.....	22
1.7.6 Global gene expression analysis	24
1.8 Rho GTPases.....	26
1.8.1 Structural changes during Rho GTPase activation.....	27
1.8.2 Regulation of Rho GTPases	29
1.8.3 Typical and Atypical Rho GTPases	30
1.8.4 The Rnd Subfamily	32
1.9 Rnd3/RhoE.....	32
1.9.1 Structure of Rnd3	33
1.9.2 Regulation of Rnd3	34
1.10 Function of Rnd3	36
1.10.1 Rnd3 and actin cytoskeletal dynamics	36
1.10.2 Rnd3 and the cell cycle	38
1.10.3 Rnd3 and Cancer	39
1.10.4 Rnd3 and Apoptosis	40
1.10.5 Rnd3 and Keratinocyte Differentiation	41
1.11 Project aims.....	42
Chapter 2	44
Materials and Methods	44
2.1 Materials.....	44
Tables 2.1-2.5 List the reagents and recipes used in this study	44
2.2 Methods.....	48
2.2.1 Molecular biology	48
2.2.2 Cell culture methods.....	48
2.2.3 Protein Biochemistry.....	51
2.2.4 RNA work	52
2.2.5 Assays	53
2.2.6 Immunofluorescence	54
2.2.7 Stable isotope labeled with amino acid in cell culture (SILAC).....	55
2.2.8 Statistical Tests.....	57
2.2.9 Analysis of Published data sets	57
Chapter 3	58

Knock down of Rnd3 leads to an enrichment of a population of ‘stem like’ keratinocytes.	58
3.1 Introduction.....	58
3.2 Results.....	59
3.2.1 Knock down in Rnd3 results in an increased cell clustering.....	59
3.2.2 Knock down of Rnd3 leads to changes in nuclear size	63
3.2.3 Knock down of Rnd3 in HaCaTs leads to an increase in cell adhesion to ECM proteins.....	67
3.2.4 Knock down of Rnd3 leads to a suppression in differentiation	69
3.2.5 Knock down of Rnd3 leads to an increase in p63	69
3.2.6 Knock of Rnd3 does not lead to changes in the expression of LRIG, MCSP and DLL1	70
3.3 Discussion	75
3.3.1 Rnd3 and Colony morphology	75
3.3.2 Rnd3 and Cell size	76
3.3.3 Rnd3 and cell adhesion to ECM.....	77
3.3.4 Rnd3 and differentiation.....	78
3.3.5 Rnd3 and p63 expression:	78
3.3.6 Why might Rnd3 be regulating some but not all stem phenotypes?	79
Chapter 4.....	82
4.1 Introduction.....	82
4.2 Results.....	83
4.2.1 Knock down of Rnd3 leads to an increase in the expression of desmoplakin.....	83
4.2.2 Rnd3 and P63 double knockdowns restore colony morphology.....	90
4.2.3 Rnd3 and p63 double knockdowns restores desmoplakin expression	95
4.2.4 Knock down does not change the expression of other p63 targets	95
4.3 Discussion	100
4.3.1 Rnd3 regulates colony morphology and desmoplakin expression in a p63 dependent manner.....	100
4.3.2 Depletion of Rnd3 does not alter the expression of other p63 targets: ..	102
Chapter 5.....	104
5.1 Introduction.....	104
5.2 Results.....	105
5.2.1 The identification of proteins regulated by Rnd3 using SILAC	105
5.2.2 Rnd3 regulates the expression of known regulators of progenitor differentiation	117
5.3 Discussion	123
5.3.1 Rnd3 regulates the expression of FOXK1.....	124
5.3.2 Rnd3 regulates the expression of JunB	126
Chapter 6.....	128
6.1 Introduction.....	128
6.2 Results.....	129
6.2.1 The identification of Rnd3 interacting proteins using SILAC immunoprecipitation.....	129
6.2.2 Functional Analysis of Rnd3 interacting proteins.....	135
6.2.3 Rnd3 regulates p63 at the protein level and not the transcriptional level	143
6.3 Discussion	147

6.3.1 Rnd3 associates with components of proteasome degradation	147
6.3.2 Rnd3 depletion leads to an increase in p63 stability	148
Final Discussion and concluding remarks.....	150
7.1 Rnd3 may regulate stem/progenitor phenotypes:.....	151
7.2 How might Rnd3 play a role in keratinocyte differentiation and stem cell maintenance:	152
References.....	154

List of Figures

Figure 1.1 The mammalian skin.....	2
Figure 1.2 The epidermis.....	3
Figure 1.3 Terminal differentiation.....	6
Figure 1.4 Desmosomal Architecture.....	8
Figure 1.5 The TP63 family of transcription factors.....	12
Figure 1.6 Models of KSC self-renewal.....	19
Figure 1.7 Evolutionary relationship between members of the Rho GTPase family.....	28
Figure 1.8 Rho GTPases- The molecular switch.....	31
Figure 3.1 Transient transfection of HaCaTs with Rnd3 siRNA for 48 hours leads to 70-80% knockdown.....	60
Figure 3.2 Knocking down Rnd3 leads to increased cell clustering and reduced inter-nuclear distance.....	62
Figure 3.3 Knock down of Rnd3 leads to a reduced nuclear diameter and nuclear volume.....	65
Figure 3.4 Knock down of Rnd3 leads to a reduction in total cell volume, nuclear volume and no change in nuclear/cytoplasmic ratio	66
Figure 3.5 Knock down of Rnd3 leads to increased cell adhesion to ECM proteins.....	68
Figure 3.6 Knocking down Rnd3 leads to suppression in confluence-induced differentiation.	71
Figure 3.7 Knockdown of Rnd3 lead to a suppression of induced differentiation.....	72
Figure 3.8 Knock down of Rnd3 leads to an increase in the expression of p63.....	73
Figure 3.9 Knock down of Rnd3 does not lead to significant changes in the expression of putative stem cell markers Lrig1, MCSP and DLL1.....	74
Figure 4.1 TP63 transcriptionally regulates multiple desmosome proteins.....	89
Figure 4.2 Rnd3 depletion leads to the increase of desmoplakin.....	86

Figure 4.3 Rnd3 depletion leads to an increase in desmoplakin transcript.....	87
Figure 4.4 Knock down of Rnd3 does not lead to a change in Perp expression.....	88
Figure 4.5 Knocking down Rnd3 and p63 at the same time does not lead to sufficient knock down of both transcripts.....	89
Figure 4.6 Knock down of both Rnd3 and p63 is efficient when oligos are transfected sequentially.....	92
Figure 4.7 Knock down of Rnd3 and p63 leads to a restoration of colony compaction.....	93
Figure 4.8 Knock down of both Rnd3 and p63 leads to reduced desmoplakin expression.....	94
Figure 4.9 Enriched GO terms using p63 chipseq data.....	97
Figure 4.9 Knock down of Rnd3 does not appear to alter the expression of p63 targets.....	98
Figure 5.1 SILAC workflow.....	107
Figure 5.2 SILAC output	108
Figure 5.3 Subcellular localization of upregulated and down regulated proteins.....	111
Figure 5.4 Molecular function of upregulated and downregulated proteins.....	112
Figure 5.5 Biological function of upregulated and down regulated proteins.....	113
Figure 5.6 STRING map showing the functional associations of upregulated and down regulated proteins.....	115
Figure 5.7 STRING map showing the functional association of each protein and ten other known associations.....	116
Figure 5.8 Rnd3 depletion leads to an increase in FOXX1 expression.....	120
Figure 5.9 Rnd3 depletion leads to an increase in junB expression.....	121
Figure 5.10 Rnd3 depletion may lead to a reduction in junB transcript and slight changes in FOXX1 transcript.....	122
Figure 6.1 SILAC immunoprecipitation set up.....	131

Figure 6.2 SILAC output.....	132
Figure 6.3 Subcellular localization of identified Rnd3 interactors.....	137
Figure 6.4 Biological processes of identified Rnd3 interactors.....	138
Figure 6.5 Molecular function of Rnd3 interactors.....	139
Figure 6.6 Rnd3 STRING map.....	140
Figure 6.7 The functional association of the submitted protein lists and 10 other known functional associations.....	141
Figure 6.8 Knock down of Rnd3 leads to an increase in p63 protein but not an increase in transcript.....	145
Figure 6.9 Knock down of Rnd3 leads to a reduction in p63 degradation.....	146

List of Tables

Table 1.1 Diseases associated with mutations in key terminal differentiation genes.....	14
Table 2.1 Buffers and Solutions.....	44
Table 2.2 siRNA.....	46
Table 2.3 Antibodies.....	46
Table 2.4 Primers.....	47
Table 2.5 Plasmids	48
Table 4.2 List of genes taken from multiple biological processes.....	86
Table 5.1 List of up regulated and down regulated proteins in Rnd3 depleted cells.....	109
Table 5.2 List of up regulated and down regulated proteins and their associated subcellular localization	111
Table 5.3 List of upregulated and down regulated proteins and their associated molecular function.....	112
Table 5.4 List of up regulated and down regulated proteins and their associated biological processes	113
Table 5.5 List of Proteins found in the molecular function ‘transcription factor activity’ and the biological process ‘Transcription’	119
Table 6.1 Full list of Rnd3 interactors and their corresponding log2 ratios.....	133
Table 6.2 Rnd interactions involved in ‘regulation of ubiquitin activity’ and ‘proteasomal degradation’	142

Abbreviations

4EBP-1 Eukaryotic translation initiation factor 4E-binding protein 1
AEC Ankyloblepharon-ectodermal defects-cleft lip/palate
ATP Adenosine Triphosphate
CHX Cyclohexamide
DAPI 4',6-Diamidino-2-Phenylindole
DDL1 Delta-like 1 protein
DH domain DBL homology domain
DNA Deoxyribonucleic acid
Dsc Desmocolin
Dsg Desmoglein
ECM Extracellular matrix
EDC Epidermal Differentiation unit
EIF4E Eukaryotic translation initiation factor 4E
GAP GTPase activating protein
GDI Guanine nucleotide disassociation inhibitors
GDP Guanosine Diphosphate
GEF Guanine exchange factor
GO Gene Ontology
GPCRS G protein coupled receptors
GTP Gunosine 5' triphosphate
KSC Keratinocyte stem cells
LC-MSMS Liquid Chromatography Mass spectrometry
MAPK Mitogen-activated protein kinases
MCSP Melanoma-Associated Chondroitin Sulfate Proteoglycan
NICD Notch intracellular domain
NSCLC None small cell lung cancer
PDGFR Platelet-derived growth factor receptor
PKC Protein Kinase C
RNA Ribonucleic acid
ROCK Rho-associated coiled-coil containing kinase
shRNA Short hairpin RNA
SILAC Stable isotope labelling with amino acids in cell culture
siRNA Small interfering RNA
SRF Serum response factor
STRING Search Tool for the Retrieval of Interacting Genes/Proteins
TP53 Tumor protein 53
TP63 Tumor protein 63
UV Ultraviolet

Chapter 1

Introduction

1.1 The Epidermis

The skin is the body's first point of contact with the external environment and functions as a protective barrier against daily microbial and chemical threats as well as regulating internal fluid homeostasis and bodily temperatures (Brenner and Hearing, 2010) (Figure 1.1).

The outermost layer of the skin, the epidermis, is a morphologically distinct epithelial tissue, which comprises of multiple cell types that act together to ensure that the skin functions as an effective barrier (Fuchs *et al*, 2007). Keratinocytes are the predominant cell type found in the epidermis, making up approximately 95% of the total cell content. Other cell types include melanocytes, langerhan cells and merkel cells (Fuchs *et al*, 1990; Brenner and Hearing, 2010). Together, these cells function to ensure that the skin is maintained as an effective barrier throughout life.

Keratinocytes are spatially organized into a number of distinct layers where each layer hosts cells at different stages of differentiation (Figure 1.2). Well-defined gene expression networks result in global changes in cell morphology and behavior and coordinates the formation of each layer. In this way, cells at different layers can be identified by distinct morphological and bimolecular phenotypes.

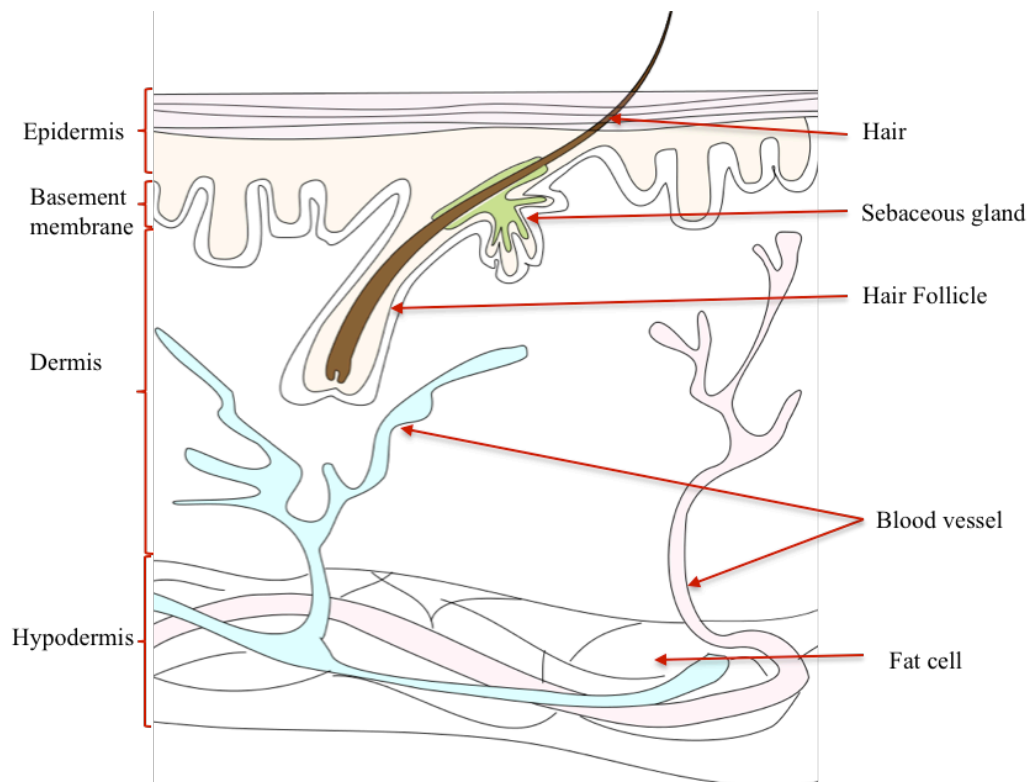


Figure 1.1 The mammalian skin

The mammalian skin is a specialized organ that functions to protect the body from external stresses. The epidermis is the outermost layer and sits directly on a basement membrane that comprises of ECM proteins. The basement membrane overlays the dermis. These tissues, in concert with one another allow the skin to function as a effective barrier.

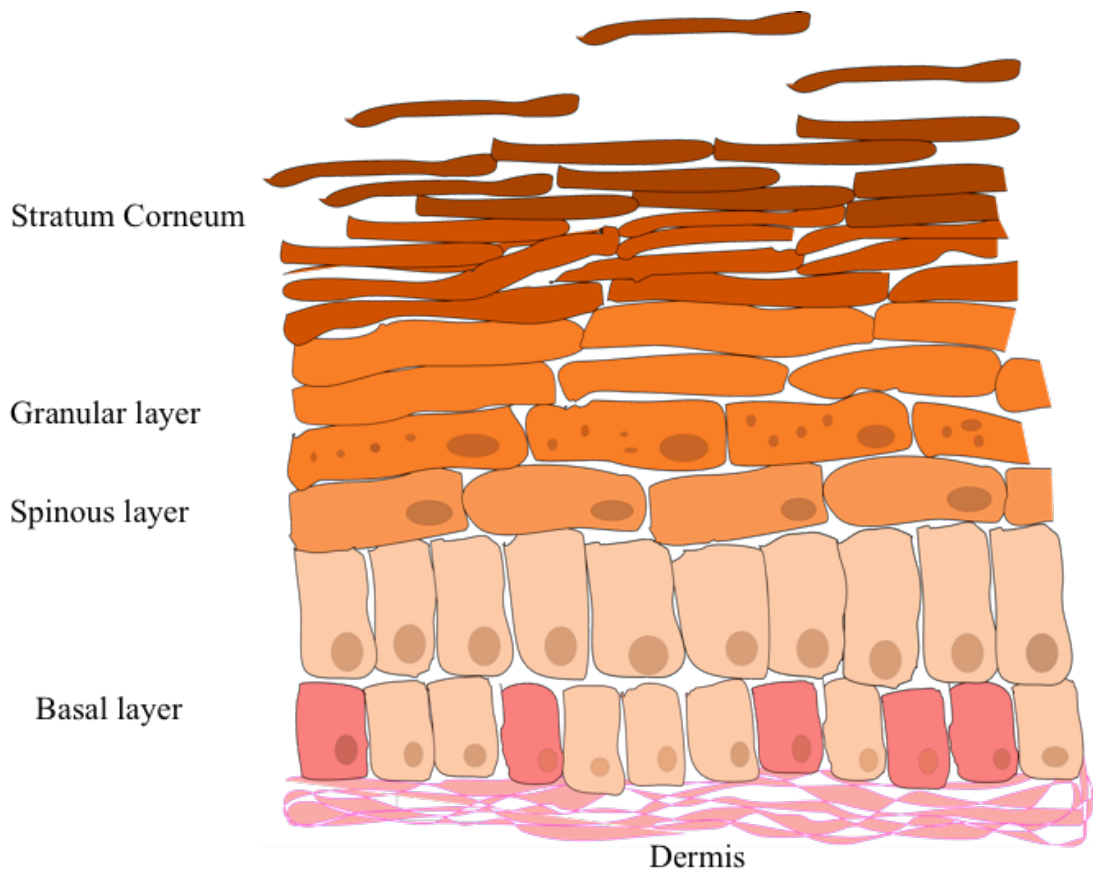


Figure 1.2 The Epidermis

The epidermis is a highly organized epithelial tissue. The basal layer consists of two pools of mitotic progenitor cells, keratinocyte stem cells (KSC) (pink) and committed progenitors (beige). Each superseding layer host's keratinocytes undergoing different stages of differentiation resulting in the formation of the highly resilient squames that makes up the outermost surface (stratum corneum). These are continuously being shed throughout life and are replaced by committed progenitors that transverse upwards.

The innermost layer comprises of a mixed population of undifferentiated progenitors whereby a sub-population of these can divide a limited number of times before leaving the cell cycle and undergoing a process of terminal differentiation. Terminal differentiation leads to the formation of superseding layers that are home to cells that are increasingly more differentiated. Fully differentiated keratinocytes or squames are located at the outermost layer and interconnect together to form a highly resilient and robust barrier that is characteristic of the skin (Watt *et al*, 2001; Fuchs *et al* 2007).

The spatial organization of keratinocytes is essential to ensure that the epidermis is maintained. Central to this, is the process of terminal differentiation and its regulation. Terminal differentiation is a multifaceted process and its regulation is finely tuned so that epidermal architecture is maintained (Figure 1.3) (Fuchs and Raghaven, 2002; Simpson *et al*, 2011).

1.2 The Regulation of Terminal differentiation

Terminal differentiation is a complex process that involves the co-ordination of gene expression changes as well as changes in intracellular adhesion and intercellular adhesion in response to numerous cell stimuli in a time dependent manner. This ensures that the epidermis is always intact as well as additionally ensuring that terminal differentiation occurs only when epidermal regeneration is required (Figure 1.3).

1.3 The regulation of intracellular adhesion during terminal differentiation

Terminal differentiation is initiated in progenitor keratinocytes located at the basal layer. The basal layer consists of a mixed population of progenitors, keratinocyte stem cells (KSC) and early progenitors that have an ability to differentiate (committed progenitors). These are attached to the basement membrane, which consist of a mix of

extracellular proteins including laminin, collagen and fibronectin (Reviewed in Breitkreutz *et al*, 2009). Attachment of basal keratinocytes to the basement membrane is facilitated largely through hemidesmosomal binding to ECM proteins. Hemidesmosomes are small multi-protein structures located at the basal side of basal keratinocytes. They function to anchor progenitor keratinocytes to the basement membrane by linking them to the intermediate filament network (IF network) consisting of keratin 5 (K5) and keratin 14 (K14) (Walko *et al*, 2015). Integrins are at the core of hemidesmosomal function and are expressed at the surface of basal keratinocytes. Integrins are multifunctional heterodimeric transmembrane cell surface receptors that are made up of one alpha subunit and one beta subunit. They function by transducing signals either via the binding of extracellular ligands or via the alterations in receptor dynamics in response to intercellular events (Walko *et al*, 2015). In the epidermis, integrins $\alpha_3\beta_1$, $\alpha_6\beta_4$ and $\alpha_2\beta_1$ are expressed predominantly.

The function of integrins in maintaining epidermal integrity can be exemplified by knock-out studies. Ablation of $\alpha_6\beta_4$ leads to a loss in hemidesmosomes and therefore a subsequent loss of binding of basal keratinocytes onto the basement membrane (Raymond *et al*, 2005).

Furthermore, it has been previously shown that terminal differentiation is regulated by cell adhesion to the basement membrane. Specifically, the expression of β_1 integrins is crucial in ensuring committed progenitors undergo terminal differentiation. Upon differentiation stimuli β_1 integrin expression is down regulated, therefore allowing committed progenitors to detach from the basement membrane and transverse upwards (Hotchin, *et al* 1992). In addition to this, cells that are artificially suspended (so are no longer adhered to the ECM) are shown to exit the cell cycle and express late differentiation genes (Watt *et al*, 1989).

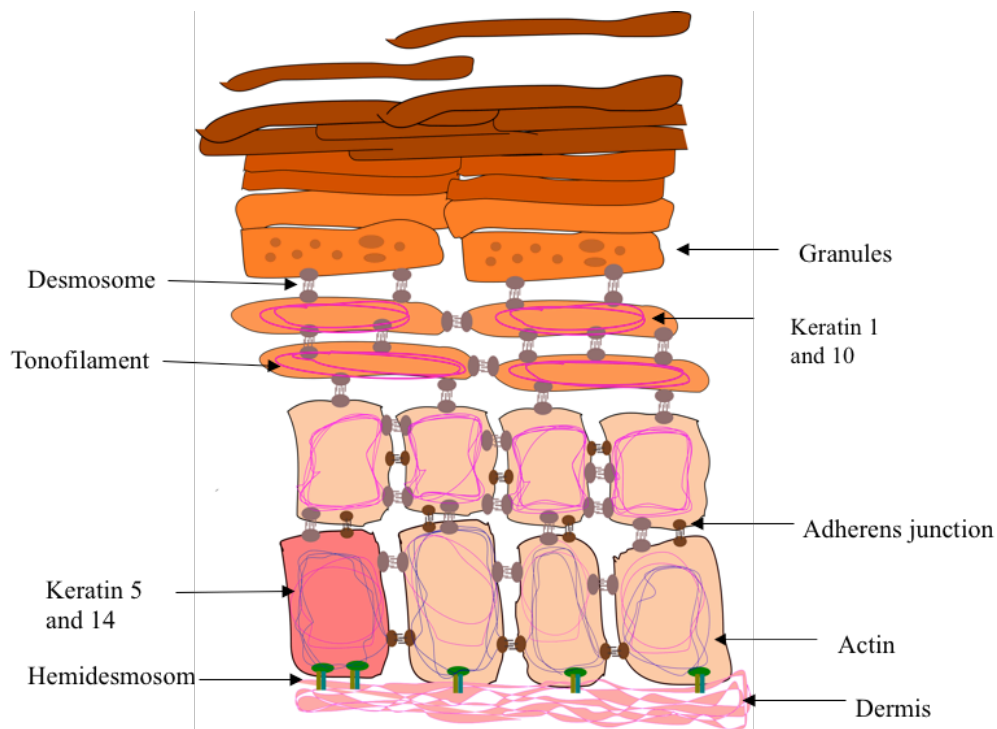


Figure 1.3. Terminal differentiation:

All basal keratinocytes are attached to the basement membrane with integrins and express K5 and K14. Upon terminal differentiation in committed progenitors (Beige), integrins are down regulated allowing them to detach from the ECM. K1 and K10 are expressed, which assemble into tonofilaments in spinous keratinocytes. Later stages of differentiation lead to the formation of granular keratinocytes that contain lamellar granules. These hold proteins that are necessary for the process of cornification such as profilligrin, a precursor to filligrin. Profilligrin is proteolysed into monomeric filligrin, which acts to bind to keratin tonofilaments, and allows for their aggregation to form extensive networks of microfibrils. These microfibrils are then cross-linked by transglutaminase resulting in the formation of a matrix of insoluble keratins. This then pulls at the plasma membrane, which as a result flattens the cell. The outermost layer or the stratum corneum is formed of these flat squames. These are metabolically inactive and release lytic enzymes, which leads to the degradation of cellular organelles as well as the lipid bilayer. The resulting lipids are deposited between squames therefore waterproofing the skin (Blanpain and Fuchs, 2009).

1.4 The regulation of intracellular adhesion during terminal differentiation

In addition to the regulation of keratinocyte ECM interactions, intracellular adhesion is involved in regulating terminal differentiation.

The differential expression of multiple keratin isoforms additionally distinguishes basal cells from differentiated cells. Keratins are thought to function as ‘stabilizers’ of intracellular adhesion. During terminal differentiation, the expression of K5 and K14 (expressed in basal cells) is switched off in favor of the expression of K1 and K10 (Fuchs *et al*, 2007). The expression of K1 and K10 is therefore up regulated in suprabasal cells and allows for the formation of extensive, highly keratinized filaments via keratin bundling. These filaments can associate with one another forming higher order bundles of keratin tonofilaments, which then interact with desmosomes in the spinous layer (Fuchs and Horseley, 2008). Keratin tonofilaments together with desmosomes give the spinous layer mechanical strength and allows for the binding of other structural proteins such as involucrin and loricrin during the later stages of differentiation.

An extensive transcellular network of anchoring junctions is vital in ensuring that the ‘living’ layer of the epidermis is held together and to ensure that the epidermis can withstand continual mechanical stress. These anchoring junctions can connect neighboring cells as well as interact directly with the cytoskeleton therefore acting to strengthen points of contact between cells. These anchoring junctions include adherens junctions and desmosomes.

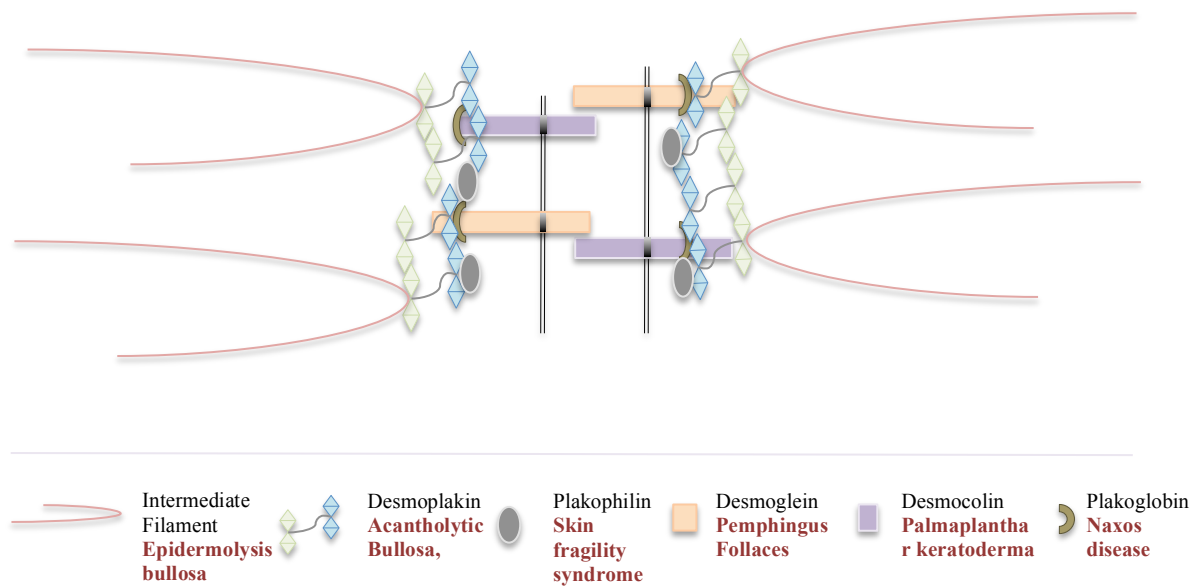


Figure 1.4. Desmosomal architecture

Desmosomes are made up of a number of components that allow cells to withstand mechanical stress. A number of epidermal disorders arise from mutations in the genes that express desmosomal proteins (red text). Symptoms usually include: skin fragility and blistering, and defects in epidermal development. For a more comprehensive review see Lai-Chong *et al*, 2007. (Adapted from Ihrie and Attardi *et al*, 2005)

Adherens junctions directly interact with the actin cytoskeleton and are composed of E-cadherin and P-cadherin. E-cadherin is expressed in all layers of the epidermis and P-cadherin is expressed exclusively in the basal layer. The intracellular domain of the cadherin directly associates with the armadillo protein β -catenin. β -catenin can associate with the actin regulator protein α -catenin, which can directly bind with actin microfilaments (Andl *et al*, 2010; Brandner *et al*, 2010; Hartstock *et al*, 2008).

Desmosomes consist of desmosomal cadherin proteins, Desmoglein (Dsg 1-4) and desmocolin (Dsc 1-3). Dsg and Dsc are crucial for desmosomal adhesion and can form homotypic and heterotypic extracellular interactions (Garrod and Chidgey 2008; Getsios *et al*, 2004). The intracellular domains of each cadherin can associate with the armadillo proteins, plakoglobin and plakophilin (pkps 1-4). These can directly bind to desmosomal plaque proteins such as desmoplakin. Desmoplakin can directly bind to the intermediate filament cytoskeletal network (Getsios *et al* 2004) (Figure 1.4). In addition to this Perp, a tetraspanin membrane protein specifically localizes to desmosomes, although whether the presence of Perp contributes to desmosome structure is unknown (Garrod and Chidgey, 2008).

The interaction of adherens junctions and desmosomes are regulated through cadherin-cadherin interactions on neighboring cells. Cadherins consist of extensive calcium binding sites and therefore cadherin-cadherin interactions are largely calcium dependent (Dusek *et al*, 2007, Al-Moudi *et al*, 2007).

The internal calcium concentration in the epidermis is thought to regulate the distribution of desmosomes throughout the different layers of the epidermis. The basal layer has a lower extracellular calcium concentration and therefore basal cells have fewer desmosomes. Conversely, spinous cells are held together with more desmosome junctions and this is thought to reflect an increase in calcium

concentration (Bickle *et al*, 2012). Interestingly, granular cells express very few desmosomes as the expression of proteins such as transglutaminases during the late stages of differentiation; crosslinks the intracellular components of desmosomes and this leads to the subsequent degradation of remaining components (Brandner *et al*, 2010; McMillan *et al*, 2003; Simon *et al*, 2001).

The adverse effects on the integrity of the epidermis exemplify the importance of the precise spatial organization of desmosomes when components of desmosomes are deregulated (Figure 1.4). Therefore, desmosomes are essential towards ensuring that correct barrier formation is obtained.

Taken together, both intercellular and intracellular adhesion are essential in regulating terminal differentiation. Both processes ensure that epidermal keratinocytes can withstand daily mechanical stresses whilst retaining its spatial organization and architecture.

1.5 Transcriptional regulation of terminal differentiation

Terminal differentiation is a complex process that consists of multiple stages leading to progressively complex changes to cell morphology and behavior. To ensure that each stage of terminal differentiation is regulated at the appropriate stage and in the appropriate way, each process is regulated by key transcriptional events. In this way, gene expression signatures can distinguish keratinocytes at each stage of differentiation as different genes are expressed in response to different differentiation events.

1.5.1 The TP63 family of transcription factors

p63 is part of the p53 family of transcription factors and is often described as the ‘master regulator’ of keratinocyte terminal differentiation (Yang *et al*, 2002). In

humans, it exists in two functional isoforms. Both of these isoforms arise from a single gene with two distinct promoters (Vanbokhoven *et al*, 2011) (Figure 1.5) One promoter gives rise to a form that contains a transactivation domain (TA isoform) and one without a TA domain (Δ N isoform). These isoforms are additionally alternatively spliced to give rise to α , β and γ forms (Koster *et al*, 2004) (Figure 1.5).

Initial studies have suggested that the TA domain is important for transcriptional activity and it was suggested that the Δ N isoforms had little or no transcriptional activity of its own. Instead, it was believed that the Δ N isoforms act to represses TAp63 transcriptional activity in a dominant negative way. However, further studies pointed towards the idea that Δ Np63 may have transcriptional activity in a way that is distinct to TAp63. Furthermore, it was suggested that the Δ Np63 isoforms have specific regions in its structure that interact with specific transcriptional targets (Koster *et al*, 2004). Therefore, suggesting that each isoform can regulate different gene expression networks.

Knockout studies in the mouse model have additionally shown that the deletion of all p63 isoforms leads to poor epidermal barrier formation and postnatal death. Furthermore, it was shown that TAp63 is primarily expressed in suprabasal layers during epithelial morphogenesis and is involved in regulating the expression of late terminal differentiation genes (Koh *et al*, 2015). Δ Np63 on the other hand is expressed almost entirely in the basal layer and is rapidly down regulated during terminal differentiation. It has been shown to be important in regulating the proliferative potential of stem/progenitor keratinocyte population (see section 1.2.5.5) Interestingly, postnatally TA isoforms are only weakly expressed whereas the Δ N isoforms are expressed in the basal layer throughout life and therefore is the primary isoform expressed in human epidermis after birth (Senoo *et al*, 2007). Furthermore,

studies that have reintroduced TA isoforms into a p63 null background lead to no obvious changes in epidermal homeostasis whereas reintroducing the ΔN isoforms leads to partial rescue of epidermal regeneration suggesting that other isoforms of p63 may be functionally redundant, postnatally (Romano *et al*, 2009)

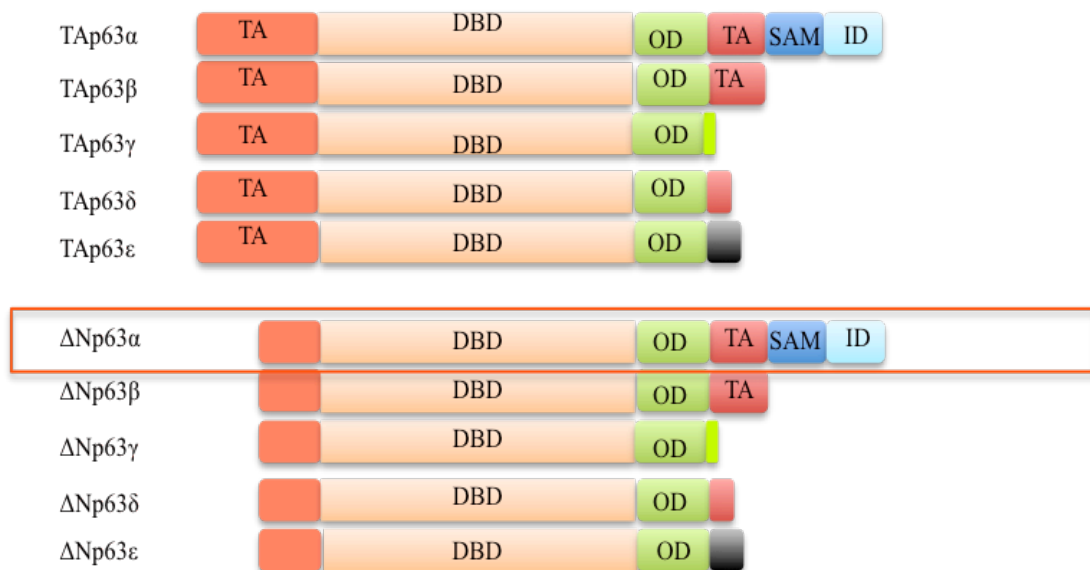


Figure 1.5. The TP63 family of transcription factors

P63 is a multidomain protein, which consists of transactivating domain (TA), DNA binding domain (DBD), OD domain (Oligomerisation domain), SAM domain (Steric alpha motif) and ID domain (inhibitory domain). p63 exists in two isoforms expressed from two distinct promoters. The TA isoform consists of a transcriptionally active transactivation domain whereas the $\Delta NP63$ isoform does not have this domain. Each isoform is alternatively spliced giving rise to five sub isotypes. Postnatally, the $\Delta NP63\alpha$ isoform is expressed predominantly (highlighted in orange). It is thought that this isoform is involved in regulating adult KSCs.

1.5.2 AP-1

AP-1 transcription factors have been additionally shown to be involved in regulating the expression of late terminal differentiation genes.

Interestingly, many late terminal differentiation genes such as involucrin, loricrin and fillagrin are clustered on a 2Mb region of chromosome 1q21. This cluster of genes is called the epidermal differentiation complex (EDC). The EDC hosts three genes families, the cornified envelope precursor family which include involucrin and loricrin, the S100 family, which express the S100 family of proteins such as S100A7 (psoriasin) S100A8 and S100A9 and the fused gene family which include fillagrin. It is not fully understood as to why these genes are clustered in this way, however it has been suggested that a single ‘master’ gene may transcriptionally regulate these collectively, however the elucidation of this factor has yet to be determined. Instead it is thought that multiple ubiquitously expressed transcription factors regulate terminal differentiation through the regulation of this gene cluster. These transcription factors include AP-1 transcription factors. AP-1 transcription factors comprise of different combinations of jun family members which include c-jun, junB and junD, as well as Fos family members which include Fra1, Fra2, c-fos and fosB. Each of these can form different dimer pairs, where each dimer pair can exert different transcriptional effects. Moreover, different members of the family are expressed in different layers of the epidermis, where different dimer pairs are thought to regulate various aspects of terminal differentiation (reviewed in Ekert *et al*, 2013). For example, junB represses involucrin and transglutaminase expression via the MAPK cascade. Whereas, JunD functions to activate loricrin and filligrin. Other transcription factors involved in the regulation of late terminal differentiation are reviewed in Kypriotou *et al*, 2012.

The importance of AP-1 transcription factors during terminal differentiation can be exemplified when the transcriptional activity of all AP1 factors are repressed using a dominant negative mutant of c-jun, TAM67. Here, it was shown that epidermal differentiation and stratification is repressed therefore suggesting that AP1 are

important factors in regulating different aspects of keratinocyte differentiation (Han *et al*, 2012).

Disorder	Mutated Gene	Effect on Terminal differentiation
Ichthyosis Vulgaris	FIL	Defective keratohyalin granules
Vohwinkels syndrome	LOR	Reduced cornification and thin barrier formation
Harlequin ichthyosis	ABCA1	Deficiency in lipid transport, disintegration of epidermal barrier
Netherton Syndrome	SPINK5	Proteolytic degradation of stratum corneum/disintegration of the stratum corneum
Atopic Dermatitis	Multiple genes in the EDC	Defective epidermal architecture, weak barrier formation
Psoriasis	Multiple genes in the EDC	Defective epidermal architecture, weak barrier formation
Bullous congenital ichthyosiform	K1, K10	Defects in formation of keratin tonofilaments
Peeling skin syndrome	TGM5, CDSN	Poor epidermal barrier formation
Ankyloblepharon-ectodermal defects-cleft lip/palate	TP63	Defective transcription of terminal differentiation genes
Epidermolysis bullosa simplex	KRT5 and KRT14	Defective intermediate filament formation
Lethal congenital epidermolysis bullosa	JUP	Defective desmosomes

Table 1.1 Diseases associated with mutations in key terminal differentiation genes. Table 1.1 lists disease states that are associated with the corresponding gene. It can be seen that mutation in key regulators of differentiation can be the causative factors for many different disease states by having an effect on different aspects of terminal differentiation.

1.6 Epidermal self-renewal

The epidermis is a regenerative tissue and therefore relies on KSCs to be constantly renewed to maintain barrier function. Terminally differentiated cells are post mitotic and are shed from the stratum corneum continuously; therefore it is imperative that KSCs divide to replenish both committed progenitor and the KSC pools (Watt *et al*, 2006). In addition to this, it is essential that the rate of KSC division is regulated

and terminal differentiation only occur when it is needed. The importance of this balance can be exemplified by a variety of skin disorders such as atopic dermatitis, ichthyosis, psoriasis and skin malignancies, where different stages of terminal differentiation are altered due to mutations in key differentiation genes (reviewed in Seagre *et al* 2006) (Table 1.1).

Central to the self-renewable capacity of the epidermis is the nature by which KSC cell division occurs. Currently a number of models have been proposed as to how KSC are regulated to maintain the epidermis (Figure 1.6).

The first model is the hierarchical model (Clayton *et al*, 2007). This model is based on the idea that the keratinocytes in the basal layer exist in discrete units that have differing proliferative capacities called 'epidermal proliferative units' or EPUs. Each unit is thought to consist of two distinct pools, a pool of committed progenitors and KSCs, which sit directly on the basal membrane. It is thought that both of these pools are maintained by a 'master' quiescent KSC. In order to ensure the epidermis is always maintained it is thought that this quiescent KSC has an ability to divide asymmetrically giving rise to KSCs as well as committed progenitors.

Committed progenitors can divide a fixed number of times before leaving the cell cycle and differentiating further. Whereas the resulting stem cells will only divide when the committed progenitor pool has been depleted. In this way the stem cell pool is both constantly being replenished as well as the more differentiated layers always being maintained (Clayton *et al*, 2007).

The second model, the stochastic model, proposes that a single undifferentiated progenitor exists at the basement membrane (Mascre *et al*, 2012). It is thought that this progenitor can undergo both asymmetric and symmetric divisions at a rate that

meets the requirements of the regenerating epidermis. This proposed progenitor can divide randomly to generate two stem progenitors, a single committed daughter and a single stem progenitor or two committed daughters (Mascre *et al*, 2012) (Reviewed in Fuchs *et al* 2014).

More recently a study conducted in mice found that there might be another way that the epidermis renews itself (Ojeh *et al*, 2015). Here, it has been suggested that in a similar way to the hierarchal model a population of quiescent stem cells divide giving rise to another stem as well as giving rise to a subset of stem cells called ‘activated stem cells’. The activated stem cell can divide over numerous generations and only a subset of these then further divide resulting in the formation of a population of keratinocytes that exit the cell cycle and go on to further differentiate. This model offers an explanation as to how the epidermis is able to respond so rapidly to external insults and undergo efficient wound healing (Ojeh *et al*, 2015).

It is currently unclear which model is the most accurate to describe how KSC and committed progenitors exist at the basal layer, however it is agreed upon that both can be distinguished by their cycling properties.

KSC are slow cycling despite having an unlimited capacity to divide. In contrast to this, committed progenitors are fast cycling so to undergo differentiation. (Watt *et al*, 2006, Clayton *et al*, 2007). Committed progenitors divide a limited number of times before undergoing terminal differentiation and therefore replenishment of the differentiating pool is dependent on subsequent KSC division in response to self-renewal signals.

The general consensus is that a KSC must undergo asymmetric division to generate two progenitor populations with different fates. Asymmetrical divisions can be achieved in two ways; either through the unequal partitioning of the mRNA and

subsequently translated proteins within the dividing cell or through the response of the newly divided cells to different external stimuli (or niches). In both cases this would result in the formation of two non daughter cells with fundamentally different fate outcomes. It has been suggested that epidermal formation during development is reliant on spindle orientation and cell polarity in relation to the basement membrane, where horizontal orientation corresponds to asymmetrical division (Simpson *et al*, 2011; Fuchs and Horseley, 2008). It has been proposed that changes in spindle orientation and subsequent asymmetrical divisions occur in response to terminal differentiation stimuli.

In contrast to this, it is thought that a vertical orientation favors the symmetrical divisions leading to the formation of two daughter KSCs (Xie and Spralding, 2000; Koster *et al*, 2005; Watt *et al*, 2006; Koster and Roop, 2007).

Although many processes have been investigated, it is still unclear as to how spindle orientation is regulated in keratinocyte progenitors during development. It is however a widely accepted view that distinct bimolecular and biochemical niches within the epidermis may regulate KSC division, whereby changes in spindle orientation may be regulated by such external stimuli (Tumbar *et al*, 2004, Williams *et al*, 2011). It is important to note that currently the effect of spindle orientation on adult epidermal homeostasis is unclear and most of this research has been conducted in pre-natal mouse models. There is therefore a need to understand how epidermal homeostasis is maintained in adult skin.

In order to do this KSC and committed progenitors need to be distinguished, both morphologically and biochemically. Current research therefore aims to identify markers that are specific to each progenitor population.

1.7 Keratinocyte stem cell markers

In order to fully understand how keratinocyte progenitor populations differ, it is important that some distinction can be made between them. A defining molecular and morphological signature would mean that KSCs could potentially be isolated to aid a deeper understanding of how KSC behave differently from committed progenitors.

Currently, a molecular signature for KSCs has not been identified, therefore a clear distinction between progenitor populations has been a challenge. In theory, being able to purify each individual population would be highly advantageous for clinical applications and would be helpful in understanding molecular basis for epidermal disorders further. If the underlining mechanism of how these disorders arise is understood, more targeted therapies can be developed to treat them. Many markers for the stem cell compartment have been proposed which range from morphological markers to biochemical markers, however a single marker or set of criteria that distinguishes one population from the other has not been established. This is especially true for when attempting to identify a biochemical signature for the KSC population, as it is thought that KSC exist in smaller numbers and therefore are more difficult to isolate (Fuchs *et al*, 2014).

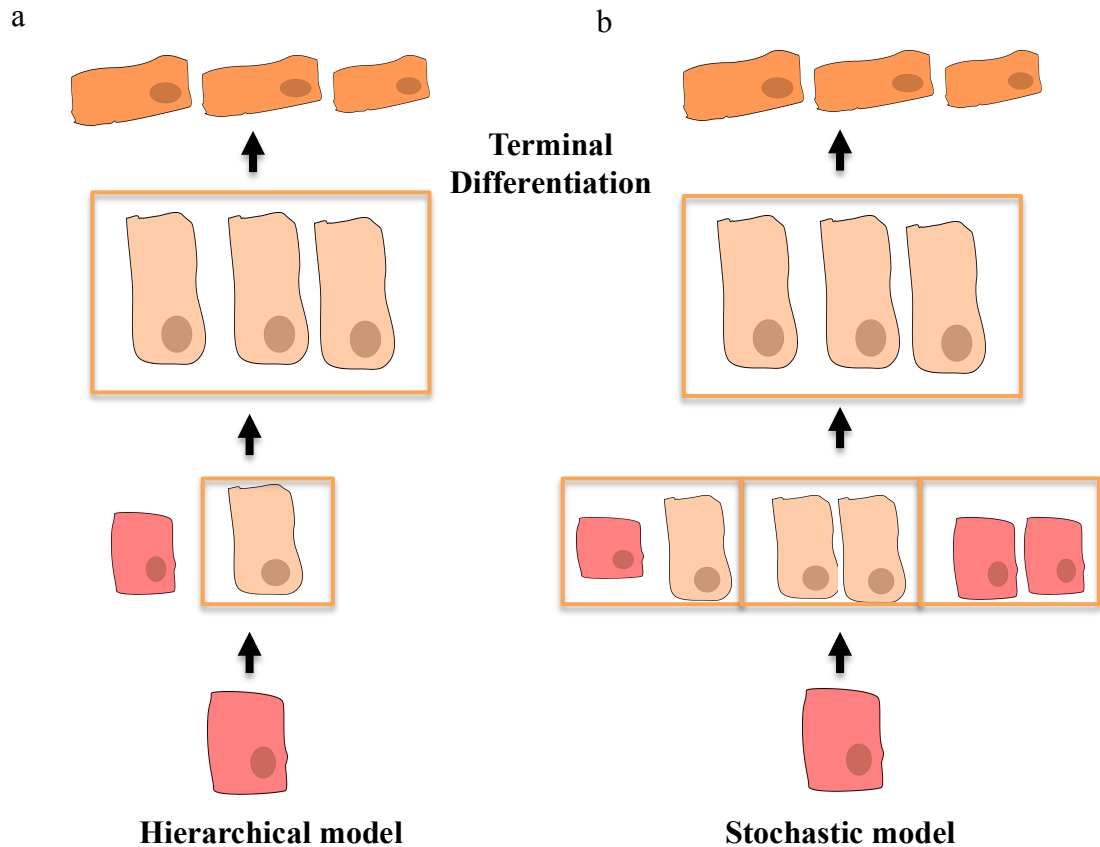


Figure 1.6 Proposed models of KSC self-renewal

Two models of KSC self renewal have been proposed the Hierarchical model (a) proposes that KSC divide asymmetrically generating a daughter KSCs and committed progenitor. In response to differentiation signals, the KSC divides giving rise to a committed progenitor and a KSC. The committed progenitor can divide a limited number of times before exiting the cycle and the going on to differentiate. The KSC maintain contact with the basement membrane and only further divides if the committed progenitor pool is depleted. The stochastic model (b) proposes that a single undifferentiated progenitor exists at the basement membrane and can undergo both assymetrical and symmetrical divisions to generate either KSC and committed progenitors in different combinations depending on the requirement for epidermal regeneration and replenishment of the KSC pool.

1.7.1 Clonogenic markers

Keratinocytes in culture have different growth properties and differ in the way that they form colonies (clonogenic capacity). Because of this it is thought that a mixed population of progenitor keratinocytes can be sub-cultured and then be distinguished depending on their growth potential and size of the colony they can form. Clonogenic assays involve culturing keratinocytes on a predefined matrix and then analyzing the size of the colonies after a number of days. They can be classified as so called holoclones, meroclones and paraclones. Holoclones represent cells, which have extensive growth potential (up to 180 divisions) and can form colonies that are progressively bigger. This coincides with the idea that stem cells have an infinite capacity to divide and can form large numbers of cells when sub cultured. In theory, holoclones should enable sub culturing onto matrixes for an unlimited number of generations. Paraclones represent cells that form small abortive colonies that have a limited capacity to divide (1-15 divisions) and are thought to represent a population of committed progenitors. Meroclones represent cells that contain a mixed population of cells that can form both large colonies and smaller abortive colonies (Barrandon and Green, 1995).

Other methods used to look at proliferative potential utilize the label retention methods such as BrdU to identify cells with differing proliferative potential. These methods measure the progression from G1 phase to the S-phase of the cell cycle (Larouche *et al* 2010; Kaur *et al*, 2004; Lavker *et al*, 2000; Barradon and Green 1987). The number of label retaining cells directly reflects the proliferative capacity of each population. The use of label retention in vivo has its limitations with regards to looking at clonogenic capacity in the human epidermis for obvious ethical reasons.

Since these techniques are largely conducted *in vitro*, an accurate assessment of proliferative capacity is hindered by the variable nature of *in vitro* proliferation techniques. Furthermore, whilst this is an interesting and useful initial technique in looking at the stem cell population, understanding how cell proliferation is regulated in a biochemical context is not fully understood when based solely on these experiments. However, cells selected for their clonogenic properties have provided a starting point in defining both populations of progenitors more closely.

1.7.2 Cell size

The use of colony forming efficiency assays has been useful in determining other features of cells in each type of clone. It was found that cells in holoclones were a lot smaller than those in paraclones (Barrandon and Green, 1985). Interestingly, a smaller cell size is a phenotype observed in other epithelial cell lines and it is thought to be a hallmark for stem cells. Furthermore, it has been proposed that most stem cells can be distinguished by an increase in the nuclear cytoplasmic ratios (Pagliara *et al*, 2014). This reflects the transcriptional dormancy of the stem population, since a closed chromatin architecture is associated with reduced transcription in stem cells.

1.7.3 Adhesion Markers

Colony forming efficiency assays have also been the starting point for identifying how keratinocyte progenitors differ in terms of their adhesive properties. Studies have proposed that KSC can be distinguished by the expression of cell surface proteins and through how attachment to the basement membrane is achieved. One of the earliest proposed potential markers for KSC was β_1 integrin. Using FACS analysis, it was found that keratinocytes with higher colony forming efficiency (CFE) expressed higher levels of β_1 integrin and has a higher capacity to proliferate as well as having an ability to form a basic epidermal surface when grafted into mice (Jones *et al*, 1995)

(Jones and Watt, 1993). In addition to this it was shown that in cultured human epidermal cells, which express high levels of β_1 integrin, have a higher colony forming efficiency and are slow cycling (Jones *et al*, 1995). However subsequent studies have suggested that β_1 integrin may additionally is expressed during the early stages of differentiation since it was found that β_1 expressing cells additionally express K10 (Kaur and Li *et al*, 2000). Therefore, this suggests that β_1 may be a marker for all cells in the progenitor population.

1.7.4 Cell clustering

It has been shown that in the oral keratinocyte stem cell compartment, that stem cells form discrete tight clusters. These clusters help to ensure that the stem cells are resilient to external and internal threats. In a similar way, it is thought that epidermal keratinocyte stem cells organize into discrete clusters. This clustering may be induced by an increase in the expression of cell-cell adhesion complexes such as desmosomes and adherens junctions (Calenic *et al*, 2015).

1.7.5 Biochemical markers

Despite these efforts it is thought that the easiest and most accurate way to distinguish progenitor populations is to identify a biochemical marker or a molecular signature, which is exclusively expressed in KSC. Currently, a few biochemical markers have been proposed (reviewed in Ghadially *et al*, 2012).

1.7.5.1 Δ NP63

As mentioned previously Δ Np63 is thought to be the primary isoform expressed in the epidermis after birth and its expression is primarily found in the basal layer. Discrepancies in two p63 knock out studies in mice have led to much confusion over the function of this isoform in relation to how this isoform functions. Both studies

deleted a common exon that is found in all isoforms of p63 (Yang *et al*, 1999, Mills *et al*, 1999).

The first study conducted by Mills *et al*, found that the deletion of p63 led to the complete absence of epidermal formation and the expression of any keratinocyte specific differentiation genes. However, the second study conducted by Yang *et al*, found that small patches resembling the epidermis were found and the cells in these patches expressed differentiation genes such as involucrin, loricrin and filaggrin. These patches however did not maintain a proliferative potential and could not sustain epidermal regeneration. Therefore, this study pointed towards a role of Δ Np63 in regulating the proliferative potential of KSC. Further studies using Δ Np63 specific knock-out studies in mice have shown that loss of Δ Np63 leads to poor epidermal development due to reduced terminal differentiation and proliferation, this resulted in postnatal lethality 3 weeks after birth (Senoo *et al*, 2007). To confirm this, a 'knock in' mouse was generated; using a p63 construct with Δ Np63 exon replaced by GFP found that epidermal formation was still impaired with little difference to the p63 null mouse (Romanno *et al*, 2012). Together, with the finding that TAp63 specific knock down has little effect on epidermal homeostasis, it was suggested that Δ Np63 is important in regulating the proliferative potential of progenitor cells.

In vitro studies have also shed light on how Δ Np63 may function. Using colony forming efficiency assays it has been shown that large colonies with a high proliferative capacity show intense nuclear staining (Pellegrini *et al*, 2001). Furthermore, when treated with shRNA constructs against p63, it was shown that keratinocytes lost their proliferative potential.

Therefore it was suggested that p63 could be a KSC marker (Pellegrini *et al*, 2001). However, much dispute has been made over whether p63 is exclusively a stem cell

marker or a marker for all basal progenitors. It has been suggested that $\Delta Np63$ may be involved in regulating the proliferative potential of all basal cells and is down regulated in committed progenitors in response to differentiation stimuli. It could be that the levels of $\Delta Np63$ expression distinguish progenitor populations rather than the mere presence or absence of $\Delta Np63$.

1.7.5.2 Notch ligand delta-like 1 (DLL1)

DLL1 is a notch ligand, which is expressed at the basal layer of the epidermis. It is thought that KSC express high levels of DLL1 to protect them from undergoing terminal differentiation (Estruch *et al*, 2008). It has been shown that DLL1 expression is high in clusters of cells, which are thought to represent KSC in human epidermis (Lowell *et al*, 2000). Furthermore, studies separating stem cells from committed progenitors based on colony-forming efficiency and integrin expression have shown that DLL1 expression was increased (Tan *et al*, 2013).

However, further studies have shown that DLL1 may not be restricted to the stem cell compartment, but rather there may be gradients of DLL1 expression. Therefore, DLL1 expression may show heterogeneity in both progenitor populations (Tan *et al*, 2013).

1.7.5.3 Melanoma-associated chondroitin sulfate proteoglycan (MCSP)

In a similar way to DLL1, MCSP is co-expressed with β_1 integrin. In culture these cells were able to form holoclones and in vivo these were found to be slow cycling. Therefore, suggesting that MCSP can be used as a marker for a population of cells which display stem like characteristics (Jenson *et al*, 2008; Tan *et al*, 2013;).

1.7.6 Global gene expression analysis

One way to characterize how the stem cell and committed progenitor pool differ is to look at differences in gene expression on a global level. In mice, label-retaining cells were further analyzed using DNA Microarray analysis to identify transcriptional networks that may regulate stem cells in the hair follicle (Tumbar *et al*, 2004). Microarrays were also used to analyze stem cells in the hair shaft regions of the human epidermis (Ohyama *et al*, 2006). However, these studies focus mainly on the expression patterns on whole populations of cells. Since a method to purify single populations of stem cells and committed progenitors has yet to be developed, it is likely that differences in the gene expression profiles may be a representation of a mixed population.

Therefore, to further understand how keratinocyte stem cells and committed progenitor cells differ, mixed populations of cells were separated based on the co-expression of DLL1, MCSP and β 1 integrin's as well as colony forming efficiency. cDNA libraries were generated from single cells and microarray analysis was performed to identify novel 'stem' markers'. In this way, Lrig-1 was identified as a putative stem cell marker (Jensen and Watt, 2006). Lrig-1 is described as being an EGFR antagonist and is thought to function to prevent the proliferation of KSCs in response to EGF signaling. Furthermore, it was shown that an overexpression of Lrig-1 led to an increase in the expression of β 1 integrin and increased cell adhesion (Tan *et al*, 2013).

Whilst these studies are interesting, some may argue that using single cell analysis may have its pitfalls. This is because both progenitor populations behave differently depending on their microenvironment and how they interact with one another. In this way, analyzing single cells takes cells away from their microenvironment and their

neighboring cells and therefore gene expression profiles may differ when looking at expression patterns in isolation.

Taken together, it can be seen that identifying the KSC pool and the committed progenitor pool is an important premise to understand how epidermal homeostasis is maintained. It is clear from the many studies that have been undertaken, a clear definitive biomolecular signature for KSC still does not exist and therefore there is still a need to further understand how each population can behave in such different ways.

1.8 Rho GTPases

Rho GTPases are a family of the Ras super family of GTPases that consists of 22 intercellular signaling G proteins, which can be grouped into 8 sub families (Wannerberg *et al*, 2005; Jaffe and Hall, 2005) (Figure 1.7) These are encoded for by at least 22 genes in mammals and are have various roles in multiple processes including actin cytoskeletal dynamics, cell migration, cell motility as well as the regulation of the cell cycle. (Heasman and Ridley, 2008).

Activation of the Rho family of GTPases is achieved through signaling via a number of cell surface receptors that include tyrosine kinases, cytokine receptors; G-protein coupled receptors (GPCRS) and integrin's (Murakoshi, *et al*, 2011). Once activated, they function as 'molecular switches' where each can cycle between a GDP bound inactive state and a GTP bound active state. When bound to GTP, Rho GTPases can undergo conformational changes that then allows for the interaction with complexes of downstream effectors. These protein complexes can then initiate cell-signaling cascades, which can activate different intercellular pathways leading to changes in cell behavior (Wannerberg *et al*, 2005; Murakoshi, *et al*, 2011) (Figure 1.8).

1.8.1 Structural changes during Rho GTPase activation

Rho GTPases share sequence and structural homology (Hakoshima *et al*, 2003, Jaffe and Hall, 2005). All family members have a structurally similar G domain, which sits next to a short Rho insert domain and a short C terminal hyper variable region (Wittinghofer *et al*, 2011). The G-domain mediates binding to guanine and contains the GTP/GDP binding sites. This domain contains switch 1 and switch 2 regions which direct the conformational changes to the effector domain in response to GTP or GDP binding (Wittinghofer *et al*, 2011; Shaefer *et al*, 2014). These conformational allow for the binding of the otherwise ‘hidden’ effector domain to downstream effectors, therefore mediating an effector specific response. The hydrolysis of GTP to GDP favors an inactive conformation, which allows for the disassociation of effector proteins (Wittinghofer *et al*, 2011; Shaefer *et al*, 2014).

Rho GTPases additionally contain a CAAX box. This consists of a N-terminal cysteine residue, followed by two aliphatic residues and a variable c-terminal amino acid. The N-terminal cysteine can be modified via the addition farnesyl group or geranylgeranyl group via the process of prenylation. This modification is thought to be involved in regulating the localization and stability of most members of the family (Wittinghofer *et al*, 2011; Shaefer *et al*, 2014).



Figure 1.7 Evolutionary relationships between members of the Rho GTPase family. There 8 sub-families in the Rho family of GTPase. The Rnd family (green) are atypical Rho GTPases however is the most closely related to the Rho A, B and C (Rho sub-family yellow). The Rnd family, BTB family, RhoH, Wrch1/RhoU and chp/Wrch2RhoV are atypical Rho GTPases. (*Adapted from Grise et al, 2008*)

1.8.2 Regulation of Rho GTPases

Rho GTPases have weak intrinsic GTPase activity and therefore require assistance by regulatory proteins such as Rho-GEFS, Rho-GAPS and Rho-GDIs (extensively reviewed in, Heasman and Ridley, 2008, Cherfils and Zeghouf, 2013; Hodge and Ridley, 2016).

Rho-GEFS functions by interacting with RhoGTPase switch domains. This interaction leads to significant changes in the conformation of the switch 1 and 2 regions, allowing for an increased affinity for GTP and enhances intrinsic GTPase activity by accelerating the exchange of GDP for GTP (Snyder *et al*, 2002).

Conversely, Rho-GAPs function to inactivate Rho GTPases through the interaction of a 150 amino acid Rho-GAP domain with the switch 1 and 2 domains. This results in a shift in conformation of the GTPase that repositions a hydrolytic water molecule, allowing for increased GTP hydrolysis leading to its inactivation (Young-Moon and Zheng, 2003). The majority of Rho GTPases are further regulated by protein chaperones called RhoGDIs. RhoGDIs function by interacting with the Rho-GDP. This is mediated through an interaction with the modified CAAX motif at the C-terminus which in effect shields the modified residue which ultimately prevents its binding with the cell membrane. This stabilizes Rho-GDP in the resting state, and stabilizes Rho-GDP in a soluble form in the cytosol. As a result, Rho-GDIs prevent the interaction of inactive GTPase with effector proteins and also prevents its degradation (Chardin *et al* 2006; Cherfils and Zeghouf, 2013).

Rho GTPases are additionally regulated by changes in gene expression and may be regulated by micro RNAs. Furthermore, Rho GTPases are thought to be regulated through post-translational modifications, such as phosphorylation, sumoylation and

ubiquitination which can alter how and which effector proteins they interact with and therefore how they function (Reviewed in Hodge and Ridley, 2016).

1.8.3 Typical and Atypical Rho GTPases

The Rho GTPase subfamily can be categorized into two groups, typical and atypical Rho GTPases. Typical Rho GTPases function as ‘molecular switches’ and are primarily activated and inactivated via the hydrolysis of GTP as described above (Figure 1.8) (Jaffe and Hall, 2005). Typical GTPases can additionally be regulated through changes in gene expression and post-translational modifications. Atypical Rho GTPases however are regulated predominantly by differential expression, posttranslational modifications and degradation (Chardin *et al*, 2006). This is because atypical Rho GTPases are constitutively bound to GTP and therefore are always activated (Foster *et al*, 1996, Nobes *et al*, 1998, Fiegan, 2002). Consequently, regulation via the interaction with GAPs and GEFs is inefficient since in most cases these GTPases have a higher affinity for GTP binding (Fiegan, *et al*, 2002). A substitution for a farnesyl group in the place of a geranylgeranyl group at the CAAX prevents GDI binding therefore atypical GTPases cannot be regulated in this way (Garavini *et al*, 2006).

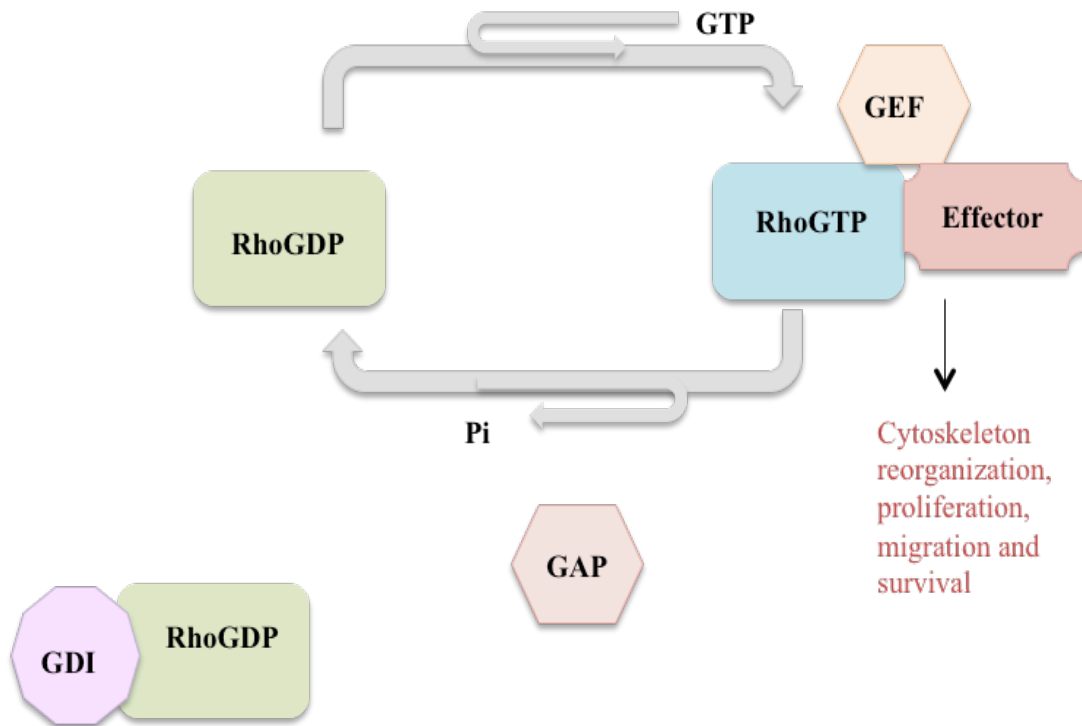


Figure 1.8. Rho GTPases- The molecular switch.

Rho GTPases cycle between GTP active form and a GDP bound inactive form. The active form of Rho-GTP allows subsequent interaction with effectors proteins due to extensive changes in structure. The active GTPase is switched off through the hydrolysis of GTP to GDP. GTPases have very weak GTPase activity and therefore are regulated by GAP proteins to increase GTPase activity. GEF proteins act to facilitate the hydrolysis of GTP to GDP. Rho-GDP is stabilized in the cytoplasm via an association with GDI. 70 GEFs have been described in humans and over 80 GAPs have been identified in mammals. (Adapted from Etienne-Manneville and Hall, 2002).

1.8.4 The Rnd Subfamily

The Rnd subfamily consists of Rnd1, Rnd2 and Rnd3/RhoE. Members of the Rnd subfamily are constitutively active and exist almost entirely in a GTP bound state (Foster *et al*, 1996, Nobes *et al*, 1998). The G domain shares some structural homology to the other members of the family however single base substitutions at some important positions mean that the ability to hydrolyze GTP is very different (Garavini *et al*, 2002, Fiegan *et al*, 2002). GTP hydrolysis in Ras is mediated by a conserved glycine at position 12 (Gly12) and a glutamate at position 61 (Gln61) in the switch 1 region. Rnd 1, 2 and 3 proteins have instead, valine (Val), alanine (Ala) or serine (Ser), respectively, at the same position. These substitutions mean that GTP hydrolysis is inefficient (Garavini *et al*, 2002, Fiegan *et al*, 2002). Furthermore, Rnd GTPases lack intrinsic GTPase activity and therefore are not regulated by GEFs or GAPs. Instead they are regulated by differential expression and posttranslational modifications (Garavini *et al*, 2002, Fiegan *et al*, 2002).

Interestingly, the Rnd subfamily arose later on during the evolution of the Rho family of GTPases as they are primarily present in vertebrates. This suggests that these are involved in more specialist roles, which have aided multi-cellular evolution. This can be exemplified by the ability for members of the Rnd subfamily of GTPases to function in a variety of cellular events. These include actin cytoskeletal remodeling, neurite extension, cell migration and cancer (reviewed in Chardin *et al* 2002).

1.9 Rnd3/RhoE

Rnd3/RhoE (referred to as Rnd3 from here) was the first member of the Rnd subfamily to be identified (Foster *et al*, 1996). Foster *et al* first discovered Rnd3 when a screen for p190Rho GAP interacting partners was undertaken. In this study it was shown that Rnd3 and RhoA show sequence homology. Because of this similarity,

Rnd3 activity was initially extensively studied in relation to actin cytoskeleton dynamics. However, more and more research is pointing to a possible role in other processes such as cell cycle regulation, apoptosis, differentiation and in cancer.

1.9.1 Structure of Rnd3

Rnd3 and RhoA show 43% sequence homology in the G domain. One of the most crucial differences is in the switch 2 region of RhoE/Rnd3, where there is a serine 32 instead of the conserved Gln63. Gln63 is a conserved residue in the active site of Rho GTPases (this corresponds to a Gln61 in the Ras family) which stabilizes the transfer of water molecules when the GTPase is in its transition state. This single base substitution is responsible for the inability for Rnd3 to hydrolyse GTP and therefore its GTPase deficiency. Furthermore, a GDP bound conformation of Rnd3 is almost entirely absent. This is because a substitution at the corresponding amino acid Ala51 (responsible for stabilizing a GDP bound conformation in other Ras family of GTPases). At this position Rnd3 instead has a Gln33 that is unable to interact with neighboring amino acids, which ensure a stabilized GDP bound conformation. In addition to this Rnd3 is not regulated by GAPs and GEFs. This is due to base substitutions in the amino acids that are responsible for binding to these regulatory proteins (Garavini *et al*, 2002, Fiegan *et al*, 2002).

Rnd3 is also modified differently at the CAAX motif at the C-terminal. Other Ras GTPases are geranylgerenylated at this motif, which favors GDI binding. Rnd3 instead is farnesylated at this position. This difference means that GDIs are unable to interact with Rnd3 and sequester Rnd3 in the cytosol (Garavini *et al*, 2002, Fiegan *et al*, 2002).

Taken together, the sequence differences and structural differences in Rnd3 are responsible for its unusual properties as a GTPase. Rnd3 is therefore a GTPase that

lacks intrinsic GTPase activity, exists always in a GTP bound conformation, has a higher affinity for GTP, and is not regulated by GAPs, GEFs or GDIs. Therefore, the function of Rnd3 must be regulated by other mechanisms so that it is not always activating downstream biological events. This is done through the regulation of its expression, its ability to be modified post translationally and through its localization (Garavini *et al*, 2002, Fiegan *et al*, 2002).

1.9.2 Regulation of Rnd3

As mentioned previously, the Rnd3 CAAX motif consists of a farnesylated cysteine residue and therefore cannot bind RhoGDIs. However, it has been shown that the residues upstream and downstream are phosphorylated and these modifications may regulate its activity and localization (Kommander *et al*, 2008). Phosphorylation by ROCK1 and PKC alpha may regulate binding to the cell membrane (Riento *et al*, 2005a; Riento *et al*, 2005b; Kommander *et al*, 2008; Madigan *et al*, 2009). It has been shown that phosphorylation at position Ser-240 (which can be phosphorylated by both ROCK1 and PKC alpha) may allow for binding with 14-3-3 (Riou *et al*, 2013). 14-3-3 proteins are regulatory proteins that exert their function by binding to various posttranslational modifications (Obsil and Obsilova *et al*, 2011). 14-3-3 functions in a similar way to RhoGDIs in that it can bind to prenylated isoprenoid groups, however have been additionally shown to bind to phospho-serine and phospho-threonine residues with high specificity (Obsil and Obsilova, 2011, Riou *et al*, 2013). It was shown that 14-3-3 has particular specificity for farnesylated groups. 14-3-3 is a dimer where one half of the dimer can bind with high specificity to the farnesylated group (Riou *et al*, 2013). The second subunit of the dimer binds with high specificity to the phosphorylated serine in the hydrophobic patch of the 14-3-3 active site. Using mutational analysis, it was shown that the changes in Ser-240 result in reduced

cytosolic Rnd3 and increased membrane bound Rnd3. This suggests that 14-3-3 proteins bound to both the farnesylation group and specific phosphosites to keep Rnd3 in the cytosol in a sequestered state (Riou *et al*, 2013). Further to this, it has been proposed that there may be a phosphatase which functions to allow for the dephosphorylation of these residues, which then allows for binding to the cell membrane and subsequent activation of Rnd3 regulated pathways (Riou *et al*, 2013). It is important to note that the CAAX motif may be modified in more than one way to alter the post translational modifications and how Rnd proteins interact with other effectors and therefore which biological pathways they regulate. This could provide meaningful insight into how localization of Rnd3 is further regulated. However, characterization of other modifications has yet to be identified.

Additionally, phosphorylation by ROCK1 has been shown to stabilize Rnd3 (Riento, *et al*, 2005b). It was shown that ROCK-1 phosphorylates Rnd3 at Ser-11 upon PDGF stimulation. This in turn stabilizes Rnd3, which then led to reduced stress fiber formation (Riento *et al*, 2005b)

Taken together this suggests that Rnd3, ROCK1 and PKC alpha may function together to regulate one another however the mechanism not clearly defined.

Rnd3 can also be regulated at a transcriptional level. Rnd3 expression is thought to be regulated by UVB radiation, chemotherapeutic agents such as cisplatin as well as NF-kappa B, TGF β and PDGFR β signaling (Boswell *et al*, 2006; Ball *et al*, 2007; Shurin *et al*, 2008; Nadiminty *et al*, 2010). However, how these transcriptionally regulate Rnd3 expression is yet to be fully elucidated.

HIF-1 α is a transcription factor that has been shown to directly bind to the Rnd3 promoter and therefore direct its transcription (Ong and Hausenloy, 2012). HIF-1 α is

involved in regulating hypoxia in response to inflammation and has been found to regulate Rnd3 expression gastric cancer cell lines (Ong and Hausenloy, 2012).

Furthermore, Rnd3 is shown to be regulated by the microRNA, miR-200b. MiR-200b is thought to post transcriptionally regulate Rnd3 via the binding onto the 3'UTR. Manipulation of the 20bp binding site meant that Rnd3 could be post transcriptionally regulated and as a result it was shown that prevention of this binding leads to increased cyclin D1 expression along with the subsequent entry into S-phase associated with cyclin D1 expression (Xia *et al*, 2010)

It is therefore evident that the regulation of Rnd3 is a multifaceted process that may be more complex than first anticipated. The number of different biological pathways that Rnd3 is involved with reflects this.

1.10 Function of Rnd3

1.10.1 Rnd3 and actin cytoskeletal dynamics

Rho GTPases have been extensively studied in relation to actin cytoskeletal dynamics and have been shown to have a role in regulating cell adhesion and cell motility (Riento *et al*, 2003). RhoA indirectly regulates actin cytoskeletal dynamics via ROCK or Rho-associated kinases. ROCKs are serine threonine kinases known to function down stream of Rho GTPases. ROCKs exist in two isoforms, ROCK 1 and ROCK 2. Both isoforms share structural homology and consist of a catalytic kinase domain (N-terminal region), coil-coiled domain and a PH domain (C-terminal). The C-terminal domain additionally contains a Rho binding domain. It has been shown that deletion of this domain leads to constitutive activation, therefore suggesting that ROCKs are auto inhibited.

The switch 1 region of active RhoA can interact with the Rho binding sites located in the C-terminal domain and this results in the activation of ROCK since binding of active RhoA triggers a conformational change thus relieving autoinhibition (Jacobs *et al*, 2005). Activation of ROCK leads to phosphorylation of MLC and LIMK both kinases that are involved in regulating actin stress fiber formation.

The switch 1 region of active RhoA shares structural homology to the switch 1 region of Rnd3 and therefore it was proposed that Rnd3 might regulate ROCK activity in a similar manner (Jacobs *et al*, 2005). Interestingly, it was found that Rnd3 firstly, binds specifically with ROCK-1 directly and secondly, it binds ROCK-1 at a region that is distinct from the RhoA binding region. Furthermore, Rnd3 binding has an opposite effect to RhoA, in that binding leads to decreased stress fiber formation through reduced phosphorylation and subsequent inhibition of MYPT-1 and as a result leads to increased cell motility and loss of focal adhesion assembly (Nobes *et al*, 1998; Riento *et al*, 2003; Komander *et al*, 2008).

In addition to this, ROCK1 has been shown to stabilize Rnd3. An interaction between Rnd3 and ROCK-1 leads to phosphorylation of Rnd3 at the C-terminal and N-terminal in Rnd3 known to regulate its stability and its stability and localization (Riento *et al*, 2005a, Komander *et al*, 2008). Taken together, it was concluded that Rnd3 acts antagonistically to RhoA and thus inhibits ROCK-1 activity.

It was also shown that Rnd GTPases also bind onto and activate p190 RhoGAP. p190 regulates Rho/Rock pathway via its interaction with RhoA (Wannerberg *et al*, 2003, Onuma *et al*, 2012). Interestingly, Rnd3 but not Rnd1 binds directly to ROCK1 however loss of Rnd1 can also induce loss of actin stress fiber formation. This suggests that activation of p190 by Rnd3 is the most likely explanation for the

function of Rnd1 and Rnd3 in stress fiber disassembly and subsequent cell rounding (Oinuma *et al*, 2012).

Furthermore, it has been shown that the effect of Rnd3 on the actin cytoskeleton may play a role in neurogenesis. It has been proposed that the polarity of both neurons and glial cells is essential during central nervous system development. It was found that Rnd3 is important in regulating the migration and length of neurons during neurogenesis, as well as regulating axon polarization and migration. It was concluded that these effects could be a consequence of the effects of Rnd3 on the Rho/ROCK/LIMC cascade, however a direct mechanism of how this occurs has yet to be identified (Pacary *et al*, 2013).

1.10.2 Rnd3 and the cell cycle

One of the best-characterized ROCK1 independent roles of Rnd3 is the effect on the cell cycle and cell proliferation. Studies have shown that Rnd3 may be involved in regulating the decision for cells to proceed into the G1 phase of the cell cycle via the regulation of cyclin D1 (Villalonga *et al*, 2004). It was shown that the expression of Rnd3 led to an accumulation of cells in G1 phase of the cell cycle and a suppression of cells entering into S-phase. It was therefore suggested that this occurred in response to the down regulation of cyclin D1 which was also observed. A direct interaction between Rnd3 and cyclin D1 promoter has not been established but it proposed that perhaps this deregulation might occur post transcriptionally via the interaction of Rnd3 with regulators of translation (Villalonga *et al*, 2004). In line with this proposal, it was later shown that when Rnd3 expression was induced, phosphorylation of 4EBP-1, a translational repressor, was reduced. Specifically, there was a suppression of phosphorylation at multiple residues that correspond to sites that are responsible for the conformational changes, which prevent 4EBP-1 binding to

translation initiation complexes such as eIF4E. Therefore, it was seen that there was a reduction in the biosynthesis of c-myc and cyclin D1, both of which are translationally regulated by EIF4E.

Additionally, it was shown that the increased expression of Rnd3 led to a reduced expression of Rb. Rb is responsible for phosphorylating cyclin D1 and therefore activating it (Villalonga *et al*, 2009).

Taken together, it was suggested that Rnd3 affects cell proliferation through the posttranslational regulation of cyclin D1 (Villalonga *et al*, 2009).

1.10.3 Rnd3 and Cancer

The function of Rnd3 in cancer is well studied. It has been found that Rnd3 functions both as a tumor suppressor gene and an oncogene. Rnd3 was shown to be overexpressed in some carcinomas such as squamous cell, hepatocellular, breast, colorectal and prostate carcinomas that Rnd3. It was suggested, that the overexpression of Rnd3 leads to tumor progression and metastasis as a result (reviewed in Jie *et al*, 2016). Conversely, it was shown that in glioblastoma multiform (GBM) there seemed to be a reduction in the expression of Rnd3 and that this was correlated to a negative clinical progression (Jie *et al*, 2016).

Interestingly, it has also been suggested that Rnd3 may play a role in tumour metastasis and invasion because of its role in actin cytoskeletal dynamics. Using DNA microarrays to determine the change in gene expression during metastasis it was shown that changes in Rnd3 expression correlated to the metastatic potential of prostate cells and their ability to migrate, which corresponds to an alteration in actin cytoskeletal dynamic also seen in these cells (Troger *et al*, 2005).

Furthermore, Rnd3 may have role in non-small cell lung cancer (NSCLC) via the regulation of notch signaling. It was shown that Rnd3 is down regulated in NSCLC

cell lines. Notch1 activation is increased in NSCLC cell lines and this increased activation is thought to be associated with hyper proliferation. It was shown that the expression of Rnd3 led to a suppression of proliferation. Moreover, the study found that Rnd3 over expression was able to stabilize the NICD portion of Notch 1 and resulted in an inhibition of cell proliferation (Tang *et al*, 2014).

Taken together, this suggests that Rnd3 plays a role in tumor progression and metastasis both via a Rho/ROCK dependent pathway and in pathways independent of its roles in actin cytoskeletal contractility. In addition to this, these studies suggest the role of Rnd3 is variable in different cell and tumor types. Therefore elucidating the functional role of Rnd3 in a cancer context is in need of further study.

1.10.4 Rnd3 and Apoptosis

Rnd3 has additionally been found to be a downstream target of p53. Studies using p53 inducible cell lines have shown that Rnd3 expression is up regulated during genotoxic stress; therefore suggesting that Rnd3 may be a p53 target gene (Ongusaha *et al*, 2006). Furthermore, actin depolymerization, stress fiber disassembly, as well as actin depolymerization were seen to correspond with the up regulation of p53, suggesting that an increase in p53 expression is ROCK dependent (Riento *et al*, 2003). Rnd3 silencing also led to a rescue of actin polymerization and stress fiber formation and this correlated to increased apoptosis (Onagusaha *et al*, 2006). Taken together, it was concluded that Rnd3/ROCK1 interaction leads to an inhibition of ROCK-1 and subsequent protection against apoptosis when cells are subject to genotoxic stress in a p53 dependent manner (Onagusaha *et al*, 2006). Other studies, which have shown that Rnd3 protects against UVB induced apoptosis in a pathway independent of both p53 and ROCK-1 activity support this notion (Boswell *et al*, 2007).

Conversely, recent studies in HaCaTs have suggested that a depletion of Rnd3 results in protection against apoptosis (Ryan *et al*, 2012). Depletion of Rnd3 using siRNA protects against cisplatin mediated cell death and this is dependent on the expression desmosomal protein plakoglobin (Ryan *et al*, 2012). One could argue that this phenotype is due to the p53 status in HaCaTs. It is important to note that HaCaTs express mutant forms of both isoforms of p53 and these mutations result in an extension of p53 half-life and reduced function (Lehman *et al*, 1993). However, p53 mutants do retain the ability to stimulate Rnd3 transcription following cell death stimuli (Reagan-Shaw *et al*, 2006, Boswell *et al*, 2007).

The study conducted by Ryan *et al* show that an increase in p53 and Rnd3 expression is not observed during cisplatin treatment in HaCaTs (Ryan *et al*, 2012).

Therefore, suggesting that Rnd3 may play a role in apoptosis in an additional pathway that is distinct from p53 mediated apoptosis.

1.10.5 Rnd3 and Keratinocyte Differentiation

The detachment of committed keratinocyte progenitors is dependent on actin cytoskeleton remodeling, since the down regulation of integrin is essential to ensuring that differentiating keratinocytes can transverse into superseding layers (Watt *et al*, 2002). Pharmacological inhibition of ROCK (using Y-27632) have shown that inactivation of ROCK results in an increase in actin fiber bundling and as a result leads to an increase in cell contraction and subsequent suppression in terminal differentiation in keratinocytes (McMullan *et al*, 2003; Colman *et al*, 2001).

Since ROCK kinases are regulated by different Rho GTPases, it has been suggested that Rho GTPases may play a role in regulating epidermal homeostasis.

Since it has been shown that ROCK1 may play a role in keratinocyte differentiation and that Rnd3 is regulated by ROCK1, it was speculated that Rnd3 might play a role

in differentiation also. It was shown that an overexpression of Rnd3 led to an increase in populations of keratinocytes, which have a higher propensity to differentiate and stratify and were larger in cell size as a result. (Liebig *et al*, 2009). Moreover, Rnd3 expression was up regulated during differentiation and stratification in a ROCK1 dependent manner. This was coupled with an increased proliferation of undifferentiated cells. The study concluded that Rnd3 might play a role in regulating the decision for keratinocyte progenitors to differentiate (Liebig *et al*, 2009)

It is clear that Rnd3 plays multiple roles in regulating very different aspects of cell biology. The current literature points to a role of Rnd3 in regulating diverse cellular and morphological events. Whilst these roles are becoming more and more defined, it is becoming clear that Rnd3 can exert its effects in numerous ways that are not necessarily Rho/ROCK dependent. Therefore, characterizing these roles further would be useful in determining how Rnd3 functions in relation to its biological and cellular context.

1.11 Project aims

The regulation of epidermal homeostasis is still a poorly understood process and it is clear from the current literature that it is a highly complex process that involves the inter-play of multiple different regulatory pathways. It is becoming more and more clear that Rnd3 is involved in regulating keratinocyte differentiation however the molecular mechanism, which underlies its role, is poorly defined and remains elusive.

Past studies have shown that increased expression of Rnd3 lead to an increased propensity to differentiate (Liebig *et al*, 2010). Therefore it is hypothesized here, that a depletion of Rnd3 would lead to an enrichment of early progenitors or KSC.

Furthermore it is hypothesized that a depletion in Rnd3 would have an effect on pathways that are known to regulate keratinocyte function.

The aim of this project is therefore to:

- Define the biochemical and morphological effects of Rnd3 depletion in HaCaTs
- Elucidate how Rnd3 may be exerting such affects by identifying ‘novel’ Rnd3 regulated proteins.

Chapter 2

Materials and Methods

2.1 Materials

Tables 2.1-2.5 List the reagents and recipes used in this study

Table 2.1 Buffers and Solutions

Buffer	Experiment	Reagents	Manufacturer
LB Broth	Bacterial culture	25% Lysogeny Buffer	Sigma
Ampicillin	Bacterial culture	15g in 25% LB broth, 100mg/ml ampicillin	
DNA extraction	Maxi Prep	Pure yield Maxi Prep system	Promega
DNA Loading Buffer	DNA loading		Bioline
Tris, Borate ethylenediaminetetracetic buffer (TBE) (10x)	Agarose gel	89mM TRIS (pH 7.6), 89mM boric acid, 2mM EDTA	Sigma
RNA Extraction kit	RNA Extraction	RNAeasy RNA extraction kit	Qiagen
DNAase treatment kit	DNAase Treatment	DNAase treatment kit	Sigma
CDNA synthesis kit	cDNA synthesis	Tetro cDNA synthesis kit	Tetro
PCR	PCR	My Taq DNA Polymerase	Bioline
1% Agarose	Agarose gel	1% Agarose in TBE buffer	Sigma
Quantitative Real time PCR kit	Quantitative Real time PCR	SensiFAST Probe Hi Rox kit	Bioline
Cell lysis buffer	Cell lysate preparation		N/A
RSB+0.5%NP40	Cell lysate preparation- Cell fractionation	1M Tris pH7.4, v1M MgCl ₂ , 1M KCL and 5% NP40 (Tergitol) +1 tablet of protease and phosphatase inhibitor cocktails per 10ml	N/A
Sample buffer	SDS PAGE	10% Glycerol, 2%SDS 1%bromophenol Blue, 20mM dithiothreitol (DTT), 100mM Tris PH 6.8	N/A

Bradford Assay	Protein Quantification	Coomassie protein assay reagent	Pierce
SDS Running buffer	SDS PAGE	0.2 M Glycine, 0.02 M Tris, 0.1 M SDS	N/A
Transfer buffer	Western blot	BioRad dry transfer buffer	N/A
TBST	Western blot	20mM of Tris pH7.5, 150mM of NaCl, 0.05% Tween20	N/A
Membrane Stripping buffer	Western blot	0.4M Sodium Hydroxide	N/A
PBST	Western blot	Phospho buffered saline, 0.05% Tween 20	N/A
Antibody dilution solution	Western blot	5% semi skimmed in TBST or 5% BSA in TBST	N/A
Blocking buffer	Western blot	5% semi skimmed in TBST or 5% BSA in TBST	N/A
Antibody cross linking buffer	Immunoprecipitation	0.02M dimethylpimelidate dihydrochloride, 0.2M TEA pH 8.2	N/A
Quenching buffer	Immunoprecipitation	0.05M Tris-HCL pH 7.5	N/A
Wash Buffer	Immunoprecipitation	0.2M Triethanolamine (TEA) pH 8.2	N/A
Elution buffer	Immunoprecipitation	1M glycine pH 3.0	N/A
Coverslip fixing buffer	Immunofluorescence	4% Paraformaldehyde	N/A
Coverslip wash solution	Immunofluorescence	PBS	N/A
Cell permeabilization buffer	Immunofluorescence	0.2% Triton X	Sigma
Blocking buffer	Immunofluorescence	5% BSA in TBST	N/A
Antibody dilution buffer	Immunofluorescence	5% semi skimmed milk	N/A
Gel Fixing buffer	In gel digestion	55% Acetic acid, 11% Methanol	N/A
Gel staining (Coomassaie)	In gel digestion	0.01% brilliant blue in gel fixing solution	N/A
Gel destain	In gel digestion	7.5% acetic acid, 5% methanol	N/A
Destain solution	In gel digestion	30% Acetonitrile	N/A
Dehydration solution	In gel digestion	50% acetonitrile in 25mM ammonium bicarbonate	N/A
Rehydration solution	In gel digestion	50% Acetonitrile	N/A

Reducing buffer	In gel digestion	10mM dithiothreitol (DTT) in 0.025M ammonium bicarbonate	N/A
Alkylation solution	In gel digestion	55mM Idoacetomide in 25mM ammonium bicarbonate	N/A
Trypsin suspension solution	In gel digestion	0.05M Acetic acid	N/A
Trypsin digestion solution	In gel digestion	12.5ng/ml trypsin in 0.025 ammonium bicarbonate	Promega
Wetting solution	Desalting	100% acetonitrile	N/A
Washing solution	Desalting	0.1% TFA	N/A
Elution solution	Desalting	0.1% Formic acid	N/A
DNA marker	Agarose gel	Hyperladder 1kb	Bioline
Protein marker	SDS PAGE	PageRuler Prestained Protein ladder	Thermo scientific

Table 2.2 siRNA

Oligo	Supplier	Catalogue Number	Target sequence
Non-silencing control	Qiagen		
ON-TARGETplus siRNA Rnd3	GE Healthcare	SO-2540035G	CUACAGUGUUGAGAAUUA UAGUAGAGCUCUCCAAAUCA CAGCAAUCUCUCCAAUCAU GCGGACAGAUGUUAGUACAA
ON-TARGETplus siRNA TP63	GE Healthcare	SO-2487849G	GCACACAGACAAAUGAAUU CGACAGUCUUGUACAAUUU UCUAUCAGAUUGAGCAUUA GAUGAACUGUUAUACUUAC

Table 2.3: Antibodies

Antibody	Antibody name	Molecular weight (kD)	Supplier	Species	Dilution for WB	Dilution for IF
Delta NP63	N-16	63	Cell signaling	Mouse	1:1000	1:100
P63	4A4	63	Novus Biosciences	Mouse	1:1000	1:100
p63	D2K8X	75	Cell signaling	Rabbit	1:1000	1:100
Desmoplakin	115F	260	Cell signaling	Mouse	1:50	1:20

FOXK-1	FOXK1	97	Cell Signaling	Rabbit	1:100 0	1:100
JunB	C37F9	42	Cell Signaling	Rabbit	1:100 0	1:50
K10	DE-K10		Thermo		1:100 0	-
Involucrin	SY5	80	Thermo		1:500	-
RhoE/Rnd3		26	Novus Biosciences	Rabbit	1:200	-
RhoE/Rnd3	-	27	Millipore	Mouse	1:200	-
α-Tubulin	DM1A	55	Sigma	Mouse	1:500	-
Perp	FL-193	25	Thermo	Rabbit	1:100 0	
IRDye Antimouse	-	-	Odyssey	Goat	1:100 0	-
IRDye Antirabbit	-	-	Odyssey	Goat	1:100 0	-
Alexa Fluro 488 (Anti Rabbit)	-	-	abcam	Goat	-	1:100
Alexa Fluro 488 (Anti mouse)	-	-	abcam	Goat	-	1:100
Hoechst 33342	-	-	Invitrogen	N/A	-	1:5000
DAPI			Invitrogen		-	1:5000

Table 2.4: Primers

Oligo	Supplier	Forward sequence	Reverse sequence
GAPDH	Sigma	CTCTGCTCCTCCTGTTCGAC	ACCAAATCCGTTGACTCCGA
RhoE	Sigma	GTCGGCTGCAAGTCTGATCT	CCATATTTGCCCCCTGGTCA
TP63	Sigma	CCTGGAGCCAGAAGAAAGG A	TCGTGTACTGTGGCTCACTAA
ΔNP63	Sigma	GAAGAAAGGACAGCAGCAT TGAT	GGGACTGGTGGACGAGGAG
LEF1	Sigma	TCCAGGCTGGTCTGCAAGAG A	GGCAGCTGTCATTCTTGGACC T
PPARB	Sigma	GGCCATCATTCTGTGTGGAG AC	CAGGATGGTGTCTGGATAG C
SMAD7	Sigma	TCCAGATGCTGTGCCTTCCT C	GCCTCCCCACTCTCGTCTTCT
Keratin 1	Sigma	GTTCCAGCGTGAGGTTTGT	TAAGGCTGGGACAAATCGAC
Keratin 10	Sigma	GGACCAAGATACTAACA ACCAGA	CTTGGTTTCTGATTCAACCAT AGAT
S100A7	Sigma	TCCCAGCTCTGGCTTTTGA	AGCAGGCTTGGCTTCTCAAT
Involucrin	Sigma	TGTGAGTCTGGTTGACAGTA GC	GGAGGAACAGTCTTGAGGAG C

Table 2.5: Plasmids

Construct	Resistance	Supplier
pCMV5 RhoE Flag	Ampicillin	Anne Ridley
pCMV5 EV Flag	Ampicillin	Anne Ridley

2.2 Methods

2.2.1 Molecular biology

2.2.1.1 Bacterial transformation:

1-5µg of plasmid cDNA was added to 45µl of *E-coli* strain DH5α. Plasmid and strains were incubated for 45 mins on ice. These were then heat shocked at 45° C for 30 seconds followed by further incubation on ice for 2 minutes.

500µl of LB broth was added and incubated with agitation for 1 hour at 37°. 250µl were spread onto ampicillin (100mg/ml) treated agar plates overnight at 37°.

2.2.1.2 Plasmid Preparation:

Individual colonies were inoculated with LB broth containing the appropriate selection overnight at 37° with agitation. The LB broth was centrifuged (Beckman 2000) at 6000 rpm for 6 minutes at 24°. Maxi preps were performed using PureYield plasmid maxi prep system (Promega) following the manufacturers guidelines. Plasmid purity and concentration was measured using NanoDrop 2000c UV-Vis Spectrophotometer at 260nm. Purified plasmids were stored at -20°C.

2.2.2 Cell culture methods

2.2.2.1 Cell culture

HaCaTs are an immortalized keratinocyte cell line that has been shown to have an ability to differentiate like normal keratinocytes and therefore have been used as a

model in this work .HaCaTs were cultured in Dulbecco's modified Eagles media (DMEM) supplemented with 5% fetal bovine serum (FBS) and 0.1mg/ml streptomycin and 100 I.U/ ml penicillin. Cells were incubated at 37° with 5% CO₂. Cells were detached from the flasks using trypsin (Gibco) and were passaged when approximately 80% confluent. Infection of mycoplasma was tested for every 4 months using MycoAlert plus mycoplasma detection kit using the manufacturers guidelines (Lonza).

2.2.2.2 siRNA Transfection

Reverse transient transfections were used to knockdown proteins of interest. Transfections were conducted in 6-well plate. 500µl of Opti-mem (Invitrogen) and 2pmol Rnd3 siRNA (GE Healthcare), 9pmol p63 siRNA (GE Healthcare), 9pmol Non-silencing control (Qiagen) (see table 2.2) was plated per well and was left to incubate for 10 minutes at room temperature. 10µl Lipofectamide RNAi max (Invitrogen) was added to the mix and was left to further incubate for 5 minutes. 1x10⁵ cells were plated with DMEM with 5% FBS. The transfected cells were left to incubate at 37° with an atmosphere of 5% CO₂ for approximately 48 hours.

2.2.2.3 DNA Transfection

Human embryonic kidney cell 293 (HEK 293) are a human embryonic kidney cell line and were used to over express FLAG-tagged Rnd3. Cells were seeded onto 6-well plates in DMEM supplemented with 10% FBS and antibiotics for 24h before being transfected with purified DNA using lipofectamine 2000. Transfected cells were incubated for 48 hours in an atmosphere of 5% CO₂.

2.2.2.4 Preparation of methylcellulose

500ml of serum free media was added to 3.5g of autoclaved methylcellulose powder into a flat-bottomed centrifuge tube. The media was stirred at 4°C O/N until viscous and clear and centrifuged at 16000 rpm. 5% FBS was then added to the media. The media was decanted in 25ml aliquots and stored at -20°C.

2.2.2.5 PolyhemA coating of tissue culture dishes

A 10% stock solution of polyhemA was made by adding polyhemA powder in 95% ethanol and dissolving at 60°C. For use, the 10% stock solution was further diluted in 50% acetone and 50% ethanol to make a 0.4% solution. The dishes were coated with 0.4% polyhemA by pouring on the solution and then immediately pouring off. The dishes were dried at room temperature before use.

2.2.2.6 Suspension induced differentiation

In order to induce differentiation a suspension-induced method was employed. Cells were transfected as described previously (Hotchin *et al*, 1992). 48 hours post transfection; cells were mixed with methylcellulose DMEM+5% FBS and were plated onto polyhemA treated plates for 24 hours. The suspended cells were centrifuged for 10 mins at 1400rpm. The cell pellet was then washed with 5 volumes of PBS a total of three times to recover cells.

2.2.2.7 Cyclohexamide Treatment

Cells were treated with 20µg/ml Cyclohexamide (Sigma) was diluted in DMEM+ 5% FBS+ p/s and incubated at 37° to inhibit protein synthesis. Cells were washed in PBS three times and samples collected at the indicated time points.

2.2.3 Protein Biochemistry

2.2.3.1 Cell lysis

Cells were lysed using scrape lysis. Cells were washed in PBS three times and treated with 2xSDS sample buffer (see table 2.1) for 5 minutes and then were scraped. The scraped cells were sonicated 3 times for approximately 15 seconds at 5amps. These samples were boiled at 95° for 5 minutes. The lysates were stored at -20°C.

2.2.3.2 Protein Quantitation

Total protein concentration was preformed using Coomassie protein assay (Peirce) kit according to the manufacturers guidelines and the absorbance was measured using Tecan infinite 5200 pro plate readers at a wavelength of 570nm.

2.2.3.3 SDS-PAGE and Western blot

10% and 12% SDS-PAGE gels were prepared with a 4% stack. Gels were run in Tris-glycine buffer (see table 2.1) for approximately 80 mins at 150V. 2µl of protein ladder (Pageruler, ThermoSci) was loaded as a molecular weight reference. Gels were transferred electrophoretically onto nitrocellulose membrane using the transblot turbo transfer system at 25W and 100V. Membranes were blocked in 5% semi-fat milk diluted in TBST at RT for 1 hour. Membranes were incubated with primary antibodies (see table 2.3) overnight at 4°. Membranes were washed 3 times for 10 minutes in TBST and incubated with Odyssey secondary antibody diluted in 10% normal goat serum (see table 2.1). They were then washed 3 times in TBST. Protein bands were detected using Odyssey infrared detection system (LI-COR Biosciences)

2.2.3.4 Co-immunoprecipitation

The appropriate volume of protein G beads, (Dynabeads protein G, Novex) were washed 3 times with PBST and incubated with concentration of antibody for 30

minutes on a rotator. These were washed once with PBST and 3 times with 0.2M triethanolamine pH 8.8. Crosslinking solution 0.02M dimethyl pimelidate dihydrochloride (Sigma-Aldrich), 0.2M TEA pH 8.2 (Sigma-Aldrich) was added to covalently attach the antibody to the beads for 30 minutes. Beads were then washed once with PBST and twice with 0.05M tris-HCL pH 7.5 (Thermo Fisher Scientific) to quench the crosslinking reaction. Unbound antibody was eluted with 1M glycine pH 2.5 for 5 minutes and washed with PBST three times. Lysates were added to the beads and incubated overnight at 4°C. The supernatant was separated from the beads using a magnetic stand. The beads were washed with ice cold PBS and 2x sample buffer was added. The sample was boiled at 95° for 10 minutes and were then subject to western blotting.

2.2.4 RNA work

2.2.4.1 RNA extraction

RNA was extracted from cells using the RNAeasy minikit (Qiagen) following the manufacturers guidelines.

The total concentration of RNA and purity was measured using a Nanodrop at an absorbance of 260nm. Samples were stored at 4°C for immediate use or at -20°C for long-term storage.

2.2.4.2 DNAase Treatment

In order to remove any genomic DNA, DNAase treatment was required. This was carried out using a DNAase treatment kit (Sigma). Briefly, RNA was treated with DNAase1 and was incubated at 37° for 15-30 minutes. EDTA stop buffer was added and the sample was the incubated at 60°C for 10 minutes to stop the reaction. The total concentration of DNAase treated RNA was measured using NanoDrop 2000c

UV-Vis Spectrophotometer at 260nm to read the absorbance. Samples were then loaded onto a 1% agarose gel to ensure that the treatment was successful. Treated samples were stored at 4°C for immediate use or -20°C for long-term storage.

2.2.4.3 cDNA Synthesis

cDNA was synthesized from DNAase treated RNA using the Tetro cDNA synthesis kit (Tetro) following the instructions provided with the kit. 1ng of cDNA was used per sample preparation. Primers are listed in table 2.4

2.2.4.4 Primer design

Primers were designed using Primer BLAST (NCBI), where the target sequences obtained from the UCSC genome browser, were set as the input. All primers were designed to cross exon-exon junctions (to reduce genomic DNA amplification) and had a T_m of approximately 60.0° and a GC ratio of approximately 50%. UCSC genome browser was used to visualize primer target. Primers were ordered from Sigma Aldrich.

2.2.4.5 Quantitative real time polymerase chain reaction

Forward and reverse primers (see table 4), SYBR green (Agilent technologies) and ROX (Agilent technologies) were added to cDNA to carry out qRT-PCR. These were plated onto 96 well plates and centrifuged. Agilent Mx3005P real time PCR machine was used to measure CT values.

2.2.5 Assays

2.2.5.1 Cell adhesion Assays

Cell adhesion assays were performed on a 96 well plate where each well was coated with 20 ug/mL fibronectin (Sigma) was diluted in serum free DMEM overnight at

4°C. Coating solution was removed, and wells were washed three times in PBS and blocked with 5% BSA for 1-3 hours at 37°. Wells were washed three times in PBS and cells were seeded at a density of 2×10^5 /well and incubated at 37°C for 30-60 minutes. Cells were flicked off in one vigorous go and wells were gently washed three times in PBS 20µl of MTT (5mg/ml) was added to each well and was incubated for 1-3 hours at 37°C. MTT was removed and crystals were solubilized with 30% isopropanol for 30 minutes. The absorbance was read using the Tecan infinite 5200 pro plate reader at a wavelength of 550/600nm. Readings were normalized to BSA only blanks.

2.2.6 Immunofluorescence

2.2.6.1 Coverslip preparation for immunofluorescence

13mm coverslips were pre-treated in nitric acid for 30 minutes diluted in water and then washed in methanol. These were left to dry O/N and were then autoclaved

2.2.6.2 Immunofluorescence

Cells were seeded onto 13mm coverslips. Coverslips were fixed in 4% paraformaldehyde in PBS for 10 minutes. They were then washed in PBS three times. Fixed cells were permeabilised by treatment with 0.2 % Triton X100 for 3 minutes. Cells were then washed in PBS 4 times and were blocked with 5% BSA+TBST for 1 hour at 37°C. Coverslips were then incubated with the primary antibody diluted in PBS for 1 hour. These were washed 3 times in PBS and were incubated with the specified fluorescent secondary antibody for 30-45 minutes. For nuclear staining µg/ml DAPI or Hoechst 3342 µg/ml was diluted with the secondary antibody. Coverslips were washed 3 times in PBS with a final wash in distilled water. Coverslips were mounted using Mowiol and stored at -20°C. Coverslips were

visualized and single section images were taken using NIKON SP2 inverted confocal microscope with a pinhole size of 1 μ m.

2.2.6.3 3D immunofluorescence

To determine cell volume, coverslips were mounted onto plastic strips after fixation and permeabilisation. Coverslips were placed onto glass slides and were immediately treated with 90% glycerol/PBS solution prior to mounting. Z-stacks were taken immediately, using a 63x objective lens, with a step size of 1nm, using NIKON SP2 inverted microscope

2.2.7 Stable isotope labeled with amino acid in cell culture (SILAC)

2.2.7.1 Cell Culture

HaCaTs and HEK 293T cells were cultured SILAC DMEM (Thermo Fisher Scientific) supplemented with 0.1mg/ml L-arginine and L-lysine ('light' R0K0, and 'heavy' $^{13}\text{C}_6$ $^{15}\text{N}_4$ L-arginine and $^{13}\text{C}_6$ $^{15}\text{N}_2$ ('heavy' R10K8). Media was supplemented with 0.1mg/ml streptomycin and 100 I.U/ ml penicillin. Additionally, 0.5mg/ml proline and 10% dialyzed FBS was added. Cells were cultured for a total of 5-6 doublings to ensure that labeled amino acids were incorporated efficiently.

2.2.7.2 In gel trypsin digestion

Cell lysates were loaded onto a 12% SDS gel (as described in section 2.4.3). Gels were subsequently fixed in gel fixation solution for 15 minutes and were stained using coomassie blue for a further 60 minutes. Gels were then destained using destaining solution for O/N. Gel bands were cut into individual bands and were subsequently destained using dehydration solution (see table 2.1) with agitation at 37°C. When

bands were dry, they were suspended in rehydration solution (see table 2.1). This process was continuous until bands were sufficiently destained.

Individual bands were dehydrated for 15 minutes using vacuum centrifugation for 10 minutes at 37°C and dehydrated in 10Mm DTT in 25mM ammonium bicarbonate for 45 minutes at 56°C. Gel pieces were then washed in destaining solution and to alkylate cysteine residues, were suspended in 55mM iodoacetamide, 25mM ammonium bicarbonate at room temperature for 45mins in the dark. Gel pieces were then washed in dehydration solution three times and were dried using vacuum centrifugation.

2.2.7.3 Tryptic Digest

Trypsin Gold (Promega) was used to digest peptides from destained gel pieces. Trypsin was suspended in at 12.5ng/μl in 50Mm ammonium bicarbonate at 37°C overnight. Proteolysis was quenched using 0.5% formic acid. Peptides were dried using vacuum centrifugation and were suspended in 0.1% formic acid.

2.2.7.4 Desalting

Ziptips C18 pipette tips (Millipore), were used to desalt the tryptic peptides according to manufacturer's instructions to remove any salts that may remain in the sample. Desalted samples were dried and suspended in 0.1% Formic acid.

2.2.7.5 Liquid Chromatography

150mm Acclaim PepMap100 C₁₈ column was used in mobile phase to separate loaded peptides (water and 0.1% formic acid). A 3.2% to 44% mobile phase B linear gradient (0.1% formic acid and acetonitrile) with a 350nl/min flow rate was used to separate peptides. The column was then subsequently washed with 90% mobile phase B before re equilibrating at 3.2% mobile phase. The Advion Triverse Nanomate was

directly connected to the LC system and was used to spray peptides into LTQ-Orbitrap ETD (Thermo Fisher) using a spray voltage of 1.7Kv.

2.2.7.6 Tandem Mass spectrometry (carried out by Jingli Yu)

Thermo Fisher Orbitrap Elite (Thermo Fisher) was used to carry out a full FT-MS scan and subsequent CID (collision induced dissociation) MS/MS scans. Data was acquired using Xcalibur 2.1 (Thermo scientific).

2.2.7.7 Maxquant

Raw MS/MS data was further processed using the Maxquant software. Raw data was searched against Andromeda search engine using the Swiss prot database. The database included forward and reverse sequences as well as ‘common contaminants’ such as keratin, trypsin and BSA.

The search parameters were: Minimum peptide length 8, precursor ion mass tolerance 7ppm, fragment ion mass tolerance 0.5Da, cleavage enzyme trypsin/P. SILAC labels corresponding to each experiment were selected for. The false discovery rate (FDR) was set to 0.01 (1%)

2.2.8 Statistical Tests

Students T-test was used to determine statistical significance where: ns $P > 0.05$, * $p < 0.05$, ** < 0.01 , *** $p < 0.001$

2.2.9 Analysis of Published data sets

Published data sets were retrieved using the GEO database. Datasets were downloaded and subsequently analyzed using GALAXY (<http://galaxyproject.org>), Submitting gene lists to DAVID bioinformatics retrieved enriched GO terms.

Chapter 3

Knock down of Rnd3 leads to an enrichment of a population of ‘stem like’ keratinocytes.

3.1 Introduction

It is clear from the current literature, that defining keratinocytes from each progenitor populations is not straightforward. Moreover, understanding how the decision for committed progenitors to differentiate and for KSCs to remain dormant is crucial towards understanding how epidermal homeostasis is regulated. Therefore, identifying potential pathways that regulate the behavior of each population is an important step towards understanding how each population has the ability to respond to different stimuli.

Previously, it has been shown that Rho GTPase signaling may play a role in regulating keratinocyte differentiation. An inhibition of ROCK1 (a serine/threonine kinase involved in the Rho/ROCK/LIMC cascade) activity has been shown to enrich for an of population keratinocytes which are ‘stem like’ (McMullan *et al*, 2003). Since Rnd3 is a known interacting partner to ROCK1, it suggests that Rnd3 may additionally play a role in keratinocyte differentiation. Rnd3 is an atypical GTPase and has been found to be involved in multiple processes such as cell proliferation, cell migration and apoptosis. Interestingly, it has been proposed that Rnd3 may be involved in regulating keratinocyte differentiation. Liebig *et al* have shown that an overexpression of Rnd3 induces keratinocyte differentiation. Furthermore, it was that in shown squamous cell carcinoma cells, which are known to have reduced Rnd3 expression, have a reduced propensity to differentiate (Liebig *et al*, 2009, Zhu *et al*, 2014). In addition to this it has been shown that Rnd3 is involved in regulating the

transportation of the cleaved portion of Notch during epidermal development prenatally (Zhu *et al*, 2014). Taken together this suggests that Rnd3 may be involved in regulating progenitor/KSC population.

This chapter aims to characterize some of the morphological and biochemical changes that occur in keratinocytes in response to Rnd3 depletion in normal keratinocytes. Since a clear defining signature has yet to be identified for the KSC population, a number of proposed putative KSC markers from the current literature have been considered. This is an approach taken by many within the field, with the notion that the more ‘stem like’ phenotypes that are observed within a given population, with more certainty it can be assumed that the cells in the population are in fact ‘stem-like’.

3.2 Results

3.2.1 Knock down in Rnd3 results in an increased cell clustering

To identify if Rnd3 has an effect on the keratinocyte behavior, Rnd3 siRNA was transiently transfected into HaCaTs for 48hours. To ensure that Rnd3 was sufficiently depleted, immunoblotting and qRTPCR was used to determine transfection efficiency. Figure 3.1a and 3.1b shows that 48 hours post transfection resulted in an 80-90% knock down at both the transcriptional level and at the protein level. The transfection efficiency was determined prior to any subsequent analysis either through immunoblotting or qRTPCR.

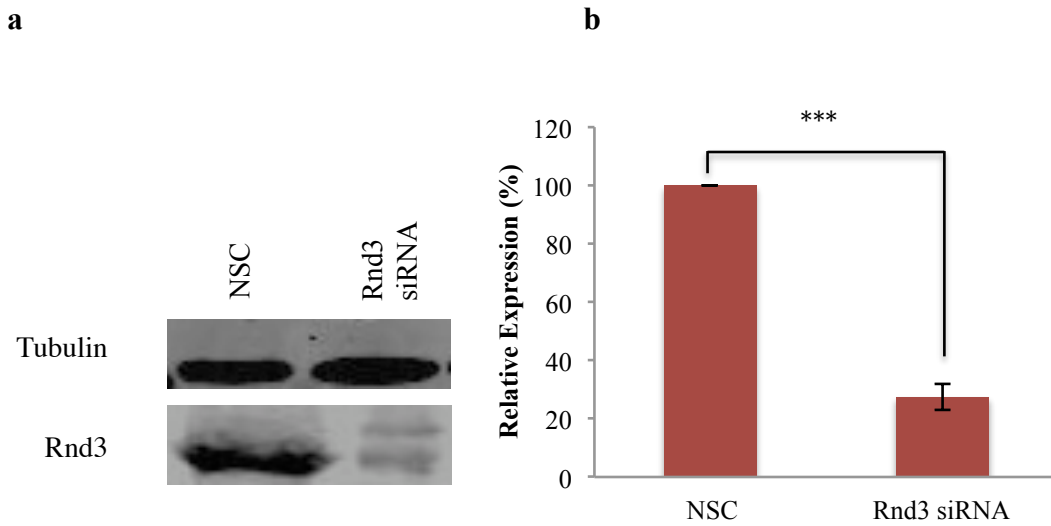


Figure 3.1 Transient transfection of HaCaTs with Rnd3 siRNA for 48 hours leads to 70-80% knock down.

HaCaTs were transiently transfected with Rnd3 siRNA for 48 hours before cell lysates were subject to immunoblotting and qRT-PCR was performed. Figure 3.1a shows that Rnd3 has been sufficiently knocked down at the protein level. Figure 3.1b shows that the knock down efficiency is approximately 80%. A total of 3 independent experiments were conducted and a Student's T-test was used to determine statistical significance where * $p < 0.05$, ** $p < 0.01$, *** $p < 0.001$. Error bars represent standard error of the mean.

As previously mentioned in section 1.7.4 keratinocyte progenitors form clusters in basal layer (Jones *et al*, 1995). Furthermore, studies in mouse models have shown that follicular epidermal stem cells can additionally form discrete clusters at the bulge region of the hair shaft (Saville *et al*, 2010).

To analyze changes in colony compaction, Rnd3 depleted cells were seeded onto glass coverslips and were stained with CellTracker green for 30 minutes. These were fixed, stained with DAPI and mounted on plastic strips with a PBS+90% glycerol mounting media (as described in methods and materials). Z-stacks were taken immediately at 1nm steps using Leica SP2 Inverted Confocal with a 63x objective lens. Inter-nuclear distance measurements are thought to be suitable to measure cell clustering since the nuclei are within a fixed position in the cell. The distance of nuclei in relation to its closest neighbor (inter nuclear distance) was measured using the measuring tool in ImageJ. The internuclear distance was measured in a total of three colonies from each sample and a total of three independent biological samples were analyzed. A Students T-test was conducted to determine statistical significance where * $p < 0.05$, ** < 0.01 , *** $p < 0.001$. The average inter-nuclear distance measurements in each cluster was normalized to the average inter-nuclear distance from all clusters analyzed in the sample. Figure 3.2a shows that Rnd3 has been sufficiently knocked down in cells that were subsequently imaged. Figure 3.2b represents a cross sectional image taken from the central stack and shows that Rnd3 siRNA treated cells cluster closer together forming discrete colonies. Furthermore, the inter-nuclear distances are reduced in Rnd3 siRNA treated cells (Figure 3.2c and 3.2d). This data is consistent with studies that have shown that increased cell clustering in Rnd3 depleted cells is correlated to increased expression of desmosome components and the number of desmosomes.

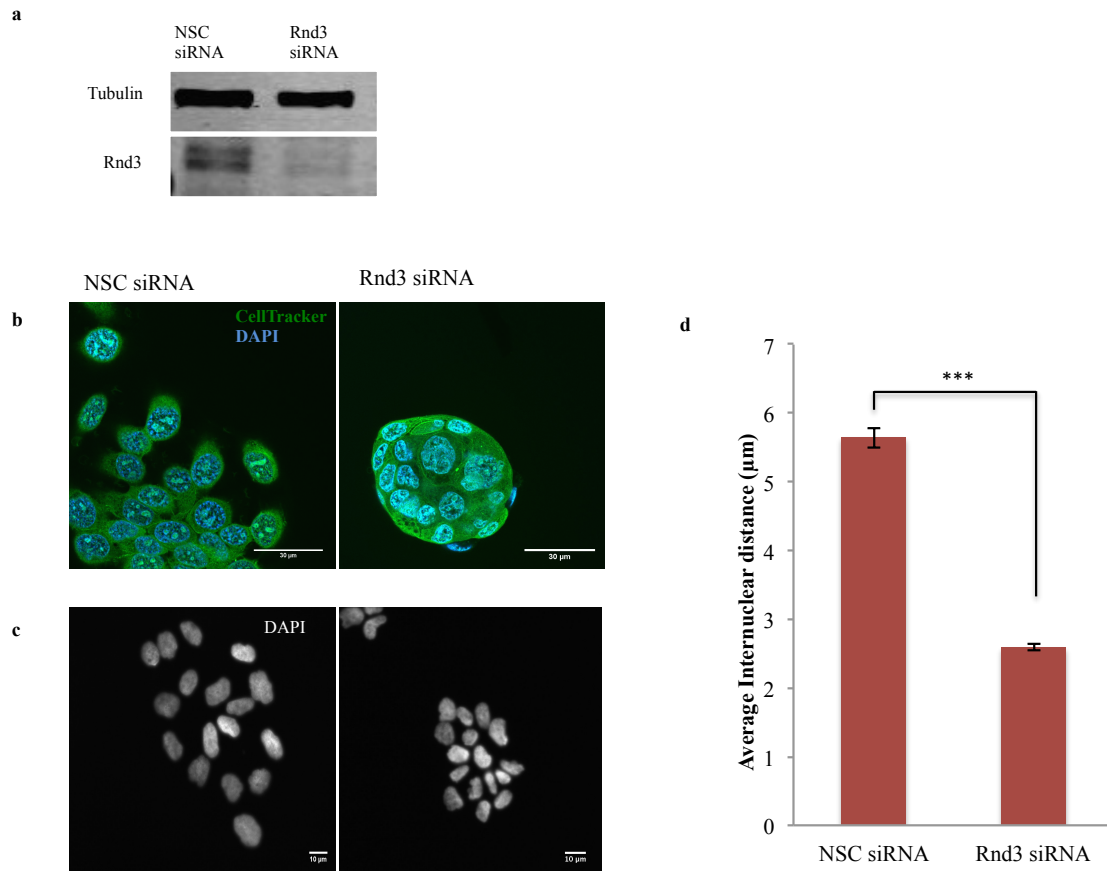


Figure 3.2 Knocking down Rnd3 leads to increased cell clustering and reduced inter-nuclear distance: Rnd3 transfected HaCaTs were seeded and stained with cell tracker and DAPI. Confocal images were taken using a 1nm step size. Figure 3.2a shows that Rnd3 was successfully knocked down in cells that were subsequently used for microscopy. Figure 3.2b represents the central stack from the z-series and shows that Rnd3 depleted HaCaTs form discrete tightly packed cell clusters. To quantify this clustering, inter nuclear distances were taken from DAPI stained nuclei (Figure 3.2c). ImageJ was used to measure the distance between each nuclei and its closest neighbour. The data was normalised to the average internuclear distance for each sample analysed (Figure 3.2d). A Students T-test was conducted to determine statistical significance where * $p < 0.05$, ** < 0.01 , *** $p < 0.001$ (n=3). Error bars represent standard error of the mean.

3.2.2 Knock down of Rnd3 leads to changes in nuclear size

Cell size may distinguish progenitor populations as it has been shown that keratinocytes that are found in holoclones are smaller in size (Barrandon and Green *et al*, 1985). In addition to this, KSC/progenitors isolated from oral epithelia have been shown to be smaller in diameter (Izumi *et al*, 2013). Furthermore, alterations in nuclear and cytoplasmic ratios are thought to be a hallmark for epithelial stem cells from other organs as well as a hallmark for ESCs (Pagliara *et al*, 2014). Figure 3.3a shows that Rnd3 has been sufficiently knocked down in cells, which have been used for subsequent analysis. To determine if Rnd3 depleted cells are smaller in size, nuclear diameter was measured with the assumption that nuclear and cytoplasmic ratios do not tend to differ and therefore can be used as a representation of cell size.

Rnd3 depleted cells were stained with DAPI and were fixed and mounted using Mowial (as described in Methods and Materials). A subset of cells were lysed and subject to immunoblotting to ensure Rnd3 was sufficiently depleted (Figure 3.3a). Images were taken using a Leica SP2 inverted microscope using a 63x objective lens. Z-stacks were taken using 1nm step size and images were taken immediately after mounting. Figure 3.3b shows a cross sectional image of a cluster of Rnd3 depleted cells, it can be seen that Rnd3 depletion leads to a smaller nuclear diameter. Nuclear diameter was quantified by measuring the periphery of each nucleus in a total of five clusters from a total of three independent experiments. A Student's T-test was conducted to determine statistical significance where * $p < 0.05$, ** < 0.01 , *** $p < 0.001$. Figure 3.3c shows that Rnd3 depleted cells have significantly smaller nuclear diameter by ~50%. It is important to note that a cross sectional image may be an inaccurate way in which to analyze nuclear size since nuclei are not always within a fixed position in a sample. This is important here since Rnd3 depleted cells cluster

together and therefore analysis of cross sectional images may be taken from smaller points of the nuclei depending on how they are clustered. Therefore, nuclear and cytoplasmic volume was additionally analyzed. To do this, Rnd3 depleted cells were seeded onto glass coverslips and were stained using CellTracker and DAPI as described in methods and materials, Z-stacks were taken using a 1nm step size and images were reconstructed in Fiji. Nuclear volume was measured by using the 3D object counter plugin in the FIJI imaging analysis software. The software calculates the total volume of voxels from each fluorescent channel in the image. Nuclei are stained blue (DAPI) and the cytoplasm is stained in green (CellTracker). Figure 3.3c shows a representation of a 3D reconstructed image of Rnd3 depleted nuclei. Figure 3.3d shows the quantification of nuclear volume by measuring the number of voxels in the blue channel. Figure 3.3c and 3.3 D shows that the depletion of Rnd3 leads to a reduction in nuclear volume. It is being assumed here that the reduction in nuclear volume reflects a reduction in cell size, therefore it was important that total cell volume was additionally measured. It should be noted that cell border measurements are inaccurate, as they do not take into account the way a cell is positioned during the imaging process. To assess if a reduction in nuclear size reflects a reduction in total cell size, total cell volume measurements were made. The total cell volume was determined by taking the sum of the volume of the blue voxels and the green voxels. Figure 3.4a shows a representation of a 3D reconstructed cluster of nuclei taken from NSC and Rnd3 siRNA treated cells. Figure 3.4b show that Rnd3 leads to a significant change in total cell volume. To ensure that nuclear and cytoplasmic ratios were not altered the ratio of nuclear volume against cytoplasmic volume were taken. Figure 3.4d shows that the Rnd3 siRNA treated cells leads to no significant change in nuclear and cytoplasmic ratio.

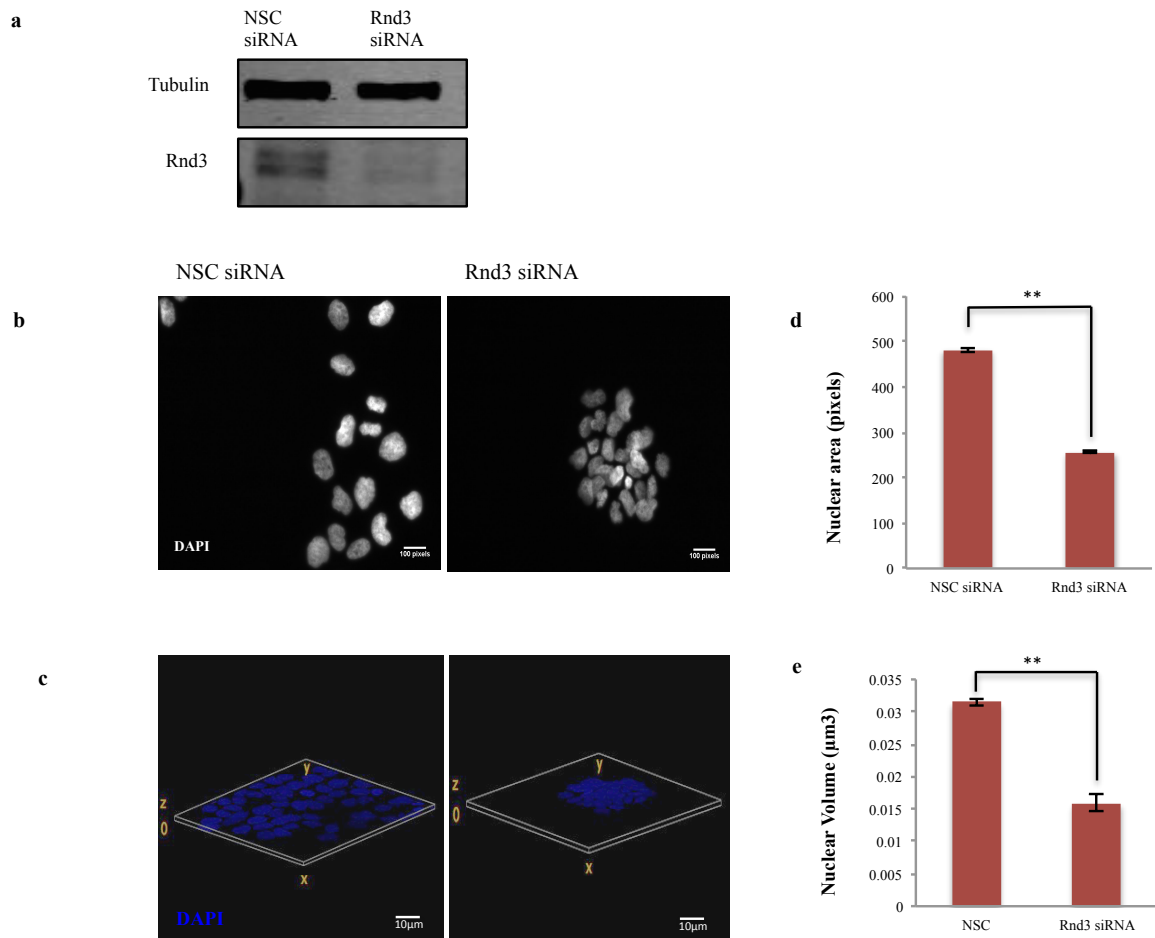


Figure 3.3 Knock down of Rnd3 leads to a reduced nuclear diameter and nuclear volume. Figure 3.3a shows that Rnd3 has been sufficiently knocked down in cells subsequently used for microscopy. To determine nuclear size, cross sectional images were initially analyzed by measuring nuclear area using the measuring tool in ImageJ. Figure 3.3a shows a representation of the images that were analyzed. Figure 3.3b shows that there is a reduction in nuclear area in Rnd3 siRNA cells. To determine nuclear volume, the 3D volume object counter was used to. Figure 3.3c shows a representation of a 3D reconstruction of z-stacks of nuclei taken of Rnd3 siRNA treated cells. Figure 3.3d shows that nuclear volume is reduced in Rnd3 siRNA treated cells. A total of three biological samples were analysed and a students T-test was conducted to determine statistical significance where * $p < 0.05$, ** < 0.01 , *** $p < 0.001$. Error bars represent standard error of the mean.

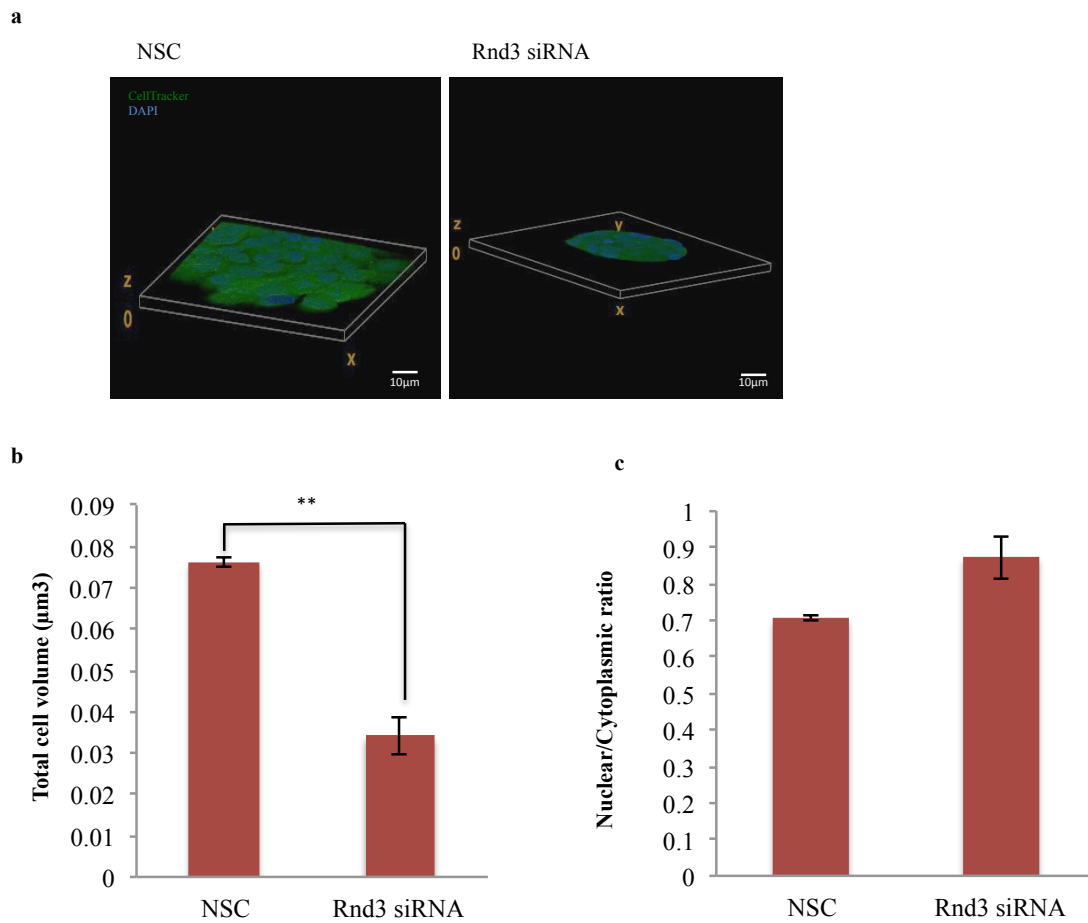


Figure 3.4 Knock down of Rnd3 leads to a reduction in total cell volume and nuclear volume and no change in nuclear/cytoplasmic ratio. To determine total cell volume, the volume of nucleus and cytoplasm was calculated using the 3D volume object counter plugin in FIJI image analysis software. The volume of green voxels (which represent the cytoplasm stained with CellTracker) and blue voxels (represent nuclei stained with DAPI) were added together to determine total cell volume. Figure 3.4a shows a 3D reconstruction of Z stacks taken from NSC and Rnd3 siRNA treated cells. Figure 3.4b shows that the total cell volume of Rnd3 treated cells is reduced suggesting that the cells are smaller. Nuclear and cytoplasmic ratios were calculated by calculating the volume of the nucleus against the volume of the cytoplasm. Figure 3.4c shows that there is no significant change in nuclear and cytoplasmic ratios in Rnd3 siRNA treated cells compared to NSC treated cells. Each experiment was conducted in three separate biological samples. A student's T-test was conducted to determine statistical significance where * $p < 0.05$, ** < 0.01 , *** $p < 0.001$. Error bars represent standard error of the mean.

3.2.3 Knock down of Rnd3 in HaCaTs leads to an increase in cell adhesion to ECM proteins.

Studies have additionally shown that keratinocyte adhesion to ECM proteins may be used to distinguish keratinocyte stem cells (as discussed in section 1.7.3)

To determine if Rnd3 has an effect on extracellular adhesion, cell adhesion assays were performed. Rnd3 siRNA transfected cells were seeded onto fibronectin and collagen pre-coated wells at the indicated concentrations. Cell adhesion was detected by the addition of MTT, which reduces in cells to form a colored salt. This salt can be solubilized using isopropanol. The colorimetric change is thought to correspond to cell uptake of MTT. The absorbance of each well was detected using a plate reader at an absorbance of 570nm. Figure 3.5a shows that Rnd3 has been sufficiently depleted prior to performing cell adhesion assays. Figure 3.5b and Figure 3.5c shows that Rnd3 depleted cells are significantly more adhesive than control cells to fibronectin and collagen respectively. This is in line with studies, which have shown that Rnd3 depleted keratinocytes have increased adhesion to collagen and additionally it can be seen that there is increased adhesion to fibronectin (Liebig *et al* 2012).

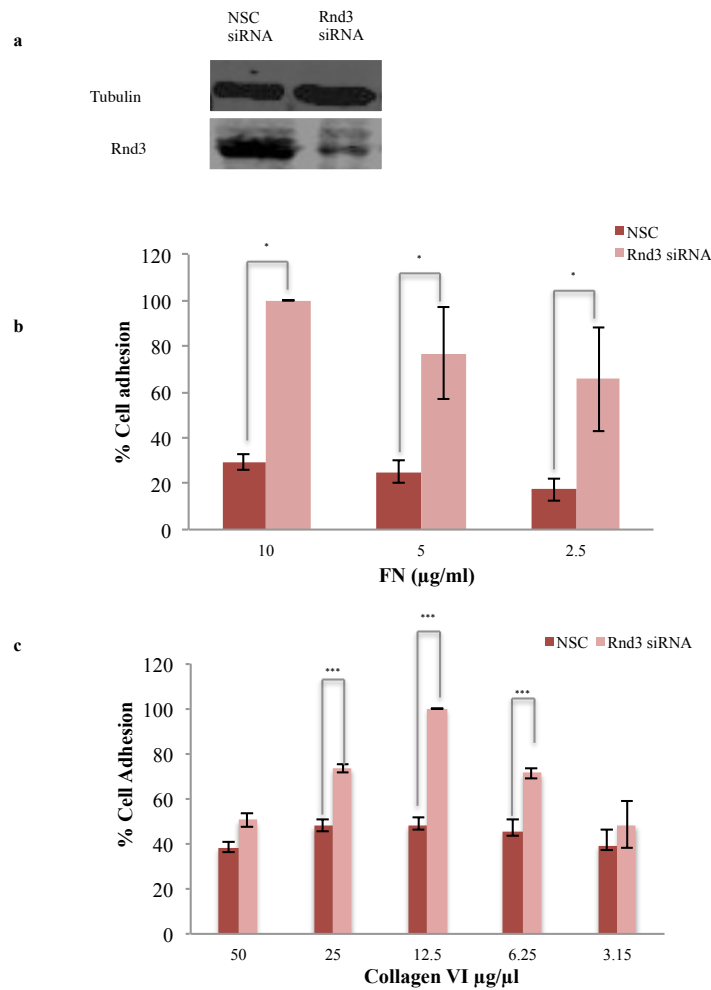


Figure 3.5 Knock down of Rnd3 leads to increased cell adhesion to ECM proteins. Figure 3.5a shows that Rnd3 was successfully knocked down. To determine if knocking down Rnd3 leads to increased cell adhesion to ECM proteins, HaCaTs treated with Rnd3 siRNA were plated on to fibronectin and collagen coated plates at the indicated concentrations for 3 hours. Cells that did not adhere were washed off and adherent cells were then treated with MTT and colorimetric changes were measured. The absorbance for each concentration was calculated relative to the maximum absorbance measured. This was calculated as the percentage of cell adhesion. Figure 3.5b shows that Rnd3 depletion results in a significant increase in cell adhesion to fibronectin (FN) at concentrations of 10µg/ml, 5µg/ml and 2.5µg/ml (* p-value <0.05). Figure 3.5c shows that Rnd3 depletion results in a significant increase in cell adhesion to collagenVI at concentrations of 10µg/ml, 5µg/ml and 2.5µg/ml. A students T-test was conducted to determine statistical significance where *p< 0.05, **<0.01, *** p<0.001 (n=5). Error bars represent standard error of the mean.

3.2.4 Knock down of Rnd3 leads to a suppression in differentiation

The differentiation capacity of Rnd3 depleted cells was analyzed to assess if Rnd3 siRNA treated cells has a capacity to initiate a differentiation induced gene expression profile. To do this, Rnd3 siRNA transfected cells were induced to differentiate. Firstly, via confluence driven differentiation and secondly via suspension induced differentiation. Figure 3.6a and Figure 3.6b show that the expression of differentiation markers, involucrin (a protein expressed in terminally differentiating cells) and S100A7 or psoriasin (a component of the epidermal differentiation complex) are reduced by ~ 80% and ~ 60% respectively when Rnd3 siRNA cells are left to reach 100% confluency. Furthermore, it can be seen Rnd3 depleted cells express ~40% more K14 than control cells in the basal state. Suspension induced differentiation was used as an additional method to determine if Rnd3 has an effect on differentiation. Figure 3.7b shows that when transfected cells were suspended in methylcellulose for 24 hours, Rnd3 siRNA treated cells express lower levels of K10. Taken together these data point to a role of Rnd3 in regulating keratinocyte differentiation confirming the data presented by Liebig *et al*, 2012.

3.2.5 Knock down of Rnd3 leads to an increase in p63

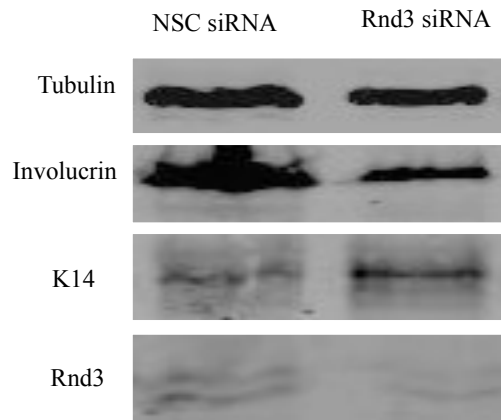
To understand how these phenotypes are being regulated, the expression of proposed stem cell markers was analyzed. p63 is a known regulator of the basal compartment and there is strong evidence that suggests that p63 levels may play a role in regulating keratinocyte progenitor cell fate decisions (see section 1.3.1.5). Therefore, immunoblotting was used to determine the expression of p63. Figure 3.8a and 3.8b

shows that there is an increase in the expression of p63 at the protein level when Rnd3 is depleted.

3.2.6 Knock of Rnd3 does not lead to changes in the expression of LRIG, MCSP and DLL1

Other biochemical markers have been proposed by analyzing the gene expression profile of keratinocytes with reduced expression of integrin expression (discussed in section 1.7.5). Therefore, the expression of putative stem cell markers LRIG, MCSP and DLL1 was assessed using qRT-PCR. Figure 3.9 shows that there is no significant change in the expression of these markers, suggesting that Rnd3 may not be regulating stem-associated transcripts.

a



b

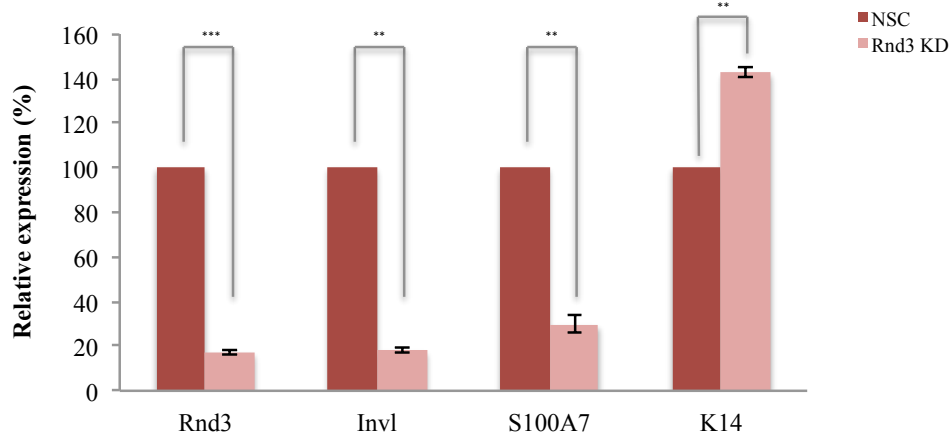
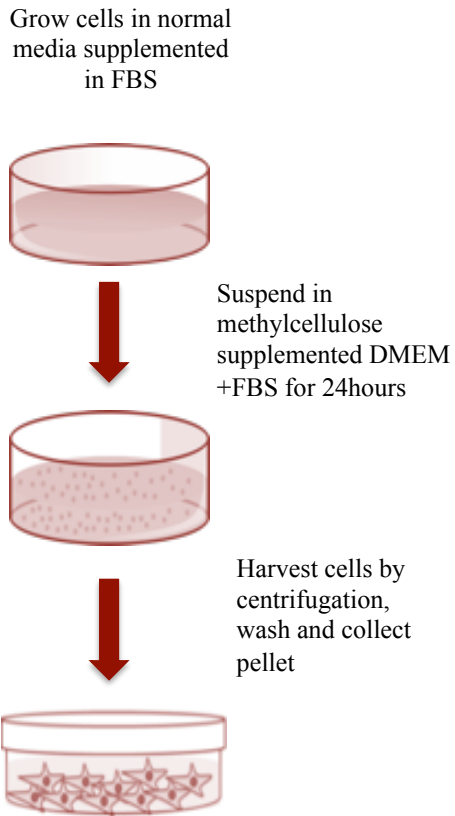
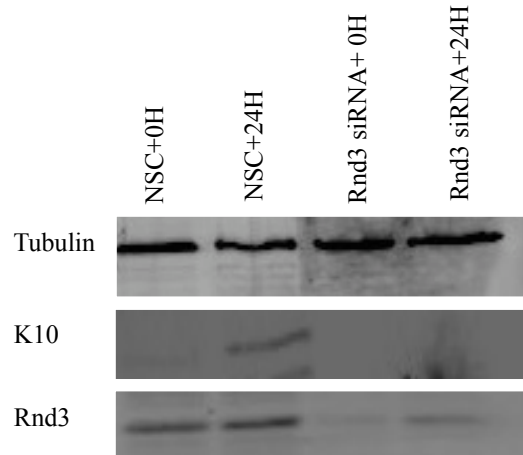


Figure 3.6 Knocking down Rnd3 leads to suppression in confluence-induced differentiation. HaCats treated with Rnd3 siRNA for 48h and were seeded at a high density. Cell lysates were collected and subjected to immunoblotting. Involucrin and K14 were used as markers of differentiation and the progenitor state respectively. Figure 3.6a shows that knocking down Rnd3 leads to suppression in the expression of involucrin and K14 on the protein levels. qRT-PCR was conducted using primers targeted against Rnd3 as well as differentiation markers involucrin and S100A7 and progenitor marker K14. Figure 3.6b shows that knocking down Rnd3 leads to a suppression of S100A7 and involucrin and an increase in the expression of K14 at the transcriptional level during confluence mediated differentiation. A students T-test was conducted to determine statistical significance where * $p < 0.05$, ** $p < 0.01$, *** $p < 0.001$. Error bars represent standard error of the mean.

a**b****Figure 3.7 Knockdown of Rnd3 lead to a suppression of induced differentiation**

HaCaTs treated with siRNA targeted against Rnd3 were suspended for 24hours in normal growth media supplemented with 0.13% methylcellulose for 24 hours (Figure 3.7a). Lysates were collected and were subjected to immunoblotting using antibodies targeted against differentiation marker K10. Figure 3.7b shows that Rnd3 siRNA treated cells have reduced expression of K10 during suspension-induced differentiation (n=3).

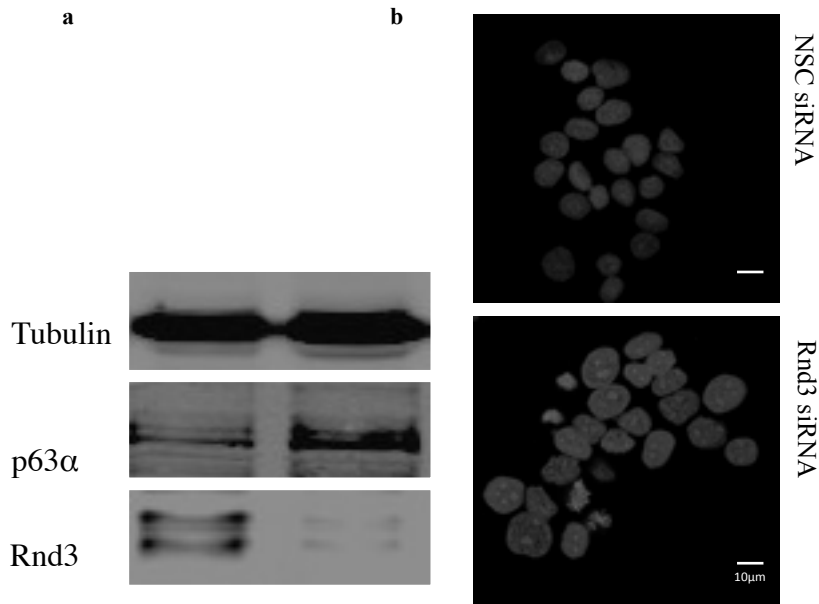


Figure 3.8 Knock down of Rnd3 leads to an increase in the expression of p63.

To determine if Rnd3 has an effect on p63 expression, immunoblotting and immunofluorescence was used using antibodies targeting p63 α . Rnd3 siRNA treated cells were lysed and subject to immunoblotting (Figure 3.8a) and immunostained (Figure 3.8b). Figure 3.8a and b shows that there is an increase in p63 α expression at the protein level. N=5.

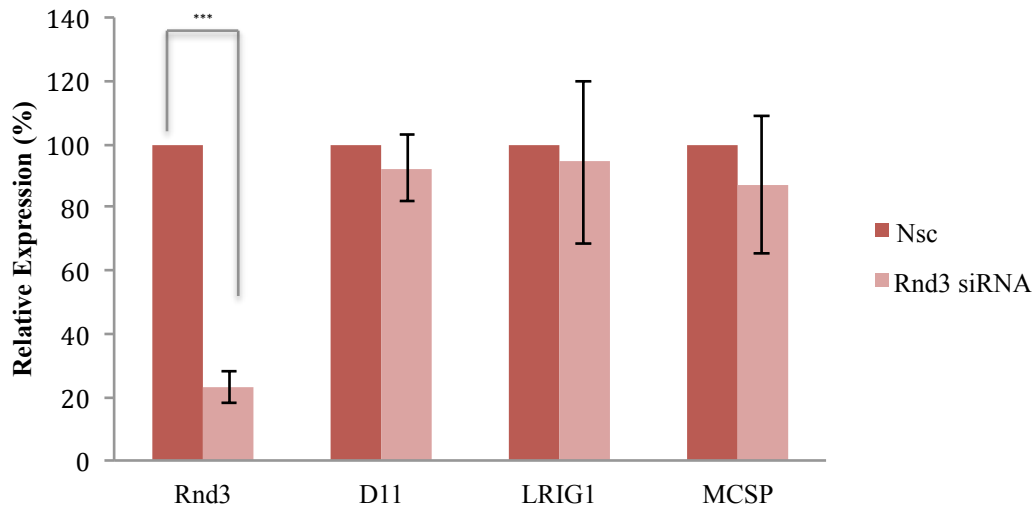


Figure 3.9 Knock down of Rnd3 does not lead to significant changes in the expression of putative stem cell markers Lrig1, MCSP and DLL 1.

To analyze if there was a change in the expression of LRIG, MCSP and DLL1, cDNA synthesized from RNA extracted HaCaTs transfected with Rnd3 siRNA and qRT-PCR was conducted. Figure 9a shows that Rnd3 has been successfully knocked down. Figures 9b, c and d show that there is no significant difference in the expression of these markers. To determine statistical significance a student's T-test was conducted across three separate experiments where * $p < 0.05$, ** $p < 0.01$, *** $p < 0.001$. Error bars represent standard error of the mean.

3.3 Discussion

Distinguishing KSCs from committed progenitors is an obstacle in determining how adult epidermal homeostasis is regulated. Whilst studies in mouse models have become increasingly successful in determining how the skin stem cell compartment is regulated, *in vitro* studies have been hindered since it is thought that KSC *ex vivo* behave differently when away from stringently controlled microenvironments (Fuchs *et al*, 2009). Furthermore, the differences between mouse and human epidermis raises of whether knowledge gained from mouse models can be transferable to the human epidermis. Whilst a single KSC biomolecular signature is highly sought after, stemness can be determined by identifying multiple proposed stem-like characteristics in conjunction with one another.

Previous studies have shown that Rnd3 may have a role in regulating keratinocyte differentiation. Liebig *et al* has shown that an overexpression of Rnd3 leads to an increased population of differentiating keratinocytes, which are less adhesive. Conversely, they have shown that a depletion of Rnd3 leads to a suppression in differentiation and increased cell adhesion to ECM proteins (validated in section 3.2.3).

Here, it can be seen that Rnd3 siRNA treated keratinocytes display multiple progenitor characteristics. These phenotypes include increased colony morphology, cell size, and cell adhesion to ECM substrates and an increase in p63 expression. In addition to this Rnd3 siRNA treated cells have suppressed differentiation. Taken together this suggests that Rnd3 regulates the keratinocyte stem/progenitor compartment.

3.3.1 Rnd3 and Colony morphology

Changes in colony morphology have been seen in stem cell populations in other keratinocyte-enriched organs such as the oral epithelium (Saville *et al*, 2010).

Here, it can be seen that Rnd3 siRNA treated keratinocytes become clustered to form tight colonies. It has been shown previously that Rnd3 depletion leads to an increase in the expression of desmosomal proteins and that an increase in desmosomal protein expression is responsible for increased colony compaction. How Rnd3 may regulate colony compaction and desmosomal protein expression will be discussed further in chapter 4.

3.3.2 Rnd3 and Cell size

Stem cells have been previously shown to be smaller in size (Calenic *et al*, 2010). Furthermore, keratinocyte holoclones (thought to represent KSC) were found to be smaller in size compared to cells that can form paraclones (Barrandon and Green, 1985). The work presented here shows that upon Rnd3 depletion, keratinocytes become smaller.

Interestingly, Liebig *et al* have shown that Rnd3 depletion does not alter cell size according to cell periphery measurements. It can be argued that this is not a true representation of cell size as the area in which a cell occupies is not fixed, and therefore the position of the cell and how it is orientated determines its measurements. Here the volume of the cell was measured as a way to measure cell size more accurately. The total volume of the nucleus and the cytoplasm was determined by taking Z-stacks of cells and reconstructing the image in 3D. This then enabled volumetric measurements to be made. It can be seen here that that nuclear volume is reduced in siRNA treated cells and that this reflects a reduction in total cell volume. Furthermore, the work here shows that no changes in nuclear cytoplasmic ratios were observed. Whilst an increase in nuclear/cytoplasmic ratios is a feature of embryonic

stem cells (ESC), it may be argued that more specialized keratinocytes are more 'mature' and that alterations in nuclear cytoplasmic ratio reflects the maturity of stem cell.

The reduction in stem cell size is thought to reflect the quiescent state of stem cells. Since stem cells are dormant unless they are required to replenish the committed progenitor pool, stem cells are thought to remain in a slow cycling state and therefore are thought to express fewer proteins (Sampath *et al*, 2008).

To further understand if a reduction in cell size reflects a reduction in protein mass, it would be important to assess if protein synthesis has been altered. One way to do this would be to do the sunSET approach to measure protein synthesis. This utilizes puromycin incorporation during protein synthesis and gives insight into the rate of protein synthesis in relation to the abundance of puromycin in newly synthesized proteins. This would therefore give insight into if Rnd3 is regulating protein synthesis on a global level (Goodman *et al*, 2013). Furthermore, polysomal analysis could be used as an additional method to identify if Rnd3 depletion leads to alterations in protein translation (Faye *et al*, 2013).

3.3.3 Rnd3 and cell adhesion to ECM

As mentioned previously KSC are more adhesive on ECM substrates. It has been previously shown that Rnd3 overexpression enriches for a population of less adhesive cells and depletion leads to an increase in a population of cells that bind to ECM substrates (Liebig *et al*, 2012). Here we confirm this and show that an increase in cell adhesion can be seen on both fibronectin and collagen.

Previous studies have shown that Rnd3 depletion does not however lead to an alteration β_1 integrin expression, which is known to bind to fibronectin. It would therefore be interesting to conduct an integrin screen to determine cell surface profile

of integrin expression. This will help aid to understand further how Rnd3 regulates cell adhesion.

3.3.4 Rnd3 and differentiation

Liebig *et al*, who showed that Rnd3 is up regulated in basal keratinocytes during terminal differentiation, have demonstrated the role of Rnd3 during differentiation. Transient over expression of Rnd3 was found to induce cell enlargement (indicative of differentiation) and this was found to correlate to induced stratification in a ROCK-1 independent manner. Furthermore, depletion of Rnd3 was found to increase the pool of undifferentiated basal cells. Here we show that Rnd3 depletion leads to a suppression of confluence and suspension induced differentiation by analyzing the expression of differentiation markers.

This suggests that the expression levels of Rnd3 may be regulating the decision for progenitors to either behave as a stem cell and remain in an undifferentiated state (and express a low level of Rnd3) or to behave as a committed progenitor and go on to differentiate (and express high level of Rnd3). It would be interesting to further see how Rnd3 expression is regulated in response to differentiation signals. This would provide insight on how Rnd3 is differentially regulated and if the mechanisms that regulate its expression can be an additional defining feature for each progenitor population.

3.3.5 Rnd3 and p63 expression:

p63 is a transcription factor and is thought to be crucial in different aspects of keratinocyte function. p63 exists in different isoforms however the $\Delta Np63\alpha$ is the isoform predominantly expressed postnatally (Senoo *et al*, 2007).

p63 is a proposed basal keratinocyte cell marker and is thought to initiate transcriptional events, which regulate KSC behavior such as the proliferative potential

of the stem cell pool (Senoo *et al*, 2007). Therefore, it has been suggested that p63 may be expressed highly in basal keratinocytes and is degraded as cells become more differentiated (Westfall *et al*, 2005).

Here it can be seen that there is an increase in p63 expression in Rnd3 siRNA treated cells (Figure 3.8). To fully understand the importance of how the increase in TP63 regulates the observed phenotype seen in Rnd3 depleted cells it is important to determine how p63 functionally regulates keratinocyte behavior (discussed further in chapter 4). Furthermore, it is important that how Rnd3 regulates p63 expression is understood so to try and establish a functional link between both proteins (discussed further in chapter 6).

3.3.6 Why might Rnd3 be regulating some but not all stem phenotypes?

Rnd3 depleted cells morphologically and biochemically resemble proposed KSC, however it is important to identify if these cells differentially express other putative stem cell markers additionally. Whilst in Rnd3 depleted keratinocytes, p63 expression is increased; conversely the expression of other putative KSC markers is unaltered.

It can be seen that the expression of LRIG, MCSP and DLL1 are unchanged (Figure 3.9). These markers have been identified by using FACS as a means of sorting cells based on the cell surface expression of β_1 integrin (see section 1.3.1.5). Keratinocytes, which have a higher expression of β_1 integrin are thought to represent KSC. Therefore, cell sorting on this basis can help identify the genomic profile of KSC and aid a further understanding of how this population is regulated. LRIG, MCSP and DLL1 were identified as KSC markers in this way. This suggests that these are markers for a KSC population with the assumption that increased β_1 integrin cell surface expression selects for KSC.

Here it can be seen that Rnd3 depleted cells do not share a similar gene expression profile to KSC since Lrig, MCSP1 and DLL1 expression does not appear to be altered following Rnd3 depletion. It is interesting to note that Rnd3 depleted cells do not show altered expression of β_1 expression despite showing a clear increase in cell adhesion (Liebig *et al*, 2009). This could highlight several things. Firstly, it raises the question of if β_1 integrin expression is expressed alongside these markers, could it be that β_1 integrin regulates the expression of these markers and therefore these markers are cooperatively regulated. Secondly it suggests that Rnd3 as previously mentioned shows a clear increase in cell adhesion to the ECM substrates and that there may be a change in the cell surface expression of other adhesion receptors. Taken together this work suggests that Rnd3 depletion may enrich for a population of cells that display stem like characteristics but are distinct in their genomic profiles.

This raises the question of whether the widely accepted models of keratinocyte self-renewal are completely accurate. Since identifying a population of cells that display all the putative features of KSC, it has been proposed that KSC may divide to give rise to two different stem cell populations, one which maintains the stem cell population and is slow cycling remains in a quiescent state and one which has a capacity to rapidly divide to allow for the expansion of committed progenitors in response to events such as wound healing which require 'quicker' self renewal'. Therefore, this suggests that and an 'intermediate' population of KSC may exist. Whilst this is a tempting concept, there is currently very little evidence that suggests that this may occur. Furthermore, there is the added obstacle of trying to identify a new set of criteria that would define each population.

Taken together, it is clear that Rnd3 depletion at the very least enriches for a population of very early progenitor keratinocytes. However, since these phenotypes

are so striking in terms of morphology and behavior it is important that how Rnd3 regulates keratinocyte behavior on global level is further understood (Discussed in chapter 7)

Chapter 4

The role of increased P63 expression in cell clustering and desmoplakin expression

4.1 Introduction

The epidermis is held together via strong mechanical adhesion that is established through an extensive transcellular network composed of anchoring junctions such as adherens junctions and desmosomes (Brandner *et al*, 2010). Anchoring junctions interact directly with the cytoskeleton, which means these junctions can impart strong intracellular adhesion at sites of mechanical stress (Brandner *et al*, 2010).

Desmosomes are architectural junctions that make contact to the intermediate filament cytoskeleton. They comprise of multiple components that act together to ensure that sufficient cell-cell adhesion is maintained. Desmoplakin links desmosomes directly to the intermediate filament network and is thought to be a major factor in strengthening cell-cell contact. This ensures that the epidermis is highly strengthened and resilient to external mechanical forces.

$\Delta Np63\alpha$ been shown to be involved in regulating cell-cell adhesion via the regulation of desmosome protein expression (Ferone *et al*, 2013). Studies using P63 knockout mice have shown that a depletion of p63 leads to a reduction in the expression of desmoplakin. In addition to this the study shows that the desmoplakin promoter has enriched TP63 binding sites. Furthermore, in disease states such as ankyloblepharon, ectodermal defects, cleft lip/palate (AEC) syndrome associated skin fragility both desmoplakin p63 expression is reduced and it is thought that this may result in poor skin development that is associated with the disease.

In chapter 3 it can be seen that depletion of Rnd3 leads to an increase in colony compaction, a phenotype previously observed by Ryan *et al.* The work conducted by Ryan *et al* have additionally shown that depletion of Rnd3 leads to an increase in desmosome proteins such as desmoplakin. The work presented here aims to identify if the increase in desmoplakin expression (and subsequent increase in colony compaction) at the cell borders of Rnd3 depleted cells is associated with the increase in p63 expression observed in chapter 3.

4.2 Results

4.2.1 Knock down of Rnd3 leads to an increase in the expression of desmoplakin.

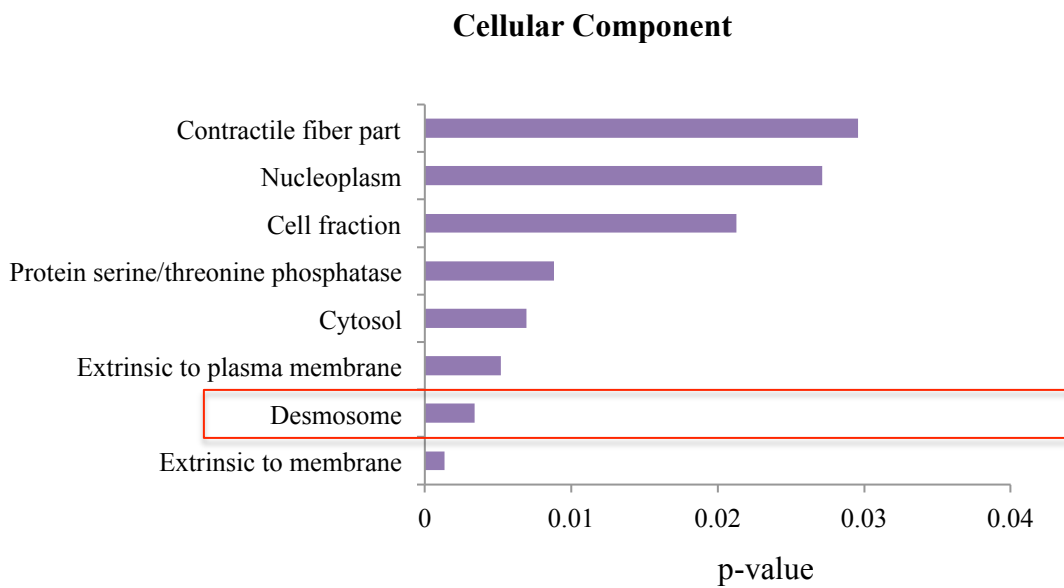
P63 has been shown to have an extensive transcriptional network which is thought to regulate many aspects of keratinocyte function. A study conducted by Pozzi *et al*, utilized ‘chip on chip’ to identify novel p63 binding sites in HaCaTs. In addition to this, the group conducted RNA sequencing in p63 overexpressing cells to determine if there was a change in the expression of transcripts that have predicted p63 binding sites. Here, data from this study was reanalyzed using Gene Ontology enrichment to identify desmosome proteins that are directly regulated by p63.

Gene ontology (GO) enrichment is a method, which enables a large gene list to be grouped according to a set of, predefined gene ontology terms. Each gene is grouped according to how functionally related it is to a given GO term. In this way, GO terms of interest can be sought after and genes that fall into that group can be further analyzed. Furthermore, GO terms can be further grouped according to their respective ‘molecular function’, ‘biological process’ and cellular components. This means that large gene lists can be functionally grouped. DAVID is an online bioinformatics tool which functions to annotate a group of submitted gene lists according to common

gene ontology terms (Huang *et al*, 2008). Here, DAVID, was used to functionally annotate ChIPseq data procured from Pozzi *et al* to identify p63 regulated genes that may regulate some of the phenotypes observed in chapter 3. Figure 4.1 shows the top ten enriched ($p=0.01$) GO terms annotated according to the cellular component that each gene falls into. Interestingly, the GO term ‘desmosomes’ was shown to significantly enriched ($p= 0.00342$). The list of p63 regulated genes that were enriched is shown in table 4.1.

It has been previously shown in that Rnd3 depletion leads to an increase in both colony compaction (confirmed in chapter 3) and an increase in desmosome expression (Ryan *et al*, 2012). To confirm this, desmoplakin expression in Rnd3 depleted cells was analyzed. Rnd3 depleted cells were seeded onto glass coverslips, fixed and stained with the desmoplakin antibody, 115F. These were subject to immunofluorescence using the Leica SP2 inverted confocal microscope. Here, it can be seen that Rnd3 transfected HaCaTs have increased expression of desmoplakin at the cell borders (Figure 4.2a). Furthermore, Rnd3 depleted cells were lysed and were subject to immunoblotting using the 115F antibody. Figure 4.2b shows that depletion of Rnd3 leads to increased expression of desmoplakin at the protein level. To determine if increased protein levels is reflected at the transcript level, qRTPCR was used to determine the relative expression of the desmoplakin transcript (Figure 4.3). Figure 4.3 shows that Rnd3 depletion leads to an increase in desmoplakin at the transcript level. Each experiment was conducted in a total of three independent samples. A students T-test was conducted to determine statistical significance where $*p < 0.05$, $** < 0.01$, $*** p < 0.001$.

Another protein regulated by p63 is PERP. PERP is a tetraspanin protein and is known to be transcriptionally regulated by p63 (Ihrie and Attardi, 2005). Knock-out studies in mice have shown that Perp associates with desmosomes and regulates desmosomal assembly and adhesion (Ihrie *et al*, 2005). Here, immunoblotting was used to determine if Rnd3 depletion leads to altered levels of PERP expression (Figure 4.4). It can be seen that Rnd3 depletion has no effect on PERP expression.



Term	P-Value	Genes
Desmosome	0.00342	B4GALT1, EVPL, PPL, PKP3, DSC3, DSP, PERP

Figure 4.1. TP63 transcriptionally regulates multiple desmosome proteins.

Chipseq dataset from pozzi *et al*, 2010 was reanalyzed using DAVID. Enriched GO terms were selected based on p-value. It can be seen that multiple desmosomal proteins are regulated by p63.

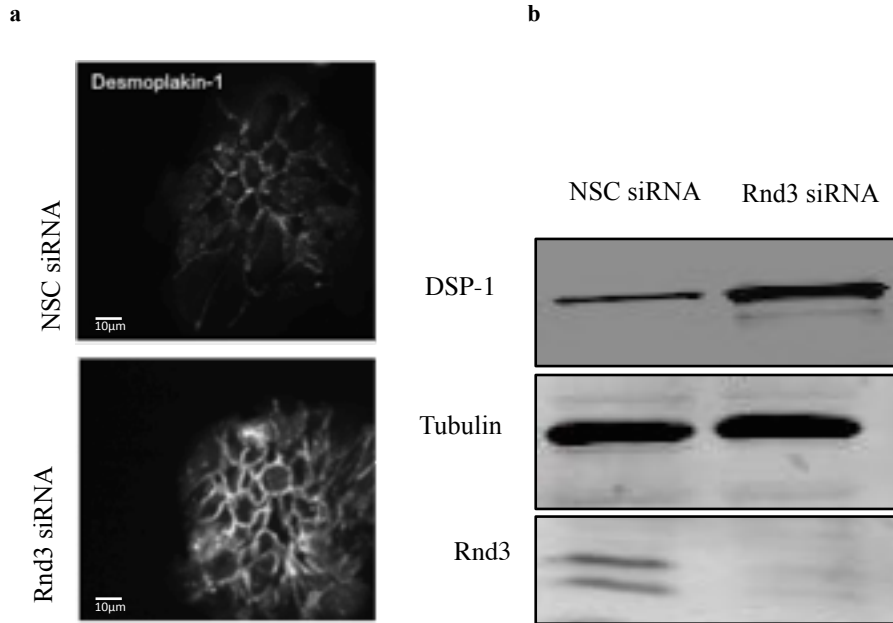


Figure 4.2 Rnd3 depletion leads to the increase of desmoplakin

To determine the expression levels of desmoplakin in Rnd3 knock down cells, immunofluorescence and immunoblotting was conducted using an antibody targeted against desmoplakin. Figure 4.2a and b show that knock down of Rnd3 leads to an increase in desmoplakin at the protein level

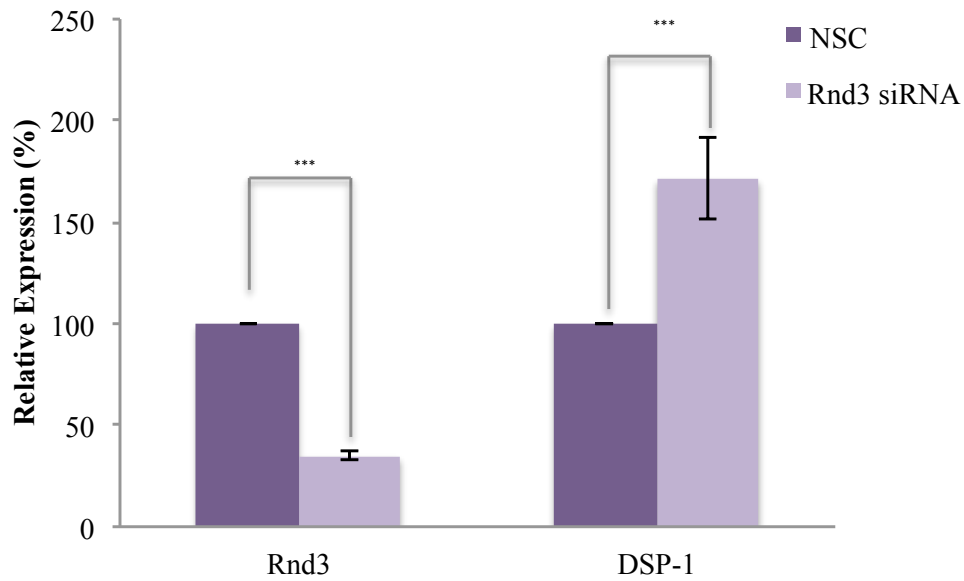


Figure 4.3 Rnd3 depletion leads to an increase in desmoplakin transcript

To determine if Rnd3 depletion leads to an increase in desmoplakin transcript, qRT-PCR was conducted using cDNA from Rnd3 depleted HaCaTs. Figure 4.3 shows that there is an approximately 90% increase in desmoplakin expression following Rnd3 depletion. Each experiment was conducted in three individual experiments were conducted and a student's T-test was conducted to determine statistical significance where * $p < 0.05$, ** < 0.01 , *** $p < 0.001$. Error bars represent standard error of the mean. (n=3)

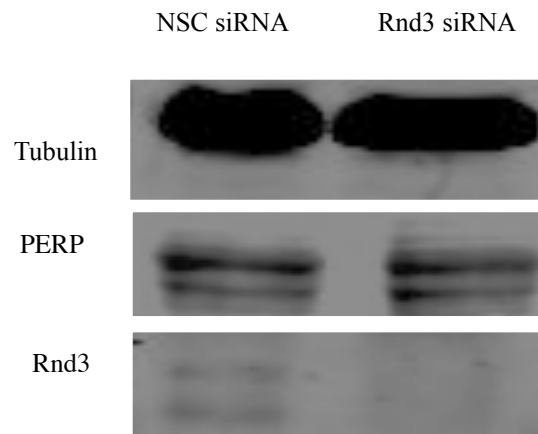


Figure 4.4 Knock down of Rnd3 does not lead to a change in Perp expression

To determine the expression levels of PERP in Rnd3 knock down cells, immunoblotting was conducted using an antibody targeted against desmoplakin. Figure 4.4 shows that there no observable increase in PERP expression following Rnd3 depletion (n=5).

4.2.2 Rnd3 and P63 double knockdowns restore colony morphology.

Desmoplakin has been shown to transcriptionally regulated by p63 (Pozzi *et al*, 2012, Ferone *et al*, 2013). To determine if the increase in colony compaction (shown in chapter 3 and by Ryan *et al*) is dependent on the observed increase in p63 expression in Rnd3 depleted cells (Figure 3.8), Rnd3 and p63 double knock downs were conducted. HaCaTs were initially transfected with both Rnd3 and p63 oligos for 48 hours before subsequent analysis. Figure 4.5a shows that at the protein level, p63 is not sufficiently depleted in double knockdowns. This suggests that the transfection with both siRNA oligos at the same time is not an appropriate way to ensure that both transcripts are sufficiently knocked down. Using qRTPCR it can be seen that p63 expression is approximately 40% depleted when both oligos are transfected at the same time (Figure 4.5c), despite Rnd3 depletion being significant in both single and double knockdowns (Figure 4.5b). To ensure both proteins are sufficiently depleted, a sequential knock down was conducted, where p63 was first transfected into HaCaTs for 24 hours before being re-transfected with Rnd3 siRNA for a further 48 hours. This ensured that both proteins were sufficiently knocked down in double knock down samples. This was validated at the protein level using western blotting (Figure 4.6). Note, for all subsequent analysis the efficiency of knockdowns were tested using western blotting and only those that showed a significant depletion were used.

To then determine if the observed increase in colony compaction seen in chapter 3 is due to the increase p63 expression in Rnd3 depleted cells immunofluorescence was used to analyze colony morphology. HaCaTs were transfected sequentially with p63 and Rnd3 oligos, and were seeded onto glass coverslips. Coverslips were stained with CellTracker Green and DAPI and were mounted using Mowial. Images were taken using Leica SP2 inverted confocal microscope. It can be seen that the double knock

down of both Rnd3 and p63 leads to an alteration in colony morphology when compared to Rnd3 single knockdown cells (Figure 4.7a). This was quantified by measuring the internuclear distance (Figure 4.7b and c). It can be seen that knocking down Rnd3 alone leads to a reduced inter nuclear distance (as seen in chapter 3) and p63 alone leads to no significant changes in inter nuclear distance compared to the NSC control. Furthermore, knock down of both transcripts leads to a rescue in colony morphology since no significant difference in internuclear distance between double knockdown cells and NSC can be seen.

Inter-nuclear distances were measured in 3 cell clusters from a total of 3 independent biological repeat. 2-way ANOVA was conducted to assess statistical significance where: ns $P > 0.05$, * $p < 0.05$, ** < 0.01 , *** $p < 0.001$.

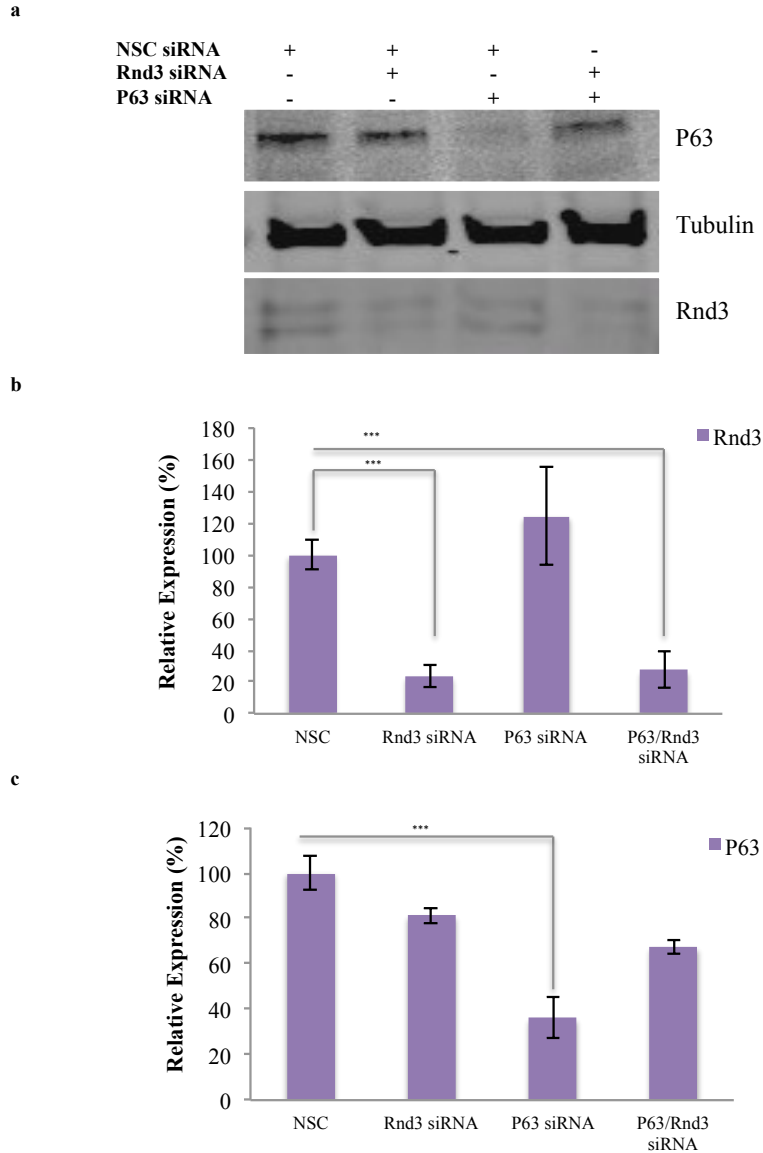


Figure 4.5 Knocking down Rnd3 and p63 at the same time does not lead to sufficient knock down of both transcripts. To determine knock down efficiency when transfecting with both oligos at the same time, western blotting (Figure 4.5a) and qRT-PCR was used (Figure 4.5b and 4.5c). Transfections were conducted by treating cells with Rnd3 and p63 oligos at the same time. Lysates and cDNA were generated 48 hours after transfection. Whilst Rnd3 remains sufficiently knocked down in the double knockdown cells (Figure 4.5b), p63 expression is only 40% depleted in double knockdown cells (Figure 4.5c), therefore double knockdowns conducted in this way are not suitable. A student's T-test was used to determine statistical significance where: ns $P > 0.05$, * $p < 0.05$, ** $p < 0.01$, *** $p < 0.001$. Error bars represent standard error of the mean. (n=3).

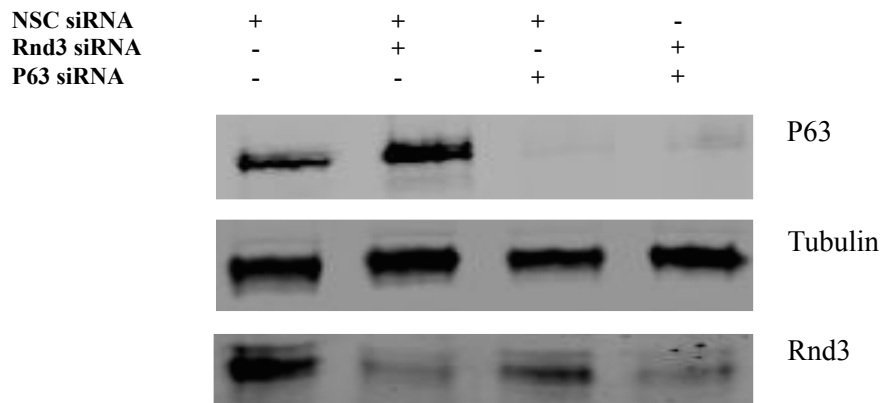


Figure 4.6 Knock down of both Rnd3 and p63 is efficient when oligos are transfected sequentially.

To optimize the efficiency of the double knock down (ensuring that both oligos are depleted sufficiently) Oligos were transfected 24 hours apart. Here, p63 siRNA was transfected in first and the same cells were then transfected with Rnd3 siRNA 24 hours later. Double transfected cells were then allowed to grown for a further 48 hours before immunoblotting was conducted. Figure 4.6 shows that knocking down p63 for 24 hours prior to re-transfecting Rnd3 was sufficient in knocking down p63 at the protein level (n=3).

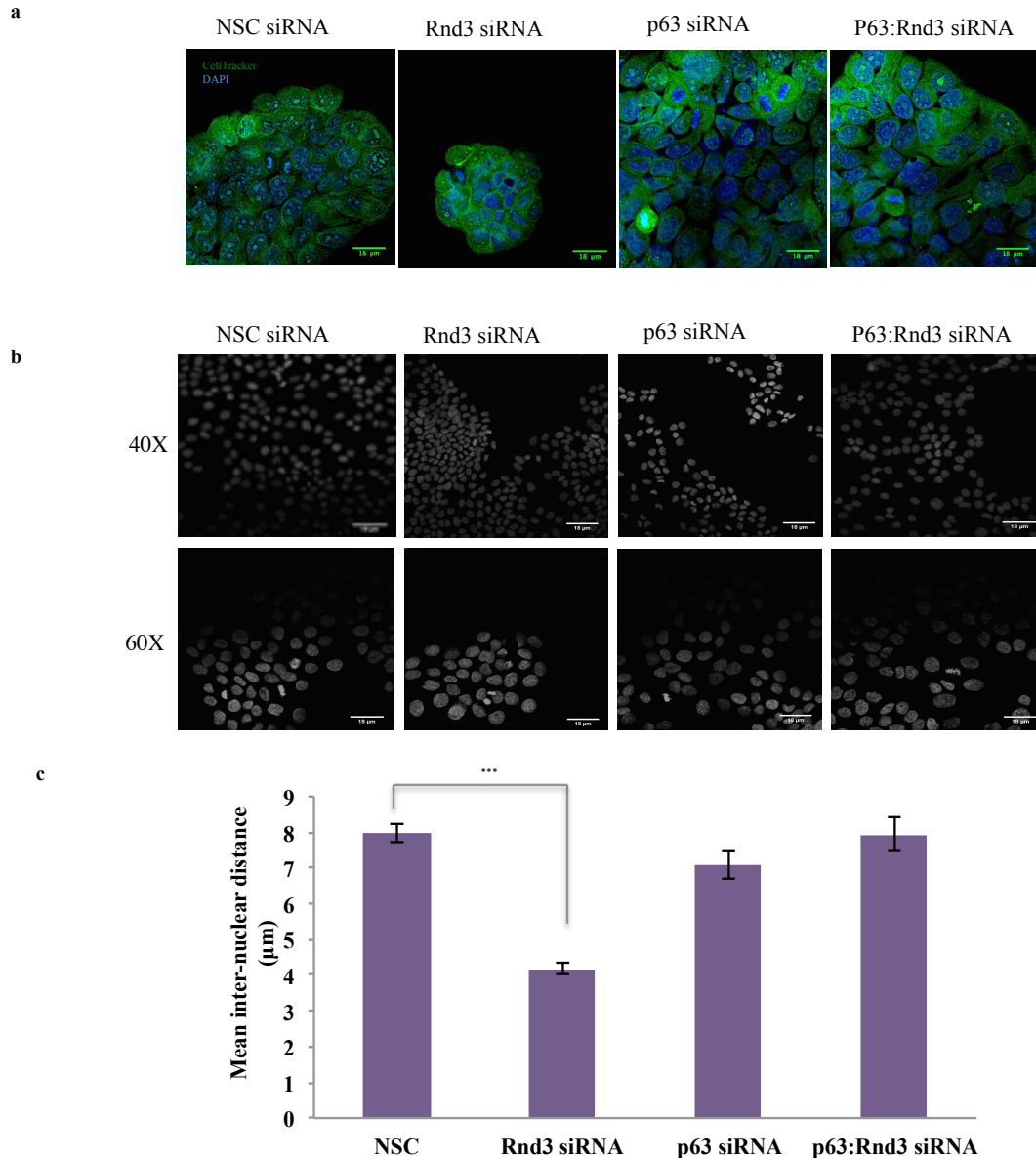


Figure 4.7. Knock down of Rnd3 and p63 leads to a restoration of colony compaction. Rnd3 and p63 oligos were transfected sequentially to determine if Rnd3 mediated colony compaction is dependent on the increased expression of p63. Briefly, cells were transfected with both Rnd3 and p63 siRNA and were subject to staining. Colony compaction was measured using internuclear distances (as described in chapter 3) Figure 4.7a shows that cells appear to be less clustered when both Rnd3 and p63 are knocked down. Figure 4.7b and c show that internuclear distances are restored in the double knock downs. Each experiment was conducted in three individual experiments were conducted and a 2 way ANOVA was used to determine statistical significance where: ns $P > 0.05$, * $p < 0.05$, ** < 0.01 , *** $p < 0.001$ Error bars represent standard error of the mean.

4.2.3 Rnd3 and p63 double knockdowns restores desmoplakin expression

To determine if the restoration of colony morphology in Rnd3 and p63 depleted cells was dependent on altered desmosomal protein expression, immunofluorescence and immunoblotting was conducted to determine desmoplakin protein expression (Figure 4.8a and 4.8b). HaCaTs were transfected using Rnd3 and p63 oligos, and were seeded onto glass coverslips, Coverslips were immunostained using 115F desmoplakin antibody. These were imaged using Leica SP2 inverted confocal microscope. Figure 4.8a shows that there is an increase in desmoplakin expression at cell borders in Rnd3 depleted cells (consistent with figure 4.1) however there is little change in the expression in the double knock down cells compared to NSC treated cells. Furthermore, immunoblotting using lysates from Rnd3 and p63 double knockdowns shows that double knock down restores desmoplakin expression.

This, therefore suggests that the change in colony morphology is dependent on the increase in p63 expression and the subsequent increase in DSP.

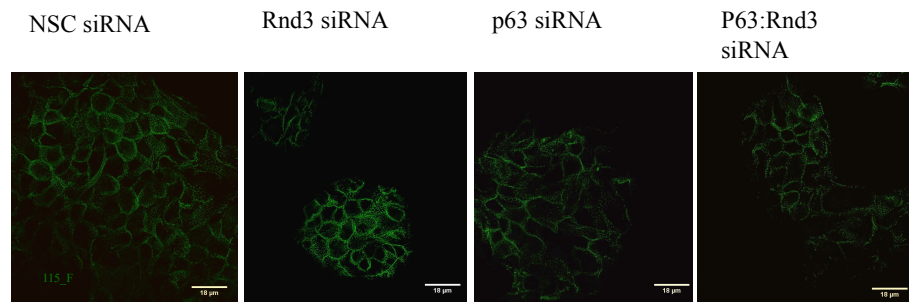
4.2.4 Knock down does not change the expression of other p63 targets

Since it can be seen that knocking down both Rnd3 and p63 leads to rescued colony morphology and desmoplakin expression, it would be interesting to see if Rnd3 has an effect firstly on the expression of any other p63 targets. To identify if p63 targets that may be related to the observed phenotypes in Rnd3 depleted cells, data from Pozzi *et al* was analyzed using Gene ontology enrichment. Genes were grouped according to their biological process (Figure 4.9). It can be seen from this that p63 regulated genes that are involved in many of the phenotypes observed in Rnd3 depleted keratinocytes shown in chapter 3 including ‘keratinocyte differentiation’, ‘cell adhesion’, ‘apoptosis’ and ‘cell size’. To further

understand how p63 may regulate these processes, genes from each GO term were investigated and those that may be involved in regulating different aspects of Rnd3 regulated phenotypes were sought after. Table 4.2 shows genes that may be involved in regulating keratinocyte behavior.

Primers targeting the transcripts of these genes were designed and cDNA from Rnd3 depleted cells were subject to qRT-PCR. Figure 4.10 shows that there is no observable change in the expression of known p63 targets. However, each experiment was conducted in two biological replicates and therefore the significance of these changes cannot be assessed without conducting a third repeat. This suggests that the increase in p63 may not have an effect on all of its known targets. This is not surprising since it is well known that an increase in a transcription factor does not necessarily mean that there is an increase in transcription. It would be interesting to see however if in Rnd3 depleted cells if there is p63 binding to new targets, which could be related back to the observed Rnd3, knock down phenotypes as seen in Chapter 3.

a



b

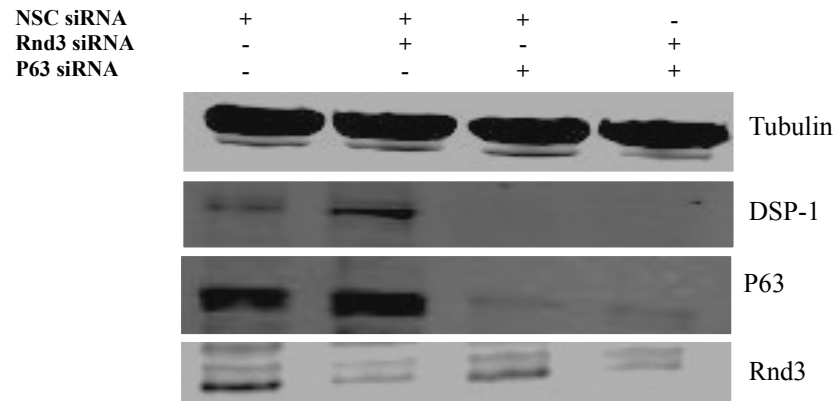


Figure 4.8 Knock down of both Rnd3 and P63 leads to reduced desmoplakin expression. P63 and Rnd3 were knocked down sequentially as described section 4.4.2. Figure 4.8a shows that desmoplakin expression is restored at cell-cell junctions in Rnd3 and p63 siRNA treated cells. Figure 4.8b shows that there is an increase in desmoplakin expression in Rnd3 depleted cells but little change in desmoplakin expression when both Rnd3 and p63 are knocked down. Each experiment was conducted a total of three times and the efficiency of each transfection was determined to ensure knockdowns were successful.

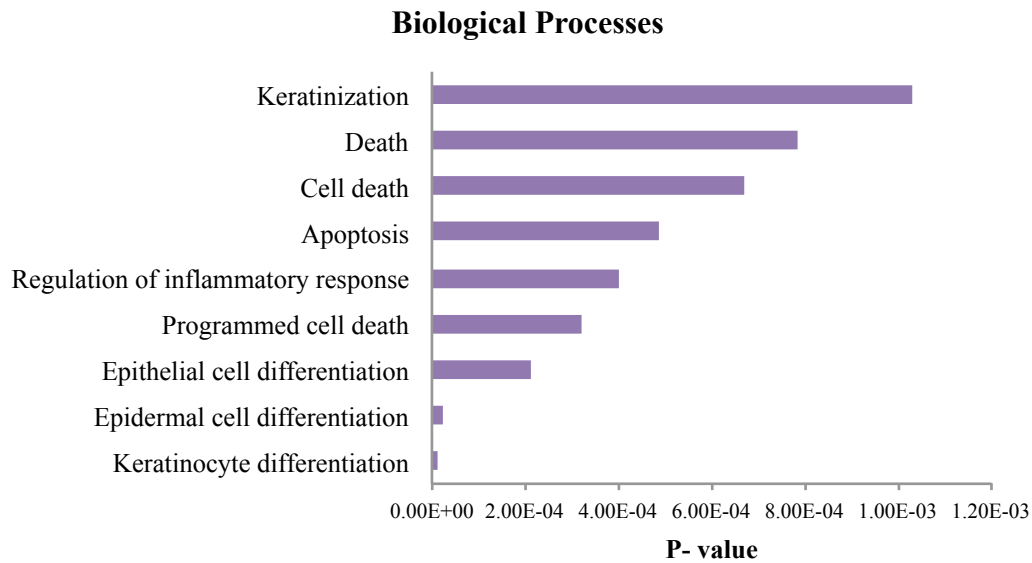


Figure 4.9 Enriched GO terms using p63 chipseq data. Chipseq dataset from Pozzi *et al*, 2010 was reanalyzed using DAVID. Genes were functionally annotated depending on their biological process.

Gene Name	Protein Name	Biological process
LEF-1	Leukocyte enhancing factor-1.	Cell size
TGFβ1T1	Transforming growth factor beta 1 induced transcript 1	Keratinocyte differentiation
PARD	Peroxiome proliferator-activated receptor delta	Programmed cell death
SMAD7	SMAD family member 7	Keratinocyte differentiation

Table 4.2: List of genes taken from multiple biological processes.

Genes were selected based on the biological process in which they may play a role in other phenotypes observed in Rnd3 depleted cells as described in Chapter 3.

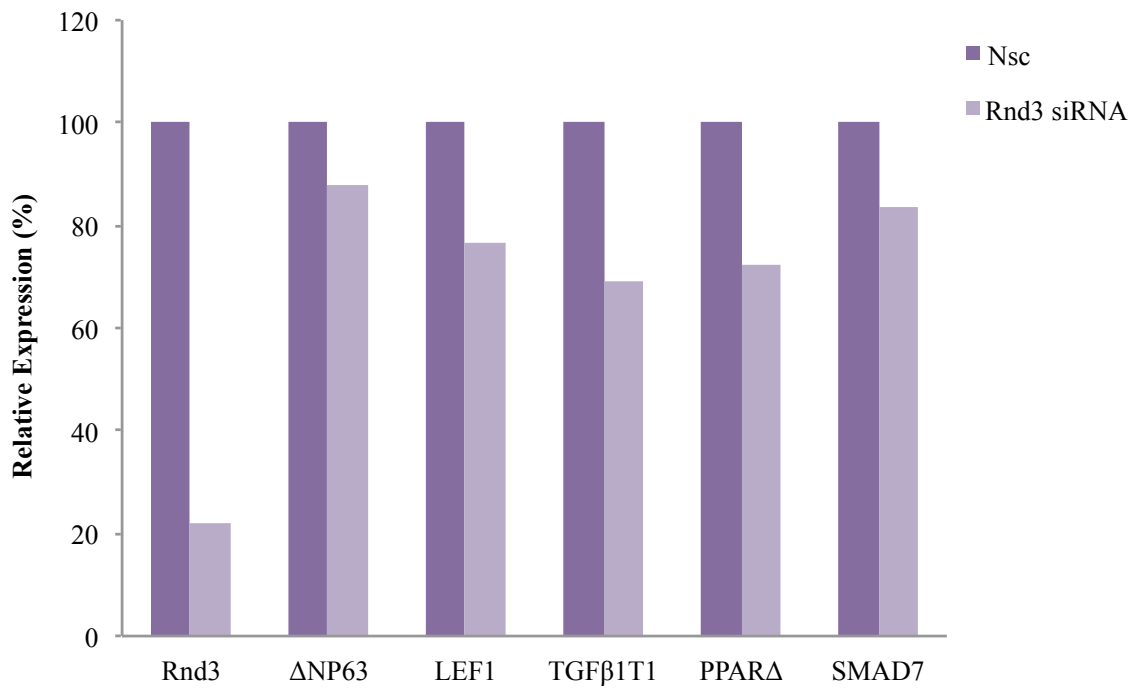


Figure 4.10 Knock down in Rnd3 doesn't appear to alter the expression of other p63 targets. Rnd3 depleted cells were subject to qRTPCR to determine the expression of other p63 targets identified from Pozzi *et al* data set. It can be seen that Rnd3 has little effect on the expression of these proteins. N=2

4.3 Discussion

The identification of p63 target genes is important towards understanding how epidermal homeostasis is regulated since p63 is often described as ‘master regulator of epidermal homeostasis’. Currently RNAi, gene profiling and ChIP on chip experiments have been routinely used to identify TP63 target genes (Kouwenhoven *et al*, 2010 and reviewed in Vigano and Motovani *et al*, 2007). These genes are associated with various cellular processes including regulators of apoptosis, development, cell cycle and cell adhesion (reviewed in Vigano and Motovani, 2007)

The work presented here suggests that the striking phenotypes observed in Chapter 3 may be regulated by the increase in p63 expression observed in Rnd3 depleted cells.

4.3.1 Rnd3 regulates colony morphology and desmoplakin expression in a p63 dependent manner

The work presented here shows that knocking down both Rnd3 leads to an increase in colony compaction and desmoplakin expression. Furthermore, knockdown of both Rnd3 and p63 restores colony compaction and desmoplakin expression. Interestingly it has been shown that desmoplakin is transcriptionally regulated by p63. Studies using ChIPseq have shown that the desmoplakin gene has conserved p63 regulatory sites as well as showing that p63 knock out leads to a reduction in the expression of desmoplakin and this is thought to be associated with skin fragility (Ferone *et al*, 2013). In this study, it was additionally shown that p63 regulates the expression of other desmosomal components such as desmoglein 1 and 3. Therefore it would be interesting to see if Rnd3 depleted cells alter the expression of these and if the expression of these components can be restored in a double knock down system.

Additionally, it has been previously shown that Rnd3 additionally regulates desmosome number. This suggests that Rnd3 may be regulating desmosomal

assembly at cell-cell junctions. P63 has been shown to transcriptionally regulate the desmosomal protein Perp (Ihrie *et al*, 2005). Perp is a tetraspanin protein and a known downstream target of p63 (Ihrie and Attardi, 2005). Knock-out studies in the murine model have shown that Perp associates with desmosomes and regulates desmosomal assembly and adhesion (Ihrie *et al*, 2005). Therefore, Perp has been associated with regulating stratification during development via the transcriptional activity of the TAp63 isoform (Beaudery *et al*, 2010, Ihrie *et al*, 2005). Here, it can be seen that there is no change in the expression of Perp in Rnd3 siRNA transfected cells. This is not a surprising result since, as mentioned previously the $\Delta Np63\alpha$ is the isoform is predominantly expressed after birth, and secondly because the function of Perp as a regulator of desmosomal adhesion postnatally is obscure. Taken together this suggests that Rnd3 could be specifically regulating the transcriptional activity of the $\Delta Np63\alpha$ isoform.

Interestingly, the expression of desmosome proteins is upregulated during terminal differentiation (Wan *et al*, 2007). Here, it can be seen that Rnd3 depletion leads to increased desmoplakin expression, however also show that there is an increase in p63 expression, as well other stem like markers. It has been demonstrated that $\Delta Np63\alpha$ is restricted to the basal layer and is essential for stem cell maintenance (Yang *et al*, 1998). Therefore, one could ask, how can Rnd3 depletion lead to an enrichment of stem/progenitor cells, but also show an increase in desmosome protein expression, even though differentiation is suppressed? Since most studies determining desmosomal protein expression are conducted in vivo, one explanation is that perhaps the number of desmosomes in the basal layer in vivo is correlated to the naturally low numbers of stem cells. Since stem cells are known to reside in small clusters in the basal layer (Jones *et al*, 1995), perhaps desmosome adhesion is additionally

upregulated so to maintain the integrity of these clusters. In addition to this perhaps in vitro studies, disturb the desmosome protein expression, since cell culturing techniques alter cell-cell adhesion and therefore the expression of desmosomal components are not truly represented.

Furthermore, it would be interesting to identify which desmosomal proteins are regulated by Rnd3 and how many of these are additionally regulated by p63. This would give insight into determining a functional link between Rnd3 and p63 and would allow for further understanding of how desmosomes are regulated in epidermal homeostasis. In addition to this, would interesting to identify if a functional link can be made between Rnd3 and epidermal disorders such as AEC. Perhaps Rnd3 expression may be altered in these disease states and may have a functional impact on p63 regulated transcription.

4.3.2 Depletion of Rnd3 does not alter the expression of other p63 targets:

Whilst it was interesting to see that in the double knockdowns colony compaction and desmoplakin expression can be restored, it is important to understand how an increase in p63 following Rnd3 depletion can have an effect on other known p63 regulated pathways. Here, it can be seen that increased expression of p63 has little effect on the expression known p63 targets such as LEF1, TGF β 1T1 and PPAR Δ and SMAD7.

This is not uncommon since an increase in transcription factor does not necessarily mean an increase in transcription, however it does raise the question of why Rnd3 depletion leads to an increase in some p63 targets (desmoplakin) and not others. This suggests that perhaps the expression of these may be regulated by transcriptional co factors that interact with p63. Perhaps Rnd3 regulates the expression or the organization of transcriptional co factors which regulates p63 transcription of specific targets

In addition to this since p63 has been shown to regulate multiple processes including cell-ECM adhesion, apoptosis and cell size (reviewed in Truong and Khavari *et al*, 2007). Therefore, it can be speculated that perhaps the other phenotypes described in chapter 3 may be regulated by p63 expression. Therefore, it would be interesting to reanalyze some of these phenotypes in a double knock down system (Discussed further in chapter 7).

Chapter 5

The identification of novel Rnd3 regulated proteins using SILAC.

5.1 Introduction

In previous chapters it has been shown that Rnd3 regulates multiple 'stem like' phenotypes. Whilst these phenotypes are interesting in their own right, little information is currently available on how Rnd3 may be regulating these phenotypes.

Currently, an 'omics' approach is routinely used to determine the biological composite of test samples on a global scale. In this way, determining key players involved in the regulation of multiple biological processes can be resolved. In addition to this, information about how these players are functionally linked can easily identify new molecular pathways.

Proteomics is a method that is widely used to measure the abundance of thousands of proteins at a given time. In the past proteomics was used almost entirely to simply identify the protein content in a sample. Currently, however the incorporation of quantitative methods with proteomics offers a more robust method towards determining the differences in relative abundance between samples. In this way, changes in protein abundance between control and test samples can be measured on larger scale.

SILAC is a method which utilises amino acids which have stable isotopes introduced into them. These amino acids are supplemented into normal growth media, where the amino acids become incorporated into newly synthesized proteins (Ong *et al*, 2002).

It is important to note that proteins remain biochemically and functionally the same except that proteins with 'heavy' amino acids incorporated into them have a larger

mass. These can be distinguished from proteins with ‘light’ amino acids using mass spectrometry by detecting the differences in mass shift (Ong *et al*, 2002). In this way the relative abundance of a protein in control and test samples can be determined as a ratio.

In previous chapters it can be seen that Rnd3 depletion leads to an increase in cell adhesion, a suppression in differentiation and a reduction in cell size. In addition to this Rnd3 depletion has been shown to alter the expression of p63, desmoplakin, involucrin and K10. The aim of this chapter is to identify the global effect of Rnd3 depletion on protein expression using SILAC and to identify novel proteins that are regulated by Rnd3 and may have an effect on keratinocyte function.

5.2 Results

5.2.1 The identification of proteins regulated by Rnd3 using SILAC

SILAC is a commonly used method used to determine the relative changes in protein abundance between control and test samples. Here SILAC was used to identify changes in protein abundance when Rnd3 is depleted. HaCaTs were grown in normal growth media supplemented with ‘Heavy’ (Arg 10 Lys 8) and ‘Light’ (Arg 0 and Lys 0) for a total of four doublings. ‘Heavy’ cells were transfected with NSC siRNA and ‘light’ cells were transfected with Rnd3 siRNA for 48 hours as described in Chapter 2. Figure 5.1a shows schematic of how samples were prepared. Cells were lysed and were subject to immunoblotting to ensure that Rnd3 was sufficiently knocked down (Figure 5.1b). Lysates were then mixed at a 1:1 ratio and were loaded onto a 12% gel and were subject to SDS-PAGE. Gels pieces were cut at the indicated bands shown in Figure 5.1c and bands were enzymatically digested using trypsin. Digested bands were then subject to LC MS-MS. To calculate the changes in protein abundance in

NSC and Rnd3 siRNA treated cells, raw MS-MS scans were submitted to MaxQuant. Maxquant is a software package that is used to analyze large scale ‘shotgun’ proteomic data. It utilizes raw MS/MS data and is able to extract the mass and intensity of peptide peaks. These peaks can then be matched against a protein database that identifies each protein depending on the sequence similarity. Ratios are calculated from the relative intensity between corresponding peaks from the same protein in both samples (Cox and Maan, 2011).

Figure 5.2 shows the log₂ ratio of all proteins analyzed within the sample. A total of 1943 proteins were identified. Proteins that were up regulated or down regulated by at least 2 fold, were considered further. Table 5.1a and b lists the proteins that are up regulated and down regulated respectively, where 13 proteins were found to be upregulated and 14 proteins were found to be down regulated.

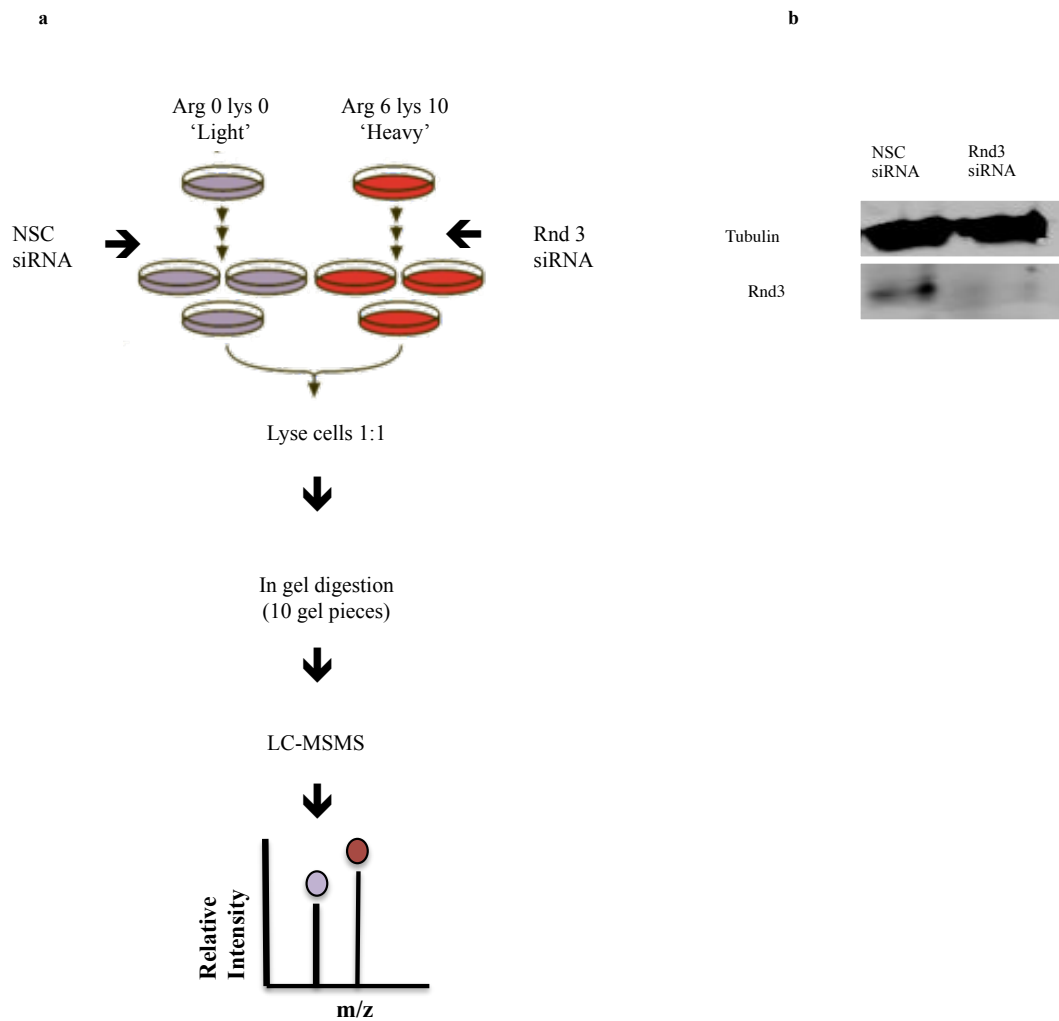


Figure 5.1. SILAC workflow. HaCaT were grown in normal growth media supplemented with heavy and light amino acids for a total of 4 doublings. Heavy and light cells were transfected with Nsc and Rnd3 siRNA for 48 hours before cells were lysed. Figure 5.1a shows a schematic of how samples were prepared. To ensure Rnd3 has been sufficiently knocked down, samples were subject to immunoblotting. Figure 5.1a shows that Rnd3 has been sufficiently knocked down. Samples were then mixed at a 1:1 ratio and loaded a 12% acrylamide gel. Lanes were cut into 10 fractions and were enzymatically digested using trypsin. Samples were submitted for LC MS-MS analysis. Each experiment was conducted a total of two times.

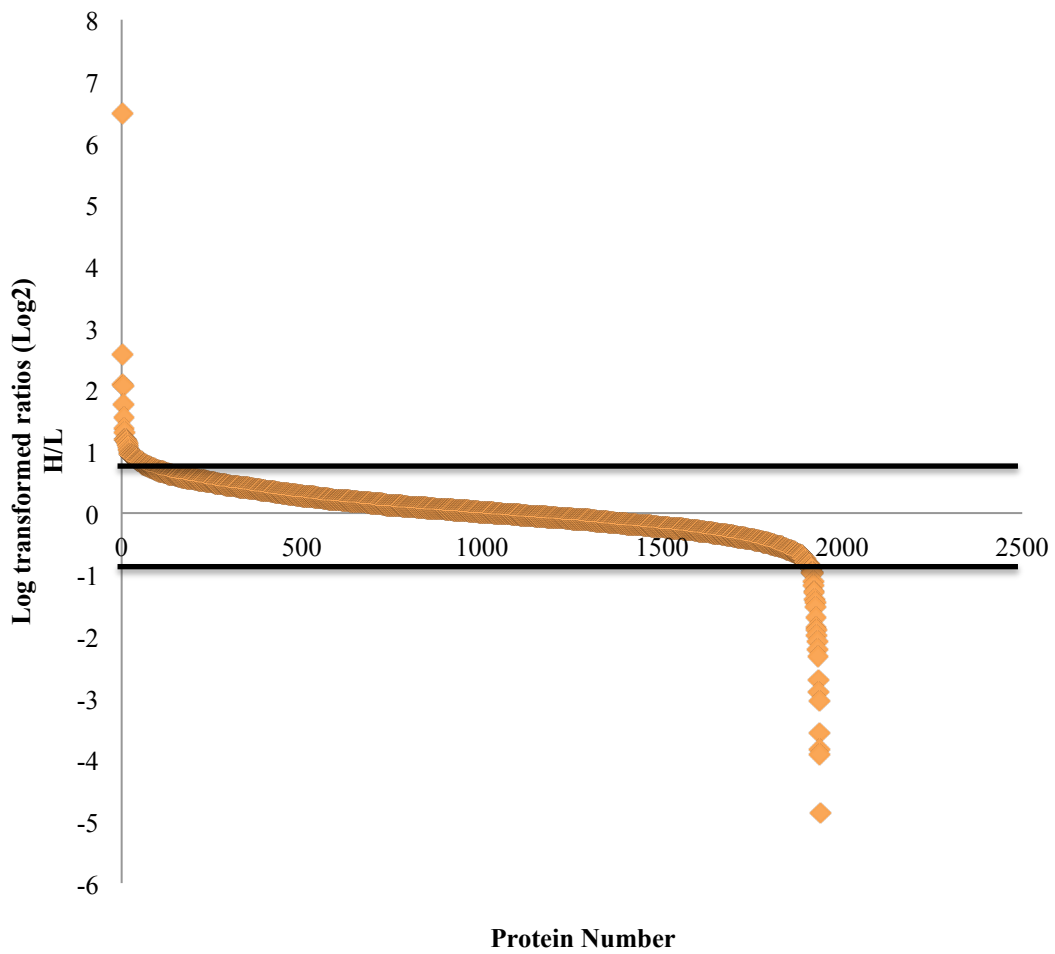


Figure 5.2 SILAC output. Raw MSMS data was submitted to Maxquant and the relative intensity of peptide peaks are calculated. Figure 5.2 shows a scatter diagram of all proteins analyzed. A total of 1943 proteins were identified. Ratios were logged. Proteins that were up regulated or down regulated by at least two fold were considered further.

<i>Downregulated</i>	
Protein	log2 ratio
S100A8	-4.251794823
OR3A2	-3.67468662
S100A9	-3.265166816
PPP3CA	-2.97652861
LTF	-2.267835392
KIF14	-2.063192281
JUNB	-1.667574266
C9orf64	-1.443659691
SERPINB4	-1.423363028
SCD	-1.420940456
PKDREJ	-1.372729271
SUN2	-1.366196301

<i>Upregulated</i>	
Protein	log2 Ratio
SARG	1.946168966
NUP153	1.982278431
LAMC2	2.05338809
SLC1A3	2.066030329
LCP1	2.077404076
SERPINB2	2.158288909
MINA	2.224397188
QTRT1	2.456640299
ZFP36L1	2.627016235
PTP4A2	2.884005307
FOXK1	3.248335228
HOOK1	3.433004909
DMD	3.777433612
HK2	-1.185486004
H2AFV	-0.947179878

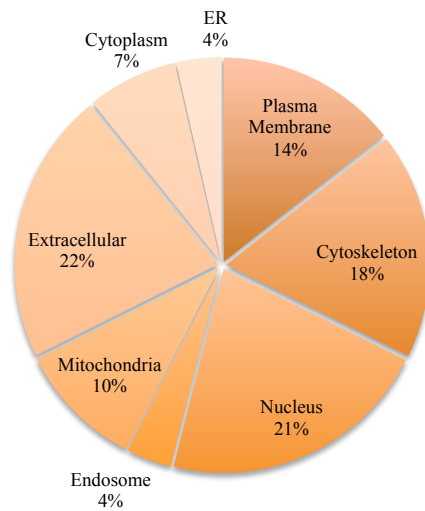
Table 5.1 List of upregulated and downregulated proteins in Rnd3 depleted cells.

Proteins that were up regulated or down regulated by at least 2 fold were considered further. Table 5.1 lists these proteins and the corresponding log2 ratio.

To understand how these proteins may be functionally relevant, up regulated and down regulated proteins were manually characterized by their subcellular localization (Figure 5.3), molecular function (Figure 5.4) and biological processes (Figure 5.5) using UniProt data. Percentages were calculated depending on the number of proteins in each corresponding class and are graphically represented as a pie chart.

To determine which class the majority of proteins could be grouped into, classes that were represented by one protein were grouped together as 'other'. Figure 5.3 shows that 21% of all proteins identified are localized in the nucleus and 22% were localized to the cytoplasm suggesting that there is no bias in the regulation of proteins in each compartment. Furthermore 14% were found to be associated with the cytoskeleton (Figure 5.3) and 11% were thought to be associated with actin binding (Figure 5.4). Interestingly, 20% of all proteins identified are involved in transcription (Figure 5.4) and 15% are shown to be involved in regulating transcription factor activity (Figure 5.5).

a



b

ID	log2 ratio	Subcellular localization
PKDREJ	-1.372729271	Plasma Membrane
DMD	1.9174064	Plasma Membrane
LAMC2	1.038006323	Extracellular
S100A8	-4.251794823	Cytoskeleton
S100A9	-3.265166816	Cytoskeleton
KIF14	-2.063192281	Cytoskeleton
LCP1	1.054781862	Cytoskeleton
H2AFV	-0.947179878	Extracellular
HOOK1	1.77947192	Cytoskeleton
HK2	-1.185486004	Mitochondrion
SLC1A3	1.046861433	Plasma Membrane
SCD	-1.420940456	Endoplasmic Reticulum
NUP153	0.987159618	Nucleus
C9orf64	-1.443659691	Nucleus
SARG	0.96063697	Cytoplasm
SERPINB2	1.109887997	Extracellular
SUN2	-1.366196301	Nucleus
PPP3CA	-2.97652861	Cytosol
PTP4A2	1.528073819	Endosome
SERPINB4	-1.423363028	Extracellular
OR3A2	-3.67468662	Plasma Membrane
LTF	-2.267835392	Extracellular
ZFP36L1	1.393425116	Cytoplasm
FOXK1	1.699700526	Nucleus
MINA	1.153414419	Nucleus
JUNB	-1.667574266	Nucleus
QTRT1	1.296686634	Mitochondria

Figure 5.3 Subcellular localization of up regulated and down regulated proteins

Proteins were manually functionally classified into their subcellular localization using uniProt data. Percentages were calculated depending on the number of proteins in each class. Figure 5.3a is a pie chart which shows the percentage of proteins which fall into each GO term. Figure 5.3b (Table 5.2) is a table that lists up regulated and down regulated proteins and their corresponding subcellular localization.

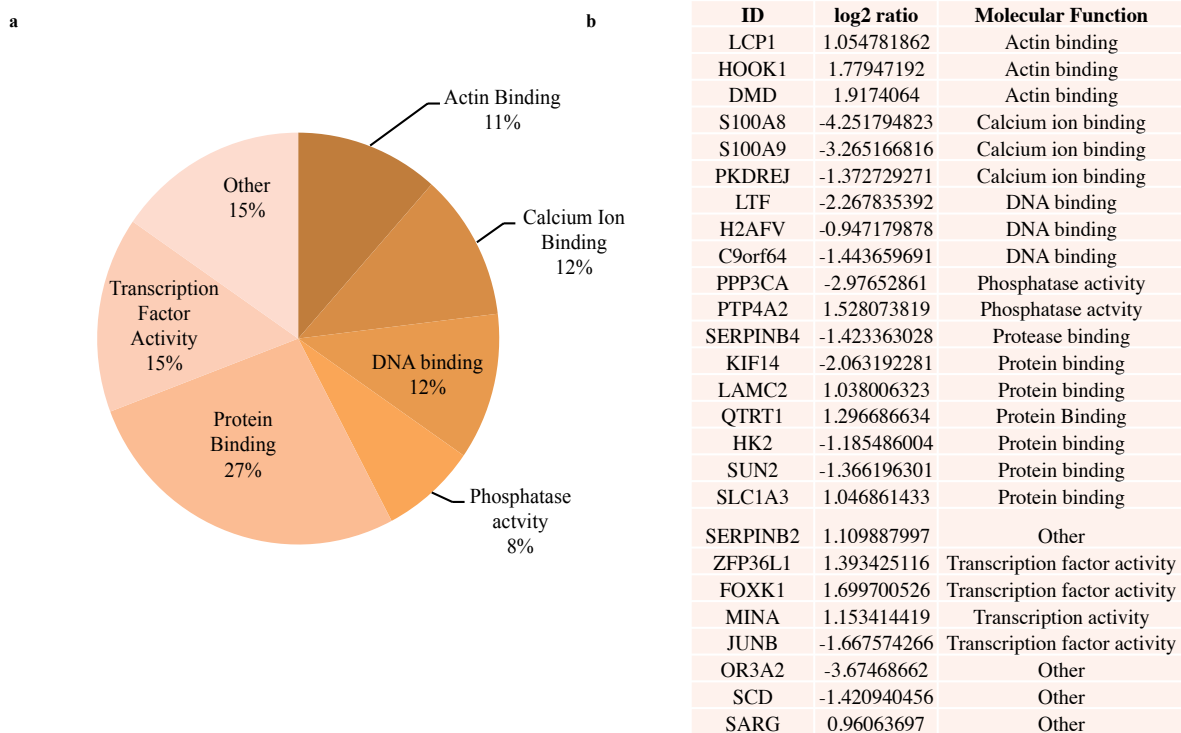
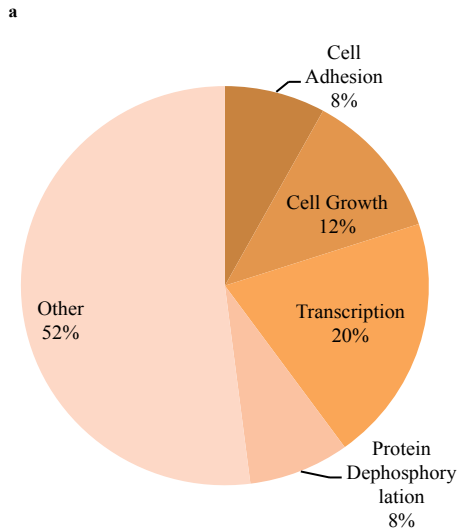


Figure 5.4 Molecular functions of upregulated and down regulated proteins

Proteins were manually functionally classified into their molecular function using uniProt data. Percentages were calculated depending on the number of proteins in each class. Figure 5.4a is a pie chart which shows the percentage of proteins which fall into each GO term. Figure 5.4b (Table 5.3) is a table that lists up regulated and down regulated proteins and their corresponding molecular function



b

ID	log2 ratio	Biological Processes
PKDREJ	-1.372729271	Calcium ion transmembrane
DMD	1.9174064	Cell Adhesion
LAMC2	1.038006323	Cell Adhesion
S100A8	-4.251794823	Cell growth
S100A9	-3.265166816	Cell growth
KIF14	-2.063192281	Cell growth
LCP1	1.054781862	Cell migration
H2AFV	-0.947179878	Chromatin organization
HOOK1	1.77947192	Endosome organization
HK2	-1.185486004	Glycolytic Process
SLC1A3	1.046861433	Ion transport
SCD	-1.420940456	Other
NUP153	0.987159618	Other
C9orf64	-1.443659691	Other
SARG	0.96063697	Other
SERPINB2	1.109887997	Negative regulation of endopeptidase activity
SUN2	-1.366196301	Nuclear envelope organisation
PPP3CA	-2.97652861	Protein dephosphorylation
PTP4A2	1.528073819	Protein dephosphorylation
SERPINB4	-1.423363028	Regulation of proteolysis
OR3A2	-3.67468662	Signal transduction
LTF	-2.267835392	Transcription
ZFP36L1	1.393425116	Transcription
FOXX1	1.699700526	Transcription
MINA	1.153414419	Transcription
JUNB	-1.667574266	Transcription
QTRT1	1.296686634	tRNA processing

Figure 5.5 Biological processes of upregulated and down regulated proteins

Proteins were manually functionally classified into their biological processes using uniProt data. Percentages were calculated depending on the number of proteins in each class. Figure 5.5a is a pie chart which shows the percentage of proteins which fall into each GO term. Figure 5.5b (Table 5.4) is a table that lists up regulated and down regulated proteins and their corresponding biological process.

To understand the functional significance of these proteins in relation to one another, protein IDs were submitted to STRING to determine the functional associations between each protein. STRING is online database which predicts ‘functional association’ between proteins/genes. These associations are predicted utilizing information from experimental data, pathway knowledge, text mining and co-expression studies. The database therefore is an interface that brings together information from multiple sources so the functional relationships between proteins can be contextualized (Szkarczyk *et al*, 2015).

Figure 5.6 shows the functional associations between upregulated and downregulated proteins. It can be seen that very few proteins from the submitted list interact with one another. To get a more general idea of how these proteins may be functionally related, STRING maps were generated utilizing both the submitted list and ten known predicted protein associations (Figure 5.7). It can be seen here that many more functional associations between the submitted list are made indirectly via the interaction with other known partners. For example, JunB can indirectly interact with SERPIN B2 and SERPINB4 via an interaction with FOS.

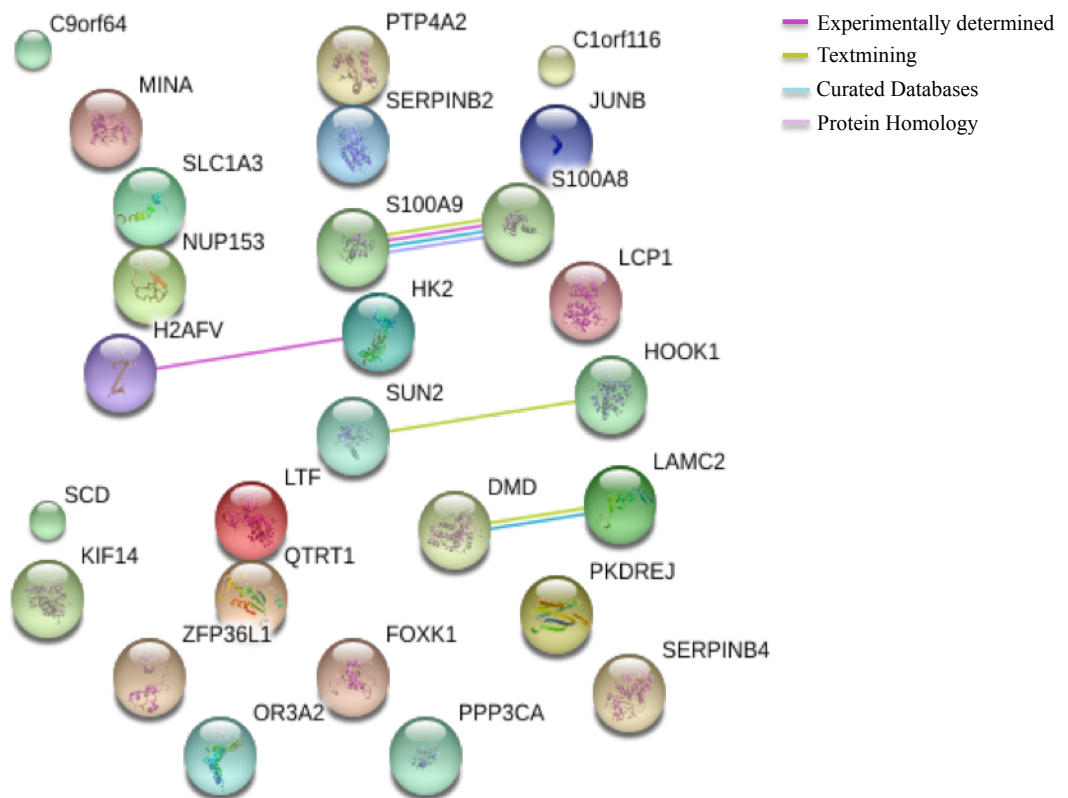


Figure 5.6 STRING map showing the functional associations of upregulated and down regulated proteins.

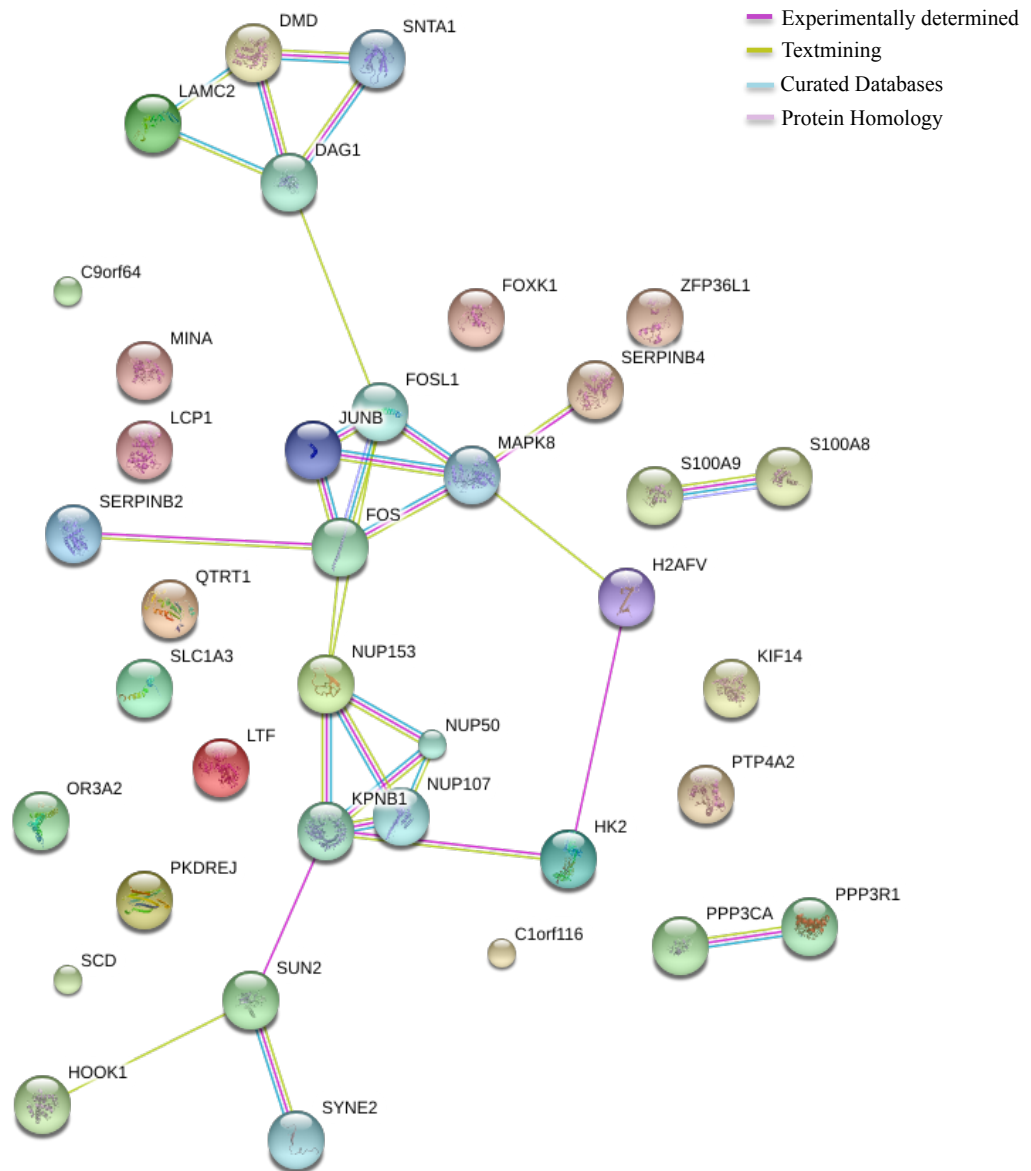


Figure 5.7 STRING map showing the functional association of each protein and ten other known associations.

5.2.2 Rnd3 regulates the expression of known regulators of progenitor differentiation

To further determine how Rnd3 may function, proteins that may be biologically relevant to the phenotypes observed in earlier chapters were analysed further.

It has already been shown in Chapter 4 that transcription factors such as p63 regulate Rnd3 depleted phenotypes. To determine if any other transcription factors may play role in regulating keratinocyte function in Rnd3 depleted cells the molecular function ‘Transcription factor activity’ and the biological process ‘Transcription’ were considered further (Table 5.5). Table 5.5 summarizes the subcellular localization, molecular function and biological process of each of the proteins in this class and how the protein functions in light of current literature.

A total of four proteins are found both ‘Transcription’ and ‘Transcription factor activity’. These include ZFP36L1, FOXK1, MINA and JunB. ZFP36L1, FOXK1, MINA were found to be up regulated in Rnd3 depleted cells and JunB was downregulated. Interestingly, JunB is a known regulator of keratinocyte differentiation, as it is involved in regulating the expression of late differentiation genes (see section 1.2.3). Furthermore, ZFP36L1, FOXK1 have additionally have been shown to be involved in regulating progenitor differentiation, therefore suggesting that these may play a role in regulating differentiation in Rnd3 depleted cells (see Chapter 5 discussion).

To ensure that this increase in expression is not an experimental artifact introduced during mass spectrometry analysis, western blotting was used to validate the changes in the expression of FOXK-1 and JunB (Figure 5.8 and 5.9). Figure 5.8a shows that FOXK1 in increase in the nucleus of Rnd3 depleted cells. It can be seen that FOXK-1 expression is increased at the protein level when using western blotting (Figure 5.8b). This was quantified by measuring the intensity of each band using imageJ to identify

if the fold change in expression shown on the immunoblot reflects the fold change in expression observed using SILAC (Figure 5.8c). It can be seen that there is a significant increase in expression of FOXK1 by 2 fold. Three replicates were conducted and a Student T-Test was performed to determine statistical significance. Figure 5.8d shows a STRING map of all the known functional protein associations. It can be seen that FOXK1 associates with SRF, a known regulator of keratinocyte differentiation (see Section 5.3). In a similar way, the expression of junB was analyzed using western blotting and quantified using ImageJ. Figure 5.9a and 5.9b shows that there is a 2 fold reduction in junB expression. Figure 5.9c shows a STRING map of known junB functional associations. It can be seen that junB with multiple FOS proteins which regulate the MAPK cascade. The MAPK cascade is additionally a known regulator of keratinocyte differentiation (see Section 5.3).

To determine if the alteration in FOXK1 and junB expression is reflected in the expression of their respective transcripts, qRTPCR was conducted. Figure 5.10 shows that upon Rnd3 depletion, FOXK-1 expression is up regulated by ~20% and junB is down regulated by ~60%. It is important to note that this experiment was only conducted twice and statistical significance cannot be determined. However, these data suggest that the up regulation FOXK1 may occur via post transcriptionally, whilst junB expression may be regulated transcriptionally.

Taken together it can be seen that Rnd3 depletion leads to an alteration of proteins that are known to regulate progenitor differentiation.

Gene ID	Name	Ratio (log2)	Biological process	Molecular function	Subcellular localization	Function	References
ZFP36L1	ZFP36 Ring Finger Protein-Like 1)	1.393425116	Transcription	Transcription factor activity	Cytoplasm	RNA binding Zinc finger protein. Binds specifically to 3' UTR and deregulates the expression of target genes	Lai <i>et al</i> , 2000
FOXP1	Forkhead Box K1	1.699700526	Transcription	Transcription factor activity	Nucleus	Member of the Forkhead box family of transcription factors. Role in regulating myogenic progenitor differentiation.	Xiaozhong Shi <i>et al</i> , 2010
MINA	MYC Induced Nuclear Antigen	1.153414419	Transcription	Transcription factor activity	Nucleus	Myc Target gene. Involved in regulating cell proliferation.	Tsuneoka <i>et al</i> , 2002; Teye <i>et al</i> , 2004
JUNB	Jun B Proto-Oncogene	-1.66757426	Transcription	Transcription factor activity	Nucleus	Member of AP-1 family of transcription factors. Role in regulating keratinocyte differentiation genes	Reviewed in Eckert <i>et al</i> , 2013

Table 5.5 List of Proteins found in the molecular function ‘transcription factor activity’ and the biological process ‘Transcription’. A basic literature search was conducted to determine the function of each protein and summarized.

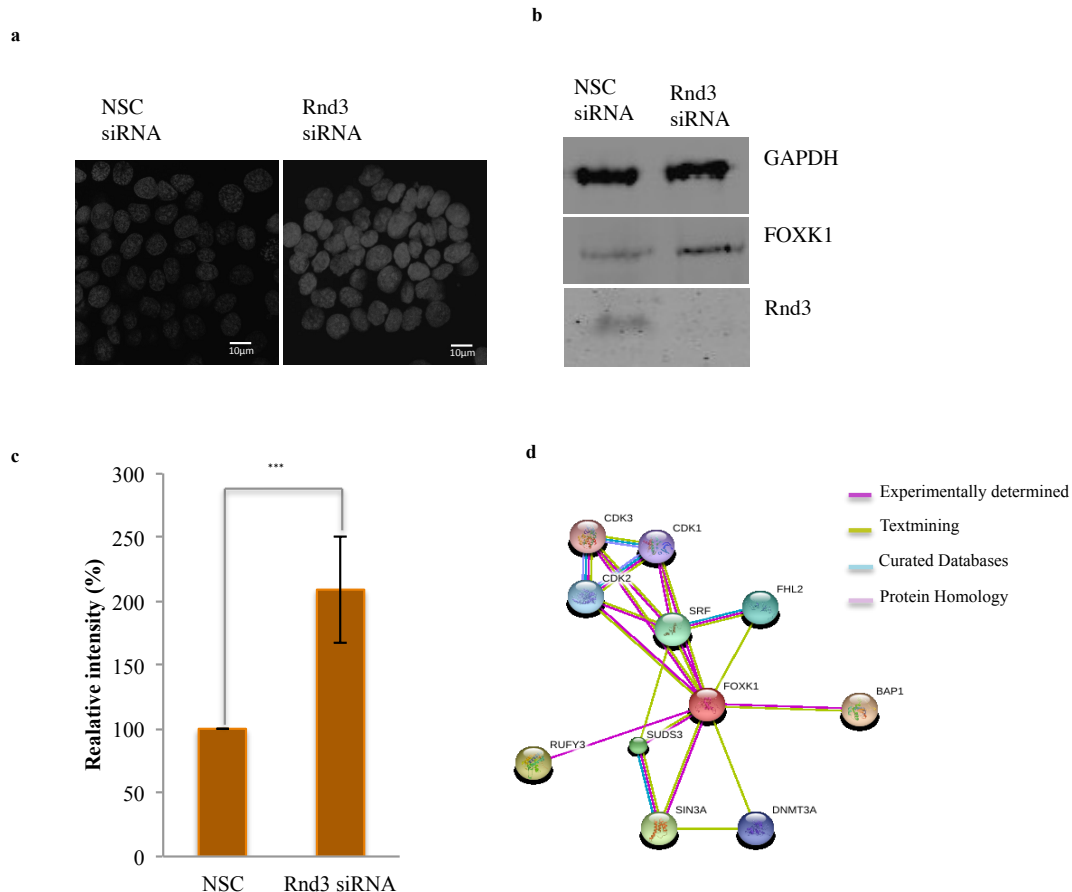


Figure 5.8 Rnd3 depletion leads to an increase in FOXK1 expression

Immunofluorescence and immunoblotting was used to validate the increase in FOXK1 expression observed in the SILAC experiment. Figure 5.8a and 5.8b show that in Rnd3 depleted cells FOXK1 is upregulated. To determine the fold change in the band intensity, image J was used. Figure 5.8c shows that FOXK1 expression has increased by 2 fold. To understand the functional significance of FOXK1, FOXK1 STRING maps were observed. Figure 5.8d shows the functional associations of FOXK1 and known protein protein interactors. Each experiment was conducted in three individual experiments were conducted and a students T-test was conducted to determine statistical significance where * $p < 0.05$, ** < 0.01 , *** $p < 0.001$. Error bars represent standard error of the mean.

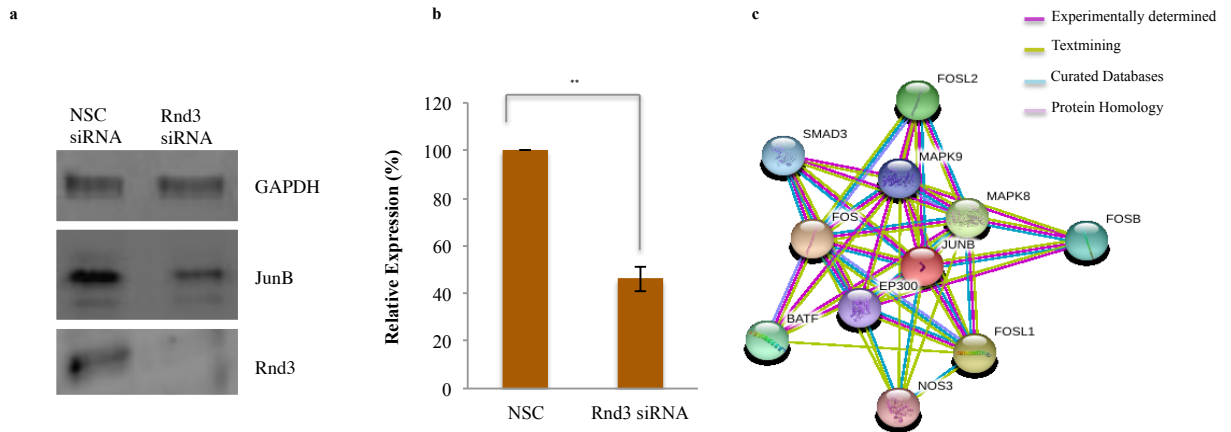


Figure 5.9 Rnd3 depletion leads to an increase in junB expression

Immunoblotting was used to validate the reduction in FOXX1 expression observed in the SILAC experiment. Figure 5.9a shows that in Rnd3 depleted cells junB is downregulated. To determine the fold change in the band intensity, image J was used. Figure 5.9b shows that junB expression has decreased by 2 fold. To understand the functional significance of junB STRING maps were observed. Figure 5.9c shows the functional associations of junB and known protein protein interactors. Each experiment was conducted in three individual experiments were conducted and a students T-test was conducted to determine statistical significance where * $p < 0.05$, ** < 0.01 , *** $p < 0.001$. Error bars represent standard error of the mean.

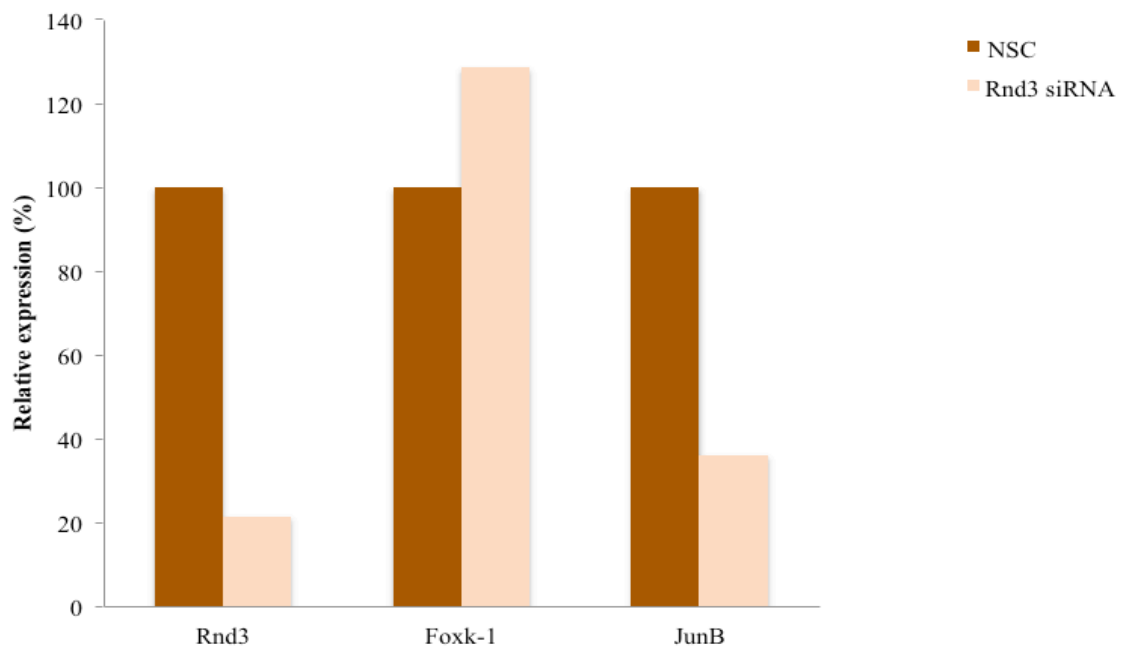


Figure 5.10 Rnd3 depletion may lead to a reduction in junB transcript and slight changes in FOXK1 transcript. To determine if alterations in the expression of junB and FOXK1 is reflected in their respective transcripts, qRT-PCR was conducted to determine relative transcript levels. Figure 5.10 shows that there is ~20% increase in FOXK1 and 70% decrease in the expression of JunB.

5.3 Discussion

SILAC is a commonly used method used to determine the differences in the abundance of protein in given sample. Previous chapters have shown that Rnd3 regulates the expression of proteins such as p63, desmoplakin, CK-19 (data not presented here), involucrin and K10. These proteins are known to play key roles in stem/progenitor cell function.

To determine the effects of Rnd3 depletion on protein expression on larger scale SILAC was used to determine the relative changes in the abundance of protein in keratinocytes treated with control and Rnd3 siRNA.

Here, an alteration in the expression of a total of 27 proteins can be seen when Rnd3 is depleted. It is important to note that quantitative proteomic approaches such as SILAC are sampling methods. Therefore, the outcome of these methods are largely dependent on how protein rich each sample analyzed using LC-MSMS is. For example, a given fraction representing a certain molecular weight may also contain a highly abundant protein, and therefore may mask the signal intensity of a lower abundant protein in the same fraction. One way to overcome this is to separate samples into a larger number of less biologically complex samples to determine the changes in less abundant proteins.

This provides an explanation to why proteins such as p63 and desmoplakin that have been shown to increase using immunoblotting in Chapter 3 may not have been identified using LC-MSMS and are therefore not present in this dataset since only ten fractions were taken and therefore the signal of these proteins may have been obscured by other higher abundant proteins. Going forward, the separation of test and control samples into less complex fractions could provide more information about how Rnd3 functions.

5.3.1 Rnd3 regulates the expression of FOXK1

FOXK1 is a member of the forkhead (FOX) superfamily of transcriptional regulators which includes almost 300 transcriptional regulators. Each member consists of an evolutionarily conserved ‘forkhead’ DNA binding domain which is involved in transcriptional activity (Katoh *et al*, 2004).

FOX proteins are involved in the regulation of apoptosis, differentiation of multiple tissue types, cell cycle progression and mutagenesis. Therefore, the family are thought to be important regulators of multiple biological processes (Reviewed in Lam *et al*, 2013).

Here, it can be seen that Rnd3 depletion leads to an increase in the expression FOXK1. Whilst the function FOXK1 in the epidermis has yet to be identified, its role in other systems may provide some insight into how it might function in keratinocytes FOXK1 has been identified as a regulator of myogenic progenitor cells in the mouse model. Studies in the FOXK1 knock out mouse has shown mice have poor skeletal muscle formation and muscle regeneration and are smaller in size. It was concluded that FOXK1 is required for the regulation of cell cycle progression and the maintenance of progenitor cell quiescence (Hawke *et al*, 2002). Further studies identified that a functional interaction between FOXK1 and the sin3 repression complex via an interaction with SDS, is involved in regulating cell cycle progression (Shi and Garry, 2012). Furthermore, FOXK1 was shown to interact with foxo4, and this interaction was found to regulate the proliferative capacity of myogenic progenitor cells. The same study additionally identified that FOXK1 interacts with Mef2, and this interaction leads to a suppression of myogenic progenitor cell differentiation (Shi *et al*, 2012) Taken together studies in the mouse model provide

evidence that FOXK1 is important in regulating the quiescent state in myogenic progenitor cells.

Interestingly, FOXK1 has additionally shown to interact with SRF. SRF is a transcription factor, which functions with different co-activators and co-repressors to exert different transcriptional responses (Freddie *et al*, 2007). It has been shown that knock down of SRF in human cells leads to an inhibition of differentiation and reduced expression of junB and fos, known regulators the expression of late differentiation genes (Connelley *et al*, 2011; Connelley *et al*, 2010).

Whilst the transcriptional effect of the SRF and FOXK1 interaction is yet to be determined, it would be interesting to see if this interaction can firstly be seen in keratinocytes and secondly if this has an effect on the expression of SRF target genes. If FOXK1 functions to suppress differentiation through an interaction with SRF, then it would be predicted that an increase in expression observed in Rnd3 depleted cells may be coupled to suppressed differentiation which is also observed. Furthermore, it would be interesting to see what happens to FOXK1 expression during terminal differentiation. Furthermore, elucidation of the transcriptional targets of FOXK1 could provide some insight into how and if FOXK1 is functionally interesting in keratinocyte function.

Interestingly FOXM1, a transcriptional regulator of stem/progenitor proliferation of oral keratinocytes, was found to be co-expressed with oral keratinocyte stem cell markers. Furthermore, an increased expression of FOXM1 leads to an enrichment of a population of cells that had a reduced propensity to differentiate (Gemenetzidis *et al*, 2010). Other studies have additionally shown that p63 regulates FOXM1 expression in a non-transcriptional mechanism and both may be required for the maintenance of

the proliferative capacity of basal progenitor keratinocytes, since an amplification of p63 was correlated to an increased expression FOXM1.

Parallels can be drawn between the above study and the work presented. Here it can be seen that depletion of Rnd3 leads to an increase a population of stem/early progenitor cells, which show increased expression of p63 and FOXK1. From this it is tempting to hypothesize that FOXK1 may be functioning in a similar way to FOXM1. Whilst this is still speculative, it would be interesting to see if a depletion of both Rnd3 and p63 leads to a restoration of FOXK1 expression.

Furthermore, it would additionally be interesting to firstly confirm that FOXK1 is regulated post transcriptionally (as indicated by figure 5.10) and if this is dependent on p63 expression.

5.3.2 Rnd3 regulates the expression of JunB

JunB is a member of AP1 family of transcription factors and is involved in regulating the expression of late terminal differentiation genes through the regulation of MAPK cascade (Eckert *et al*, 2013). Here, it can be seen that Rnd3 depletion leads to a reduced expression of JunB and this coupled with the reduced expression of involucrin shown in Chapter 3.

JunB expression in the epidermis is found almost entirely in the suprabasal layers and therefore suggests that it plays a role in keratinocyte differentiation.

To determine if the suppression in differentiation observed in Rnd3 depleted cells is due to a reduction in the expression of JunB it would be interesting to see if junB remains at low levels in Rnd3 depleted cells when differentiation is reduced. Furthermore, it would be interesting to see if changes in the expression of other members of the AP1 families are deregulated in Rnd3 depleted cells.

In addition to this it can be seen here that preliminary data indicates that junB is regulated at the transcriptional level. This was somewhat surprising as AP1 transcription factors are thought to be typically regulated post transcriptionally via the addition of various post translational modifications. Therefore, the elucidation of how junB is regulated transcriptionally would be interesting.

In conclusion the data presented here shows that Rnd3 regulates both FOXX1 and JunB both transcription factors that may be involved in the regulation of keratinocyte differentiation.

Chapter 6

The identification of Novel Rnd3 interacting partners using SILAC immunoprecipitation

6.1 Introduction

Rnd3 has been shown to be involved in regulating multiple processes, which include actin cytoskeletal dynamics, cell cycle, apoptosis and differentiation (as described in section 1.10) The role of Rnd3 in actin cytoskeletal dynamics is perhaps the most understood. This has been aided heavily through the identification of its interaction with ROCK-1. However, other studies have shown that Rnd3 plays roles in other biological processes independent of this interaction (as described in section 1.10.1).

It is therefore clear that determining how Rnd3 functions in relation to its interaction with other proteins could provide some insight into how Rnd3 regulates some of the phenotypes that have been observed in previous chapters.

So far, it has been shown that Rnd3 regulates many aspects of keratinocyte behaviour and function including cell size, expression of differentiation markers, as well as the expression of numerous proteins. However, understanding how Rnd3 regulates these processes and the biological pathways that are involved are unknown. Therefore, understanding how Rnd3 functions in relation to its interacting partners will give some insight into how Rnd3 depletion can have such varied effects

SILAC immunoprecipitation incorporates affinity protein purification methods with quantitative proteomics. It is an approach that combines traditional affinity purification methods such as immunoprecipitation with SILAC (Emmet, *et al* 2014).

This method enables the quantification of proteins between control and test samples by measuring the relative abundance of a given protein by analysing the differences in mass shift during mass spectrometry analysis. This has additional benefits to using

none labelling methods, since specific interactions of a given protein can be quantified, therefore reducing the number of false positives. In this way, non-specific binding can be distinguished from specific binding depending on the ratio of isotopically labelled proteins.

Here, SILAC immunoprecipitation was used to pull down Rnd3 and its interacting partners. The aim of doing this is to identify novel Rnd3 interactors that may be involved in regulating Rnd3 function.

6.2 Results

6.2.1 The identification of Rnd3 interacting proteins using SILAC immunoprecipitation

SILAC immunoprecipitation was used to characterise Rnd3 interacting partners. A quantitative approach allows for a more accurate means of determining protein-protein interactions since relative quantification of protein abundance can be determined in control and test samples. This ensures that interactions can be distinguished as either, specific and non specific, depending on their respective relative abundances. In this way experimental contaminants can be easily disregarded. HEK293T cells were grown in normal growth media supplemented with either ‘light’ and ‘heavy’ Arg and lys for 6 doublings to ensure that amino acids have at least 98% incorporation. Figure 6.1a shows a schematic of how samples were prepared. ‘Heavy’ cells were transfected with Flag-Rnd3 and ‘Light’ cells were transfected with Flag-EV for 48 hours before being lysed. Lysates were loaded onto a 12% gel and were subject to immunoblotting to determine transfection efficiency prior to immunoprecipitation. Figure 6.1b shows that Rnd3 is sufficiently over expressed. Lysed cells were then initially subject to immunoprecipitation separately to ensure

that immunoprecipitation was efficient. Immunoprecipitation was performed using a FLAG antibody crosslinked onto a protein G bead. Immunoprecipitates were loaded onto a 12% gel and subject to SDS PAGE. Gels were then comassie stained so to identify protein bands (Figure 6.1c (2rd and 3rd lane). Immunoprecipitation was performed again in the same way but this time, lysates were mixed at a 1:1 ratio before they were applied to flag beads. The gel lane was cut into 10 pieces and in gel digestion was conducted (Figure 6.1c). Peptides were subject to LC-MS MS to determine relative abundance based on the relative intensity of each corresponding peptide peak. Raw MS data was analysed using Maxquant, which calculated the ratio of heavy and light peptides and identified the protein each peptide belonged to.

Figure 6.2 shows the log₂ H/L ratio of all proteins found in the sample that was analysed. Proteins that were upregulated by at least 2 fold were deemed to be true interactors. A total of 79 specific proteins were found to significantly upregulated therefore suggesting that these specifically bind to Rnd3. Table 6.1 lists the proteins that were upregulated and their corresponding log₂ ratios.

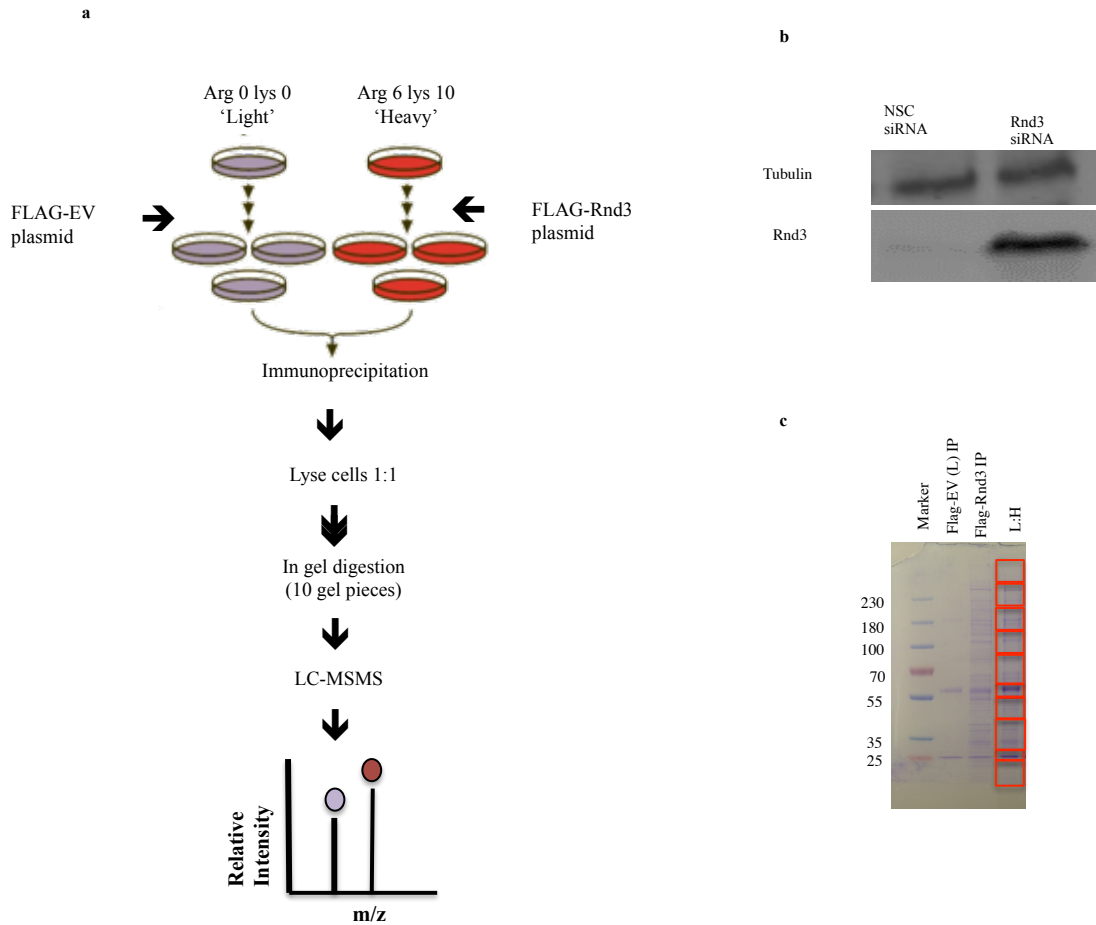


Figure 6.1 SILAC immunoprecipitation set up

To identify and quantify novel Rnd3 interacting partners HEK 293T cells were grown in SILAC DMEM supplemented with heavy and light amino acids. 'Light' cells were transfected with Flag-EV and 'Heavy' cells were transfected with Flag-Rnd3. Figure 5.5a shows a work flow depicting how samples were prepared. Figure 5.5b shows that Rnd3 has been sufficiently overexpressed in 'heavy' cells. Figure 5.5c shows the pieces the lane was cut into. Two biological and two technical repeats were analysed.

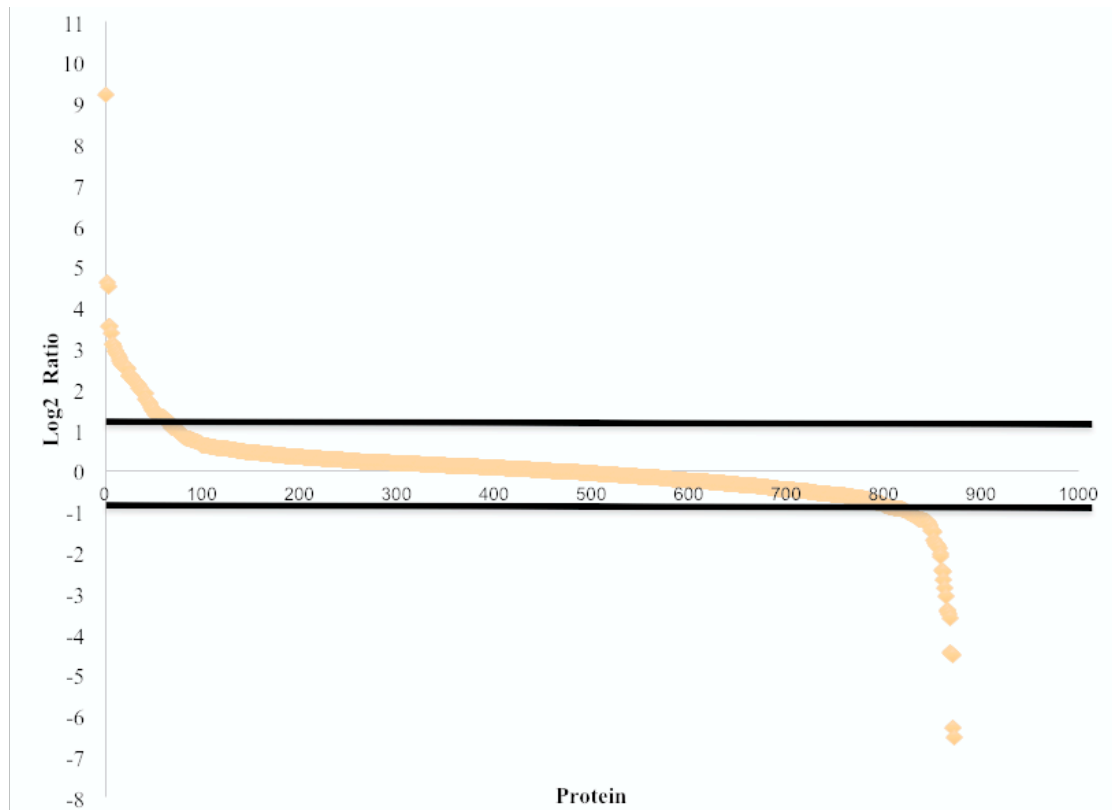


Figure 6.2. SILAC output

Maxquant was used to measure the relative abundance of proteins as a ratio. The log₂ of each ratio was calculated and plotted onto a scatter graph. Proteins which showed a > 2 fold increase or decrease were deemed to be significant hits and were further analysed. A total of 75 proteins were significantly upregulated or downregulated.

Table 6.1 Full list of Rnd3 interactors and corresponding log2 ratio.

Protein	Log2 Ratio
DMD	4.617180918
STPG2	4.52123923
KV204	3.553851968
HSPB1	3.535555333
SYVC	3.372116318
PRPS2	3.122258568
HCDH	3.119322973
SFXN1	3.035060797
CYFP1	2.954047379
TOP2A	2.941613419
PPME1	2.882799537
DCTN1	2.84478735
SLK	2.723820647
RENT1	2.653770868
SF3B2	2.650741586
AQR	2.615698782
APEX1	2.561081695
PSD10	2.542728552
EXOS4	2.536152393
GTF2I	2.520547968
PSMD2	2.501668429
CND1	2.341587315
UBC9	2.323197108
IF5A1	2.322591582
IDH3A	2.307370233
USO1	2.247046441
NTM1A	2.226724301
NIPS2	2.21992743
CSK2B	2.175748134
SP16H	2.155457815
YAP1	2.152215875
CHRD1	2.118226814
CPSF5	2.02994754
CBX3	2.027967904
KAD4	1.971479177

SMCA4	1.927251742
MARE1	1.925885517
SRSF9	1.909888285
UBP24	1.891574725
IF4E	1.776188231
COPB	1.720541148
ROAA	1.686253987
PRS4	1.678702946
HCFC1	1.628353671
GDIR1	1.574392198
PHF6	1.527720953
GSTO1	1.497382436
HUWE1	1.474721569
RL13	1.409798228
ELP1	1.383718115
GEMI5	1.370331702
MP2K1	1.358846331
RS17	1.332335577
CYBP	1.331705216
SYQ	1.330615763
IF4H	1.324234562
IDH3B	1.309001516
P08579	1.280778192
HNRDL	1.244887059
ROA0	1.222433641
HMGB1	1.202449067
RU2A	1.18922364
SPTB2	1.119289768
SF3B3	1.079224489
RAB5A	1.058939855
CHTOP	1.051998468
TFAM	1.048166421
G3BP1	1.040962548
THOC4	1.023823091
GSTM3	1.006764782
CMBL	0.964287722
FGD6	0.962215841

6.2.2 Functional Analysis of Rnd3 interacting proteins

After identification, proteins were manually classified according to subcellular localization using uniprot data and the percentage of proteins in each corresponding GO term is represented graphically using a pie chart (Figure 6.3a, 6.4a and 6.5a). Percentages were calculated depending on the number of proteins in each class and classes represented by one protein were sub classified as 'other'. Proteins along with their corresponding subcellular localization (Figure 6.3b), biological processes (Figure 6.4b) and molecular function (Figure 6.5b) are listed. DAVID was used to additionally functionally annotate proteins according to their biological processes and molecular function to determine enriched GO terms (Figure 6.4c and Figure 6.5c).

It can be seen that 42% off all proteins identified associate with the cytoplasm which suggests that Rnd3 associates with cytoplasmic proteins (Figure 6.3). Interestingly, 11% of the protein identified can be grouped into the biological process 'proteasomal degradation' and 8% can be classified into the molecular function 'Regulation of ubiquitin ligases'. Furthermore, GO terms such as 'negative regulation of ubiquitin protein ligase activity' and 'positive regulation of ubiquitin activity' were statistically enriched.

To further characterize these interactors STRING was used to determine if any functional associations exist within the group of proteins. Figure 6.6 shows the STRING map of known interaction between the list of proteins submitted.

To understand how these functional associations might be of biological significance in light of other known protein-protein associations, STRING parameters were altered to include the interaction networks of each protein in the submitted list (Figure 6.7). It can be seen that Rnd3 indirectly interacts with known components of proteosomal degradation. To determine how these proteins may function a literature search was

conducted to determine their biological significance. Table 6.2 summarizes proteins classified in biological function 'Proteasomal degradation' and molecular process 'regulation of ubiquitin ligase activity'.

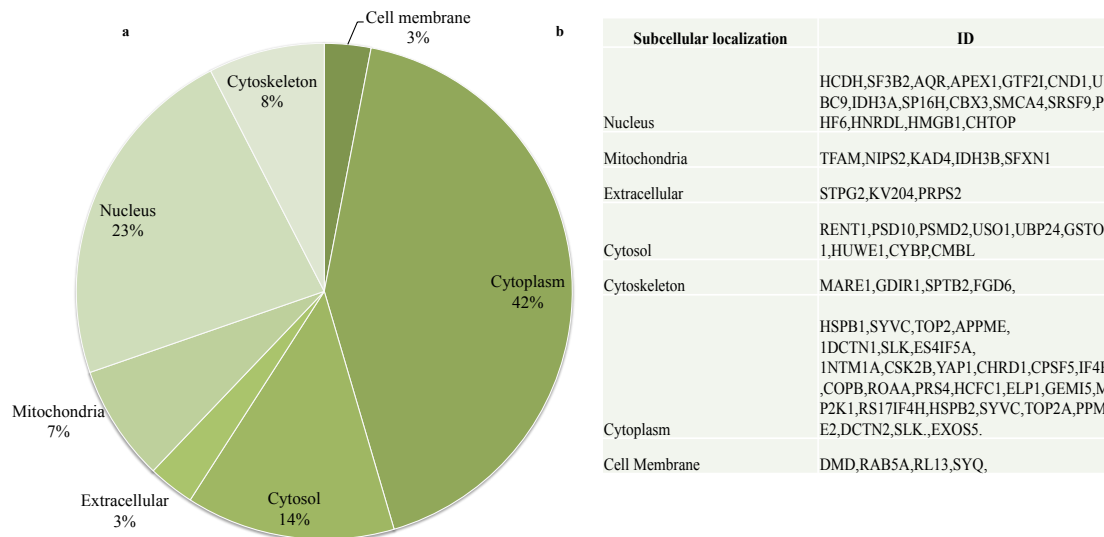


Figure 6.3 Subcellular localization of identified Rnd3 interactors

Proteins IDs were converted into Gene IDs before functional analysis was conducted. Genes were manually grouped according to predefined gene ontology terms. Figure 6.3a shows a pie chart representing the percentage of proteins manually classified into each subcellular compartment. Percentages were calculated depending on the number of proteins in each class and classes represented by one protein were sub classified as ‘other’. Figure 6.3b lists the genes and the corresponding GO term.

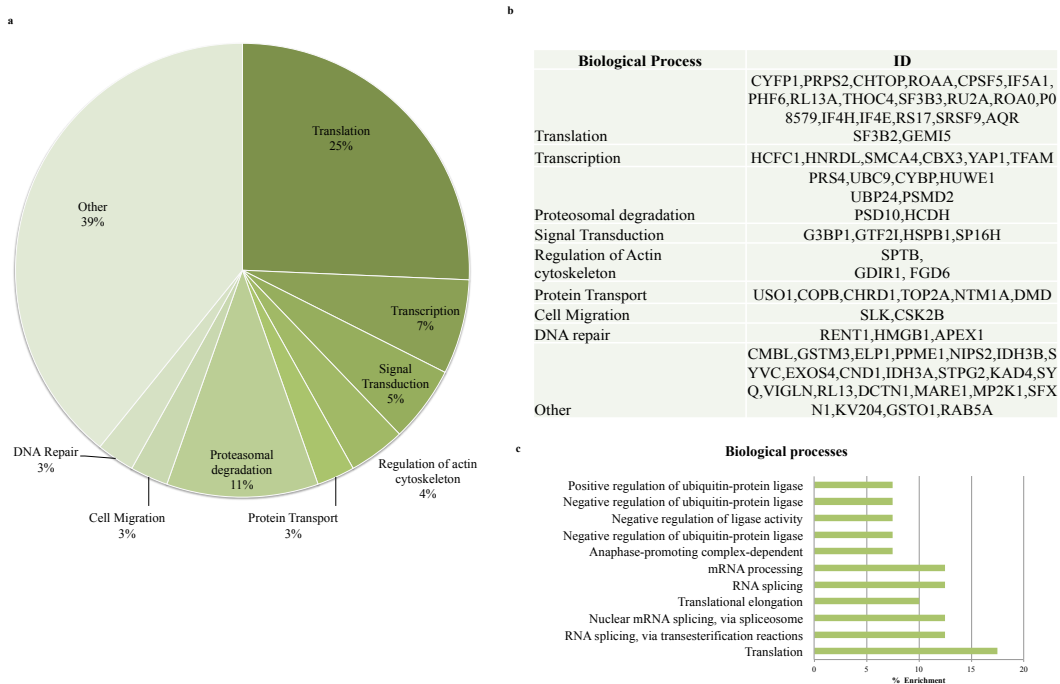


Figure 6.4 Biological processes of identified Rnd3 interactors

Proteins IDs were converted into Gene IDs before functional analysis was conducted. Genes were manually grouped according to predefined gene ontology terms. Figure 6.4a shows a pie chart representing the percentage of proteins manually classified into each biological process. Percentages were calculated depending on the number of proteins in each class and classes represented by one protein were sub classified as ‘other’. Figure 6.4b shows lists the genes and the corresponding GO term. Figure 6.4c shows the enriched GO terms using DAVID .

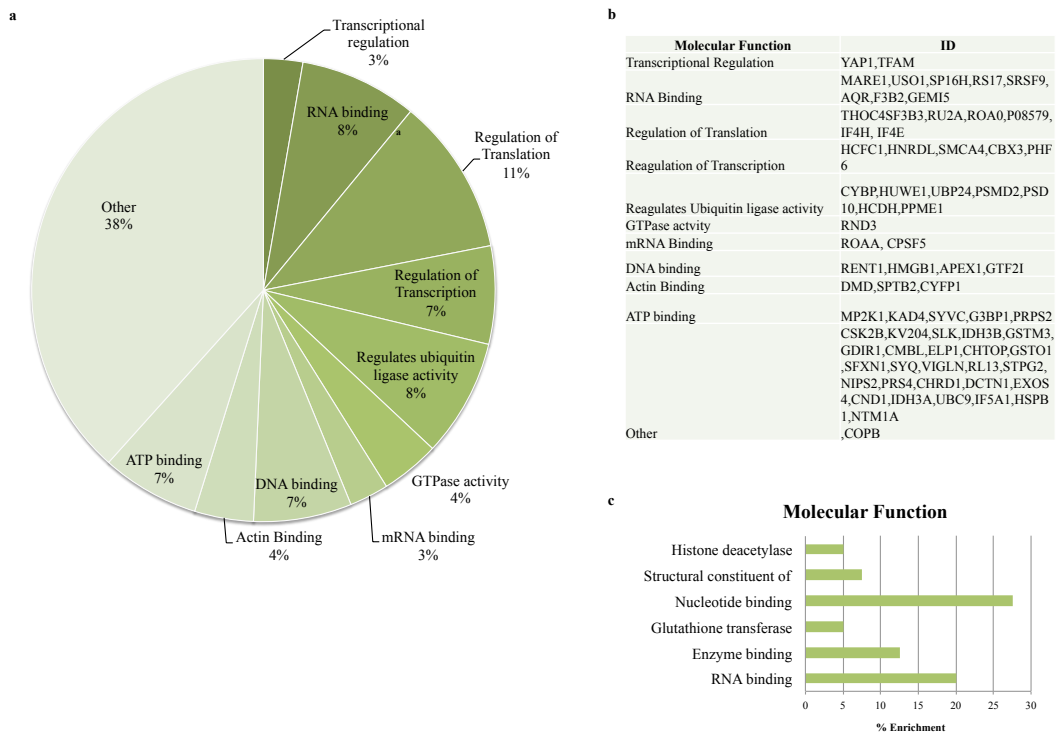


Figure 6.5 Molecular function of Rnd3 interactors

Proteins IDs were converted into Gene IDs before functional analysis was conducted. Genes were manually grouped according to predefined gene ontology terms. Percentages were calculated depending on the number of proteins in each class and classes represented by one protein were sub classified as ‘other’. Figure 6.5a shows a pie chart representing the percentage of proteins manually classified into each molecular function. Figure 6.5b lists the genes and the corresponding GO term. Figure 6.5c shows the enriched GO terms using DAVID.

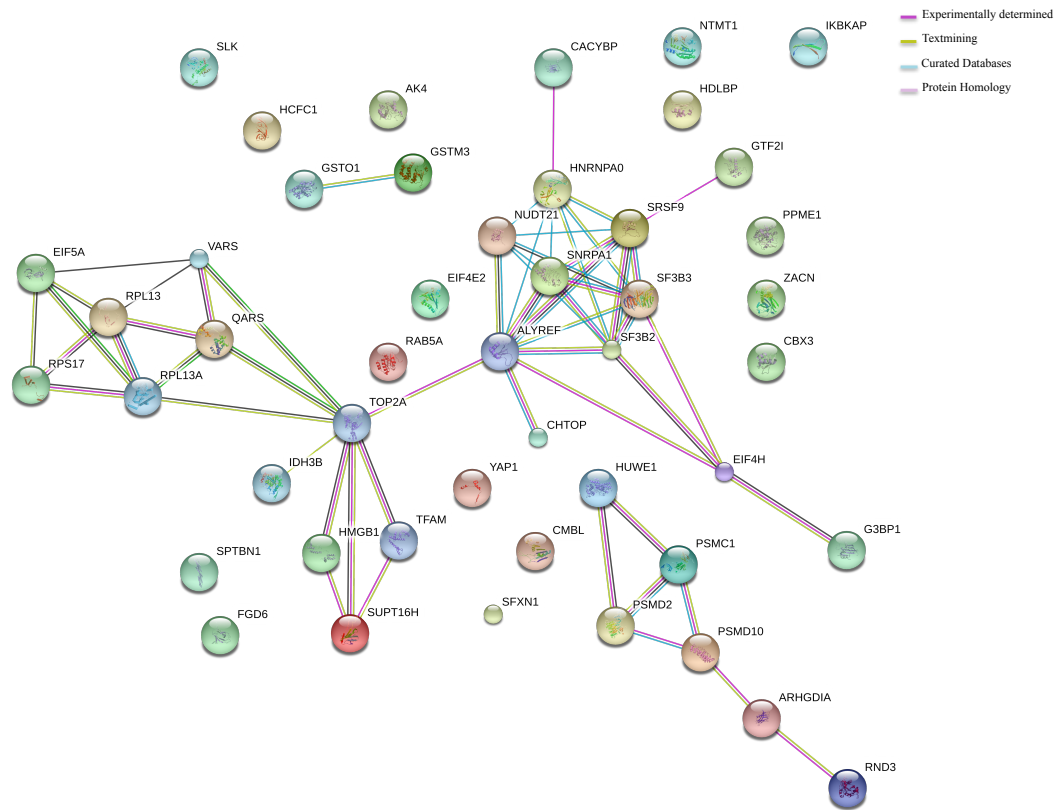


Figure 6.6 shows the functional associations between proteins that were found to interact with Rnd3

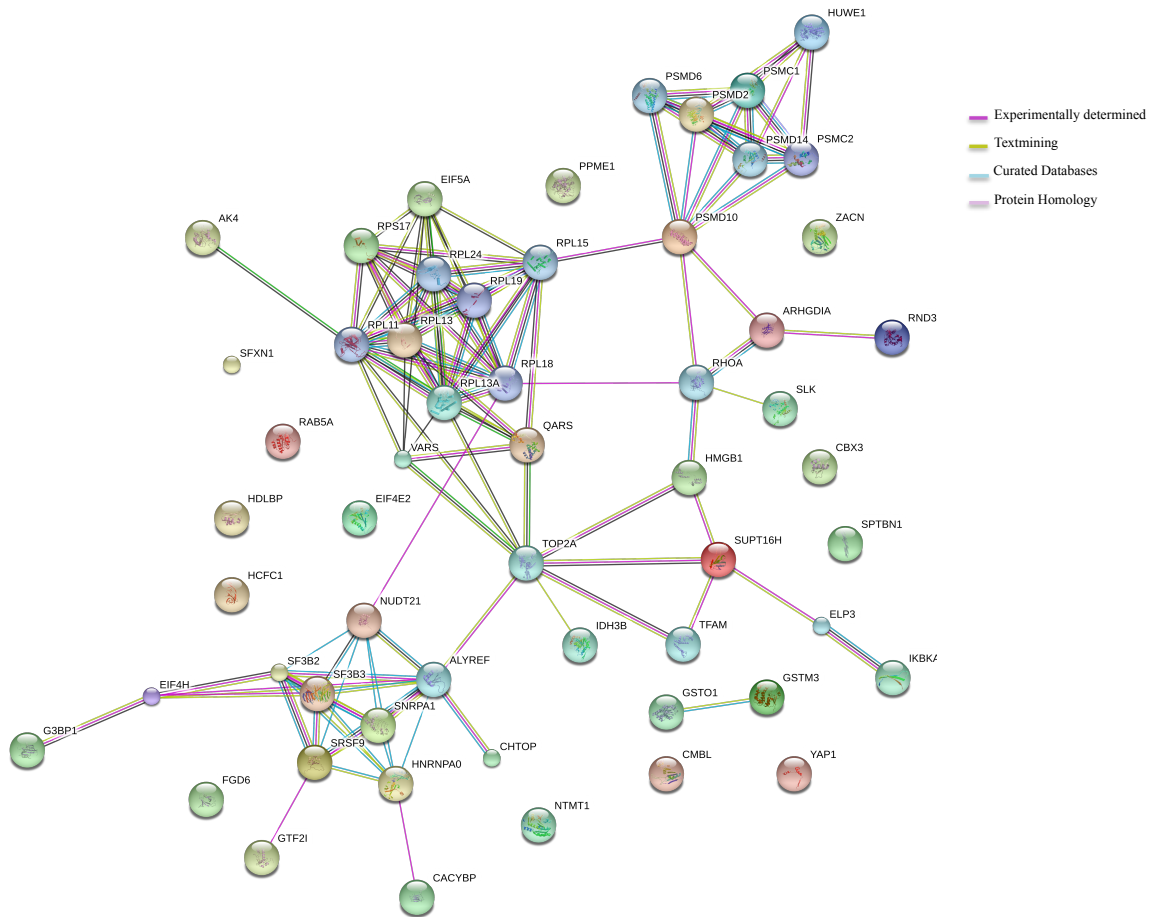


Figure 6.7 The functional association of the submitted protein lists and 10 other known functional associations.

ID	Log2 Ratio	Subcellular localization	Molecular Function	Biological Processes	Function
PSMD2	2.501668429	Cytosol	Regulation of ubiquitin ligase activity	Proteasomal degradation	Component of 26s proteasome
UBP24	1.891574725	Cytosol	Regulation of ubiquitin ligase activity	Proteasomal degradation	Involved in deubiquitination
HUWE1	1.474721569	Cytosol	Regulation of ubiquitin ligase activity	Proteasomal degradation	E3 ubiquitin protein ligase
CYBP	1.331705216	Cytosol	Regulation of ubiquitin ligase activity	Proteasomal degradation	Molecular bridge to E3 ligases
PSDM10	2.542728552	Cytosol	Regulation of ubiquitin ligase activity	Proteasomal degradation	Component of 26s proteasome
HCDH	3.119322973	Nucleus	Regulation of ubiquitin ligase activity	Proteasomal degradation	Regulates APC complex

Table 6.2 Rnd interactors involved in ‘regulation of ubiquitin activity’ and ‘proteosomal degradation’.

A literature search was conducted to determine the biological process and molecular function of these proteins and is summarized here.

6.2.3 Rnd3 regulates p63 at the protein level and not the transcriptional level

To determine if the interaction between Rnd3 and components of the proteasome degradation pathway may be functional, the regulation of p63 expression was analysed.

As shown in Chapter 3, Rnd3 depletion leads to an increase in p63 expression and in Chapter 4 it can be seen that an increase in p63 expression leads to an increase in the expression desmoplakin, which was shown to regulate colony compaction.

P63 is predominantly regulated post translationally and has been shown to be regulated by proteosomal degradation. To determine how p63 expression is regulated in Rnd3 depleted cells the transcript levels of p63 were analysed first using qRTPCR using cDNA synthesised from Rnd3 depleted cells. Primers targeted against the Δ NP63 α isoform and one that targets all isoforms (4A4) were used. Figure 6.8 shows that upon Rnd3 depletion there is no significant difference in the relative expression of any of the isoforms of p63.

Since there appeared to be no significant change in the expression of p63 at the transcript level, protein stability was measured next. To determine protein stability, cyclohexamide (CHX) was used. CHX is a known inhibitor of eukaryotic protein synthesis and functions by blocking the elongation stage of translation (Schnieder-Poetsch, 2010). 20 μ g/ml of CHX was supplemented into normal growth media described in (Rossi *et al*, 2006) for the indicated time points before cell lysates were collected and analysed by immunoblotting. Figure 6.9 shows that Rnd3 depletion leads to an increase in p63 stability. It can be seen that after 12 hours of treatment with CHX, NSC treated cells expressed approximately 80% of p63 protein was degraded when compared to the 0 hours' time point. However, in Rnd3 siRNA treated cells only approximately 20% was degraded. Furthermore, it can be seen that protein

degradation is delayed in Rnd3 siRNA treated cells. P63 in NSC cells started to degrade between 0-3 hours whereas in Rnd3 siRNA treated cells degradation was apparent between 6-9 hours. This preliminary data suggests that Rnd3 may regulate the expression of Rnd3 by regulating its stability and perhaps through its interaction with components of proteasome degradation pathway.

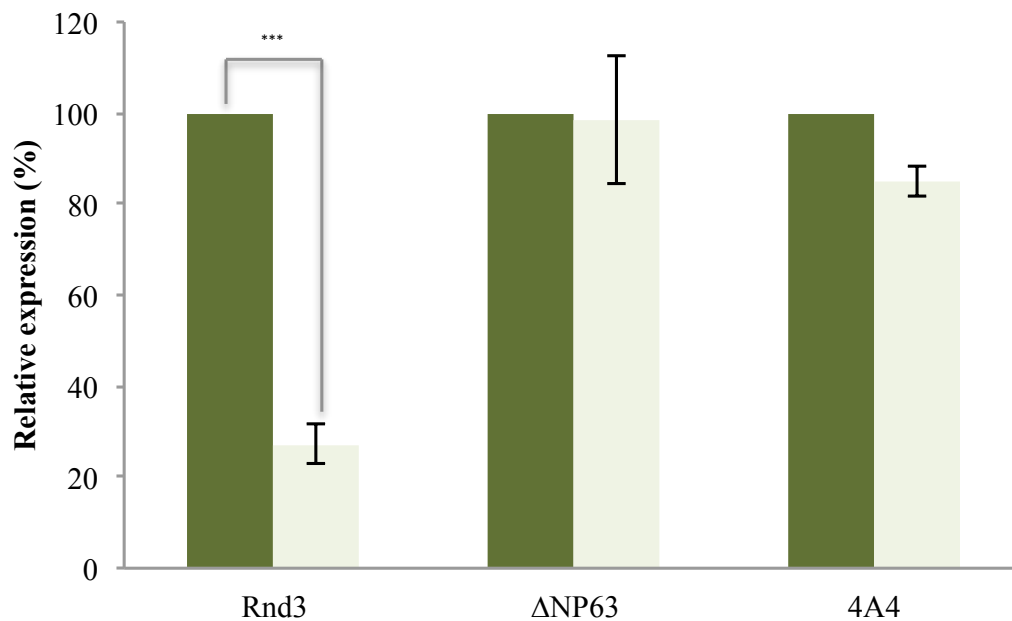
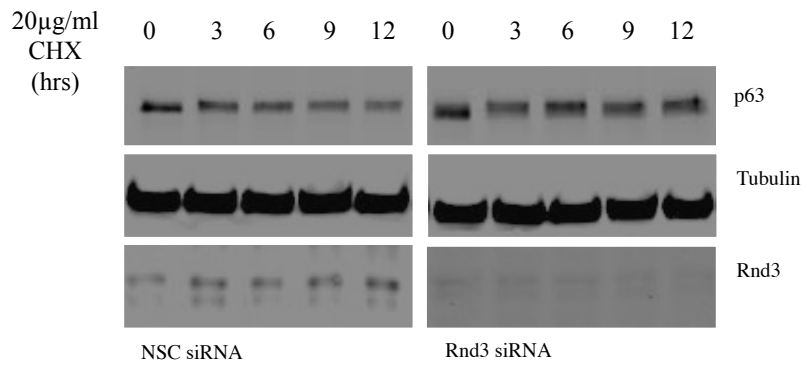


Figure 6.8. Knock down of Rnd3 leads to an increase in p63 protein but not an increase in transcript. To determine if there is an increase in p63 transcription qRTPCR was used to quantify p63 transcript in Rnd3 siRNA treated cells using primers that specifically targets the Δ NP63 α isoform and a primer that targets all isoforms (4A4). Figure 6.8 shows that there is no significant difference in transcript of any isoform can be seen. A students T-test was used to determine statistical significance where: ns $P > 0.05$, * $p < 0.05$, ** < 0.01 , *** $p < 0.001$. Error bars represent standard error of the mean. (n=3).

a



b

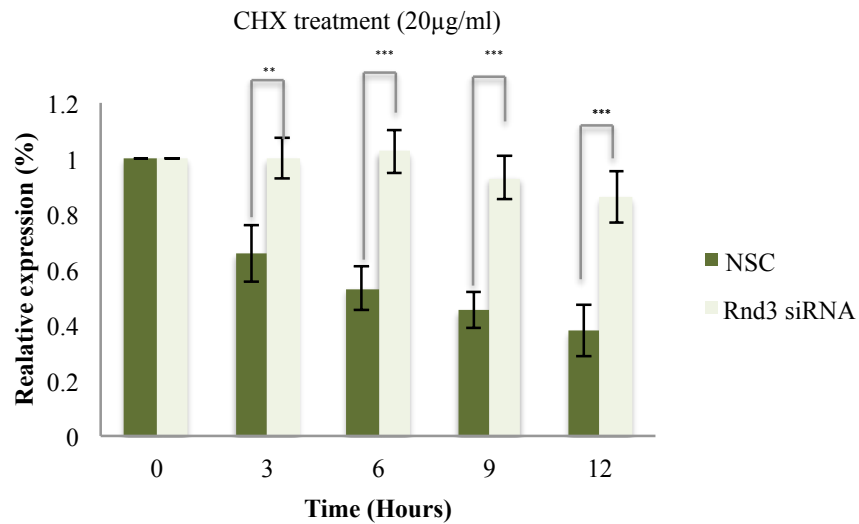


Figure 6.9 Knock down of Rnd3 leads to a reduction in p63 degradation

To determine if p63 becomes more stabilized in Rnd3 siRNA treated cells, protein degradation was inhibited. Cells were first transfected for 48 hours before being treated with 20 µg/ml Cyclohexamide (CHX) for the indicated time points. Figure 6.9a and b shows that after 12 hours of treatment, 80% of p63 remains in the cell. A student's T-test was used to determine statistical significance where: ns $P > 0.05$, * $p < 0.05$, ** $p < 0.01$, *** $p < 0.001$. Error bars represent standard error of the mean. (n=3).

6.3 Discussion

Determining the function of a protein can be aided by identifying protein-protein interactions. A number of techniques can be used to determine novel interacting partners which help aid the understanding of how a protein functions in a biological context. Here, SILAC immunoprecipitation was used to identify novel Rnd3 interactors in Rnd3 overexpressing cells. HEK 293T cells were used since the over expression of Rnd3 in keratinocytes has been shown to induce differentiation and therefore the Rnd3 ‘interactome’ may be altered to reflect this. Therefore, Rnd3 was overexpressed in HEK293T cells as an initial model to identify the proteins Rnd3 may be interacting with. It is important to note that the data presented here are preliminary data, and is a screen of potentially interesting proteins that Rnd3 may interact with. Further studies using affinity purification methods to determine if these interactions are, firstly specific and secondly direct, will be required to determine the biological significance of these predicted interactions.

6.3.1 Rnd3 associates with components of proteasome degradation

The ubiquitin proteasomal pathway (UPP pathway) is the most common mechanism for protein degradation in eukaryotic cells and involves the conjugation of ubiquitin to proteins to mark for them for proteasomal degradation (Lecker *et al*, 2006). This conjugation is mediated by three types of enzymes, E1 ligases (ubiquitin activating), E2 ligases (conjugating proteins) and E3 ligases (ubiquitin-protein ligases). E3 ligases are the most important in the UPP since it is these ligases function to target specific substrates and catalyse the transfer ubiquitin chains onto them (Lecker *et al*, 2006). Once proteins have been ubiquitinated, they are targeted for by the 26s proteasome. The proteasome is a large (~2.5MDa) multi-domain complex that consists of 31 different subunits. The proteasome functions to recognise ubiquitinated

proteins, unfold them and subsequently proteolysis them into a mix of small peptides. These are subsequently targeted for by components of the adaptive immune system (Lecker *et al*, 2006).

During keratinocyte differentiation in committed progenitors, proteins involved in self-renewability are required to be downregulated at a fast rate so to meet the demands of the newly regenerating tissue. Proteins in the cell need to be degraded so that newly synthesising proteins can have the required effect to go on to differentiate (Fuchs and Raghaven, 2002).

Here, it can be seen that Rnd3 may interact with the E3 Ligase, HUWE1 and components of 26S proteasome, PSMD10 and PSMC2. In addition to this Rnd3 depletion leads to the stability of p63 (figure 6.9). Therefore, it is tempting to speculate that Rnd3 may be involved in regulating the interaction between E3 ligases and the proteasome.

It is important to note that Rnd3 binding to the proteasomal components may be an artefact in response to overexpressing and therefore may not have any biological significance. Affinity purification techniques determining Rnd3 binding to specific targets may shed some light in terms of understanding these interactions further.

6.3.2 Rnd3 depletion leads to an increase in p63 stability

Interestingly, Huwe1 is an E3 ligase that interacts with mdm2. It was found that mdm2 (also a E3 ligase) bound to HUWE1 and ubiquities it marking it for degradation. In this way, mdm2 indirectly regulates the abundance of HUWE1 targets (Kurokawa, *et al*, 2013). In addition to this, PSMD10 (26S proteasome non-ATPase regulatory subunit 10) also known as gankyrin, independently of proteasome function, interacts with mdm2. PSMD10 additionally functions by binding to mdm2 and regulates the degradation of p53 (Lazano *et al*, 2005). Mdm2 has additionally been

shown to interact with p63, however why and how this interaction is important is still obscure (Shin *et al*, 2015).

Interestingly, it has been shown that p63 is predominantly regulated post translationally via the UPP pathway (Armstrong *et al*, 2016).

Going forward it would be interesting to see if any of the modifications made on p53 are made on p63 and what effect this has on p63 degradation.

Furthermore, it would be interesting to determine if any modifications are made on p63 post translationally after Rnd3 deletion and if this corresponds to known modifications that effect p63 stability.

Final Discussion and concluding remarks

The epidermis is stratified morphologically distinct epithelial tissue that functions as a specialist barrier against daily stresses. The outermost layer is continuously being shed throughout life and therefore must be replenished so that the epidermis is always intact. Keratinocytes that are lost from the surface are replaced by terminally differentiating cells that start off as committed progenitors. Committed progenitors exit the cell cycle and undergo various changes in cell morphology and biochemistry which results in the formation of a highly robust and resilient keratinocytes that interconnect together forming the outer layer of the skin. Because committed progenitors exit the cell cycle it is important they are continuously replenished by KSC. Therefore, the regulation and maintenance of both populations of progenitors is essential to ensuring that barrier formation is always maintained.

Accurately identifying committed progenitors from KSC is a major obstacle in determining the biomolecular mechanisms that regulate self-renewal and the initiation of terminal differentiation. This is important since the identification of how the stem/progenitor pool is regulated could provide some insight towards understanding how some epidermal disorders arise as well as aiding the identification of novel therapeutic targets.

Whilst some putative 'stem markers' have been identified, a single definitive marker is yet to be identified. Moreover, most current research is conducted in in vivo mouse models. This is particularly useful since ideally the biochemical markers within in stem/progenitor cell is likely to be dependent on a stringently controlled microenvironment. However, the regulation of murine epidermis is different to human epidermis and therefore it might be argued that the research conducted in these

models may be limited in terms of how transferable they are. Furthermore, many of these experiments cannot be carried out in humans for obvious ethical reasons. Therefore, to understand how the human epidermis is regulated, *in vitro* methods are particularly useful.

The work presented here demonstrates that the depletion of Rnd3 in HaCaTs induces a stem/progenitor phenotype. These cells show increased colony compaction, a reduction in cell size, increased cell adhesion to the ECM, suppressed differentiation and an increase in the expression of putative progenitor markers. In addition to this it can be seen that Rnd3 may exert these effects through the regulation of p63, junB and FOXK1.

7.1 Rnd3 may regulate stem/progenitor phenotypes:

p63 is a transcription factor that is essential in regulating skin morphogenesis (Koster *et al*, 2004). Δ NP63 is located at the basal layer and has been shown to regulate the proliferative potential of the stem/progenitor population (Senoo *et al*, 2007). Therefore, it has been suggested that p63 may be expressed in basal cells differentially, where expression is upregulated in KSC and is rapidly degraded in committed progenitors in response to differentiation stimuli.

Here, it can be seen that Rnd3 depletion leads to increased levels of p63 expression (shown in chapter 3) and this regulation is mediated via an increase in p63 protein stability. Interestingly, it can additionally be seen here that the increase in p63 in Rnd3 depleted cells is responsible for the increase in the expression of desmoplakin, a known transcriptional target of p63 (Chapter 4).

Going forward it would be interesting to determine if any of the other phenotypes observed in Rnd3 depleted cells are dependent on the expression of p63. For example, p63 is known to regulate the expression of beta 1 integrin as well as regulating YAP.

Furthermore, using a proteomics approach it can be seen that the depletion of Rnd3 leads to an increase in the expression of junB and FOXK1, both of which are involved in the regulation of differentiation genes junB and FOXK-1. Interestingly, both of these which are members of gene families that have been shown to regulate keratinocyte differentiation. Therefore, it would be interesting to determine what, if any role they play in keratinocyte regulation and if any other of the family members play a similar role.

7.2 How might Rnd3 play a role in keratinocyte differentiation and stem cell maintenance:

The data presented here suggests that the depletion of Rnd3 results in the enrichment stem/progenitor cells. These data are partly consistent with a study conducted by Liebig *et al* demonstrated that Rnd3 is up regulated in basal keratinocytes during terminal differentiation. Therefore, this suggests that Rnd3 may be differentially expressed at the basal layer. Studies determining Rnd3 expression in the basal layer in vivo would inform this hypothesis. Furthermore, the use of keratinocytes with stable depletion of Rnd3 could be used to grow keratinocytes in 3D, forming organotypic cultures. Therefore, if Rnd3 depletion does enrich for a stem population, it would be expected that the formation of 3D culture would be limited. Furthermore, it would be interesting to see if Rnd3 and p63 are co-expressed and if this co-expression determines stemness.

This work additionally raises a question of whether it is the intrinsic nature of the cell that determines stemness or whether it is the stringently controlled microenvironment.

If Rnd3 is involved in the regulation of the pathways discussed here, then all that remains to be answered is the question of; how is Rnd3 expression being regulated? If Rnd3 expression is spatially regulated, how and why is it spatially regulated?

Currently it is unknown how keratinocyte stem cells are maintained in the basal layer amongst transit amplifying cells, however it is becoming clear that the microenvironment regulates cell behaviour (Fuchs *et al*, 2009).

It is therefore necessary to identify upstream regulators of Rnd3 and determine if these are co-expressed alongside Rnd3 in the epidermis.

References

- Al-Moudi A, Diez DC, Betts MJ, Frangakis AS (2007). “The molecular architecture of cadherins in native epidermal desmosomes”. *Nature* 450: 832-837.
- Andl CD (2007). “The misregulation of Cell adhesion components during Tumorigenesis: Overview and Commentary”. *Journal of Oncology*, 2010:174715.
- Armstrong SR, Wu H, Wang B, Abuetaf Y, Sergi C, L (2016). “The Regulation of Tumor Suppressor p63 by the Ubiquitin-Proteasome System”. *Int J Mol Sci.* (12):6;17.
- Attardi.LD, Reczek.EE, Cosmas.C, DeMicco.EG, McCurrach.ME *et al*, (2001). “PERP, n apoptosis associated target of p53, is a novel member of the PMP-22/gas3 family”. *Genes and Development*; 14:704-718.
- Barrandon Y and Green H (1987). “ Three clonal types of keratinocyte with different capacities for multiplication”. *PNAS* 84, 2302-2306.
- Beaudery VG, Jiang D, Dusek RL, Park EJ, Knezevich S *et al* (2010). “ Loss of the p63/p53 regulated desmosomal protein Perp promotes tumourigenesis” *Plos Genetics*, 6:10.
- Bikle DD, Xie Z, and Chia-LiTu (2012). “Calcium regulation of keratinocyte differentiation” *Expert Rev Endocrinol Metab*, 7(4): 461–472.
- Blanpain C, Fuchs E (2009). “Epidermal homeostasis: a balancing act of stem cells in the skin”. *Nature Review Molecular Cell Biology* 10, 207-17 .
- Boswell SA, Ongusaha PP, Nghiem P. and Lee SW (2007). “ The protective role of a small GTPase RhoE against UVB-induced DNA damage in keratinocytes”. *Journal of Biological Chemistry* 282, 4850-4858 .

Brandner JM, Haftek M, Niessen CM (2010). “Adherens Junctions, Desmosomes and Tight Junctions in Epidermal Barrier Function’. *The Open Dermatology Journal*, 4:14-20.

Breitkreutz D, Mirancea N, and Nischt R. (2009). “Basement membranes in skin: unique matrix structures with diverse functions?”. *Histochemistry and Cell Biology*, 132, 1:1–10.

Brenner M, Hearing VJ (2007). “The Protective Role of Melanin Against UV Damage in the skin”. *Cell Cycle*, 6 233–239

Calenic B, Ishkitiev N, Yaegaki K, Imai T, Kumazawa Y, Nasu M, Hirata T (2009). “Magnetic separation and cahrefertization of keratinocyte stem cells from human gingiva”. *Journal of periodontal research*; 45:703-708 .

Carroll DK, Carroll JS , Leong CO, Cheng F, Brown M, Mills AA, Brugge JS, Ellisen LW (2006) “p63 regulates an adhesion programme and cell survival in epithelial cells”. *Nature Cell Biology*, 8:551–561.

Chardin, P. (2003) “GTPase regulation: Getting a Rnd Rock and Rho inhibition”. *Current Biology* 13, 702–704

Cherfils J, Zeghouf M. (2013). “Regulation of small GTPases by GEFs, GAPs, and GDIs”. *Physiol Rev*; 93,269-309.

Clayton E, Doupé DP, Klein AM, Winton DJ, Simons BD, Jones PH. (2007). “ A single type of progenitor cell maintains normal epidermis”. *Nature*, 446, 185-9.

Coleman ML, Sahai, EA, Yeo M, Bosch M, Dewar A and Olson MF (2001). “Membrane blebbing during apoptosis results from caspase-mediated activation of ROCK1.”. *Nature Cell Biology* 3: 339-345 (2001).

Connelly JT, Gautrot JE, Trappmann B, Tan DW, Donati G, Huck WT, Watt FM (2010). “Actin and serum response factor transduce physical cues from the

microenvironment to regulate epidermal stem cell fate decisions.” *Nature cell bio*, 2(7):711-8.

Connelly JT, Mishra A, Gautrot JE, Watt FM (2011). “Shape-induced terminal differentiation of human epidermal stem cells requires p38 and is regulated by histone acetylation”, *Plos one*, (11): e27259

Cox J and Mann M. (2008). “MaxQuant enables high peptide identification rates, Individualized p.p.b.-range mass accuracies and proteome-wide protein quantification”. *Nat Biotechnol*, 26:1367-72.

Dusek RL, Godsel LM, Chen F, Strohecker AM, Getsiosis S, Harmon R, Muller EJ, Caldelari R, Cryns VL and Green KJ (2007). “Plakoglobin Deficiency protects keratinocytes from apoptosis”. *Journal of investigative dermatology*, 127: 792-801 .

Eckert RL, Adhikary G, Young CA et al (2013) “AP1 Transcription Factors in Epidermal Differentiation and Skin Cancer,” *Journal of Skin Cancer*, Article ID 537028,

Estrach S, Cordes R, Hozumi K, Gossler A, Watt FM. (2008). “Role of the Notch ligand Delta1 in embryonic and adult mouse epidermis.” *J Invest Dermatol*, 128(4):825-32.

Faye MD, Graber TE, Holcik M. (2014). “ Assessment of Selective mRNA Translation in Mammalian Cells by Polysome Profiling”. *J. Vis. Exp*, 134: 234-239

Ferone G, Mollo MR, Thomason HA, Antonini D, Zhou H, Ambrosio R, De Rosa L, Salvatore D, Getsios S, van Bokhoven H, Dixon J, Missero C (2013). “ p63 control of desmosome gene expression and adhesion is compromised in AEC syndrome”. *Hum Mol Genet* 1;22(3):531-43.

Fiegen D, Blumenstein L, Stege P, Vetter IR, Ahmadian MR (2002). “ Crystal structure of Rnd3/RhoE: functional implications”. *FEBS Lett* 525, 100–104

Fingar DC, Salama S, Tsou C, Harlow E, and Blenis J (2006). "Mammalian cell size is controlled by mTOR and its downstream targets S6K1 and 4EBP1/eIF4E". *Genes and Dev*, 16(12): 1472-1487.

Finlan LE and Hupp TR (2007). "p63: the phantom of the tumor suppressor". *Cell Cycle*, 6:9: 1062–1071

Foster R, Hu KQ, Lu Y, Nolan KM, Thissen J and Settleman J (1996). "Identification of a novel human Rho protein with unusual properties: GTPase deficiency and in vivo farnesylation". *Mol Cell Biol*, 16 (6):2689-2699.

Freddie CT, Ji Z, Marais A, Sharrocks AD (2007). "Functional interactions between the Forkhead transcription factor FOXK1 and the MADS-box protein SRF". *Nucleic acids*, (15):5203-12

Fuchs E and Horseley V (2008). "More than one way to skin". *Genes and Development*; 22, 976-985 .

Fuchs.E (2007). "Scratching the surface of skin development". *Nature* 445, 834-842.

Garavini H, Riento K, Phelan JP, McAlister MS, Ridley AJ, Keep NH (2002). "Crystal structure of the core domain of RhoE/Rnd3: a constitutively activated small G protein". *Biochemistry* 41, 6303–6310.

Garrod D, Chidgey M (2008). "Desmosomes structure, composition and function". *Biochem at Biophy Acta*, 17778:572-587.

Gemenetzidis E, Elena-Costea D, Parkinson EK, Waseem A, Wan H, Teh MT (2010). "Induction of human epithelial stem/progenitor expansion by FOXM1". *Cancer research*, (22):290.

Getsios S, Simpson CL, Kojima S, Harmon R, Sheu LJ, Dusek RL, Cornwell M, Green KJ (2004). "Desmoglein 1 dependant suppression of EGFR signalling

promotes epidermal differentiation and morphogenesis”. *Journal of cell biology*, 29: 1243-58.

Ghadially R (2013). “ 25 years of epidermal stem cell research”. *J Invest Dermatol.* 132 (3 Pt 2):797-810.

Goodman CA and Hornberger T (2013). “Measuring protein synthesis with SUnSET: a valid alternative to traditional techniques?” *Exerc Sport Sci Rev*, (2); 107-115

Guasch.G, Greco.V, Blanpain.C, Lowry.WE, Rendl.M, and Fuchs.E; Defining the Epithelial Stem Cell Niche in Skin; *Science*; 303: 359-363 (2004).

Hakoshima T, Shimizu T, Maesaki R (2003). “Structural basis of the Rho GTPase signaling”. *J Biochem*, 134(3): 327-331

Hartstock.A and Nelson.WJ (2008). “Adherens junctions and tight junctions; Structure, function and connections to the actin cytoskeleton”. *Biochimica et Biophysica Acta*; 17778:660-669.

Hawke T. J., Jiang N., Garry D. J. (2003a). “Absence of p21CIP rescues myogenic progenitor cell proliferative and regenerative capacity in Foxk1 null mice”. *J. Biol. Chem.* 278, 4015–4020

Heasman SJ, Ridley AJ (2008). “Mammalian Rho GTPases: new insights into their functions from in vivo studies”. *Nature Review Molecular Cell Biology*; 9:690-701.

Hodge RG, Ridley AJ (2016). “Regulating Rho GTPases and their regulators.” *Nat Rev Mol Cell Biol*, (8) 496-510

Hotchin. NA, Ganderillias A, Watt FM (1995). “Regulation of cell surface beta 1 integrin levels during keratinocyte terminal differentiation”. *The Journal of Cell Biology.* 128(6):1209-1219.

- Huang DW, Sherman BT, Lempicki RA (2009). "Systematic and integrative analysis of large gene lists using DAVID Bioinformatics Resources". *Nature Protocols*, 4(1):44-57
- Ihrle RA and Attardi LD (2005). "A new PERP in the lineup". *Cell cycle*; 4:873-876.
- Ihrle RA, Marques MR, Nguyen BT, Horner JS, Papazoglou *et al* (2005) "Perp is a p63 regulated gene essential for epithelial integrity". *Cell*, 120:843-856.
- Jacobs M, Hayakawa K, Swenson L, Bellon S, Fleming M, Taslimi P, Doran J (2006). "The structure of dimeric ROCK I reveals the mechanism for ligand selectivity". *J Biol Chem*, (1):260-268
- Jaffe AB, Hall A (2005). "RhoGTPases: Biochemistry and Biology". *Annu Rev Cell Dev Biol* 21:247-69.
- Jensen K. B., Watt F. M. (2006). "Single-cell expression profiling of human epidermal stem and transit-amplifying cells: Lrig1 is a regulator of stem cell quiescence". *Proc. Natl. Acad. Sci. USA* 103, 11958–11963
- Jie W, Andrade KC, Lin X, Yang X, Yue X, & Chang J. (2015). "Pathophysiological Functions of Rnd3/RhoE." *Comprehensive Physiology*, 6(1), 169–186.
- Jones PH, Harper S and Watt FM (1995). "Stem cell patterning and fate in human epidermis". *Cell* 80, 83-93.
- Jones PH. and Watt FM (1993). "Separation of human epidermal stem cells from transit amplifying cells on the basis of differences in integrin function and expression." *Cell* 73, 713-724.
- Katoh M, Katoh M (2004). "Human FOX gene family (Review)". *Int J Oncol.* 25(5):1495-500.

Kaur, P, Li, A (2000). “Adhesive properties of human basal epidermal cells: An analysis of keratinocyte stem cells, transit amplifying cells, and postmitotic differentiating cells” *J Invest Dermatol* 114, 413–420.

Kaur. P, Li.A, Redvers.R and BertocellonI (2004). “Keratinocyte stem cells: An evolving science”. *Journal of Investigative Dermatology Symposium Proceedings* 9, 238–247 .

Koh LF, Ng BK, Bertrand J, Thierry F. (2015). “Transcriptional control of late differentiation in human keratinocytes by TAp63 and Notch”. *Exp Dermatol.* 24(10):754-60.

Komander. D, Garg.R, Wan PTC, Ridley. AJ and Barford.DJ (2008). “Mechanism of multi-site phosphorylation from a ROCK-I:RhoE complex structure”. *EMBO* 27: 3175–3185.

Koster MI, Kim S, Mills AA, DeMayo FJ, Roop DR (2004). “p63 is the molecular switch for initiation of an epithelial stratification program”. *Genes and Development*; 18, 126-31.

Koster MI, Roop DR (2007). “Mechanisms regulating epithelial stratification”. *Annual Reveiw Cell Developmental Biology* 23, 93–113.

Kouwenhoven EN, van Heeringen SJ, Tena JJ, Oti M, Dutilh BE, *et al* (2010). “Genome-Wide Profiling of p63 DNA–Binding Sites Identifies an Element that Regulates Gene Expression during Limb Development in the 7q21 SHFM1 Locus”. *PLoS Genetics* 6: e1001065 .

Kretz M, Webster DE, Flockhart RJ, Lee CS, Zehnder A, Lopez-Pajares V, Qu K, Zheng GX, Chow J, Kim GE, Rinn JL, Chang HY, Siprashvili Z, Khavari PA (2012). “Suppression of progenitor differentiation requires the long noncoding RNA ANCR”. *Genes Dev.* 15;26(4):338-43.

Krieg. T and Aumailley. M (2011). “The extracellular matrix of the dermis: flexible structures with dynamic functions,” *Experimental Dermatology*, 20, 8:689–695.

Kurokawa, M., Kim, J., Geradts, J., Matsuura, K., Liu, L., Ran, X., ... Kornbluth, S. (2013). “A Network of Substrates of the E3 Ubiquitin Ligases MDM2 and HUWE1 Control Apoptosis Independently of p53”. *Science Signaling*, 6(274),

Kypriotou M, Huber M, Hohl D (2012). “The human epidermal differentiation complex: cornified envelope precursors, S100 proteins and the 'fused genes' family”. *Exp Dermatol* 21(9):643-9.

Lai Y, Di Nardo A, Nakatsuji T et al. (2009). “Commensal bacteria regulate Toll- like receptor 3-dependent inflammation after skin injury”. *Nat Med* 15:1377–82

Lam EW, Brosens JJ, Gomes AR, Koo CY (2013). “Forkhead box proteins: tuning forks for transcriptional harmony”. *Nat Rev Cancer* (7):482-95 .

Larouche.D, Hayward.C, Cuffley.K and Germain.L (2005). “Keratin 19 as a stem cell marker in vivo and in vitro”. *Methods in Molecular Biology*; 289:103-10.

Larouche.D, Lavoie.A, Paqueat.C, Simard-Bisson.C, Germain.L (2010). “Identification of Epithelial stem cell in vivo and in vitro using Keratin 19 and BrdU”. *Methods in Molecular Biology*; 585:383-400.

Lavker.RM, Sun.T (2000). “Epidermal stem cells: Properties, markers and location”. *PNAS*, 97: 13473-13475.

Lecker SH, Goldberg AL, Mitch WE (2006). “Protein degradation by the ubiquitin-proteasome pathway in normal and disease states”. *J Am Soc Nephrol.* (7):1807-19.

Lehman, T. A., Modali, R., Boukamp, P., Stanek, J., Bennett, W. P., Welsh, J. A., *et al* (1993). “p53 mutations in human immortalized epithelial cell lines”. *Carcinogenesis* 14, 833-839.

Liebig, T, Erasmus J, Kalaji, R, Davies D, Loirand G, Ridley A, and Braga,V. M

(2009). “RhoE is required for keratinocyte differentiation and stratification”. *Molecular Biology of the Cell*, 20, 452-463.

Lock, F. E. and Hotchin, N. A (2009). “Distinct roles for ROCK1 and ROCK2 in the regulation of keratinocyte differentiation”. *PLoS ONE* 4:e8190.

Lozano, Guillermina et al (2005). “Gankyrin: An intriguing name for a novel regulator of p53 and RB”. *Cancer Cell* , 8(1):3 – 4

Madigan JP, Bodemann BO, Brady DC, Dewar BJ, Keller PJ, Leitges M, Philips MR, Ridley AJ, Der CJ, Cox AD (2009). “Regulation of Rnd3 localization and function by protein kinase C alpha-mediated phosphorylation”. *Biochem J* 424: 153-161.

Mascre G, Dekoninck S, Drogat B, Youssef KK, Broheé S, Sotiropoulou PA, Simons BD, Blanpain C (2012). “Distinct contribution of stem and progenitor cells to epidermal maintenance”. *Nature*, 489(7415):257-62.

McMullan, R., Lax, S., Robertson, V.H., Radford, D.J., Broad, S., Watt, F. M., Rowles, A., Croft, D. R., Olson, M. F. and Hotchin, N. A (2003). “Keratinocyte differentiation is regulated by the Rho and ROCK signaling pathway”. *Current Biology* 13, 2185-2189

Moon SY, Zheng Y (2003). “Rho GTPase-activating proteins in cell regulation.” *Trends Cell Biol*, 13(1):13-22.

Murakoshi, H., Wang, H., & Yasuda, R. (2011). Local, persistent activation of Rho GTPases during plasticity of single dendritic spines. *Nature*, 472(7341), 100–104.

Nadiminty N, Dutt S, Tepper C, Gao AC (2010). “Microarray analysis reveals potential target genes of NF-kappaB2/p52 in LNCaP prostate cancer cells”. *Prostate* 70: 276-287.

Nobes, C.D *et al* (1998). “A new member of the Rho Family Rnd1 promotes disassembly of actin filament structures and loss of cell adhesion” *J. Cell Biol*, 141, 187-197.

Obsil T, Obsilova V (2011). “Structural basis of 14-3-3 protein functions”. *Semin Cell Dev Biol*. 22(7):663-72

Ohyama, M., Terunuma, A., Tock, C. L., Radonovich, M. F., Pise-Masison, C. A., Hopping, S. B., ... Vogel, J. C. (2006). “Characterization and isolation of stem cell-enriched human hair follicle bulge cells”. *Journal of Clinical Investigation*, 116(1), 249–260

Ong SE, Blagoev B, Kratchmarova I, Kristensen DB, Steen H, Pandey A, Mann M (2002). “Stable isotope labeling by amino acids in cell culture, SILAC, as a simple and accurate approach to expression proteomics.” *Mol Cell Proteomics*.(5):376-86.

Ong SG, Hausenloy DJ. Hypoxia-inducible factor as a therapeutic target for cardioprotection. *Pharmacol Ther*. 2012;136:69–81.

Pacary E, Azzarelli R, Guillemot F (2013). “Rnd3 coordinates early steps of cortical neurogenesis through actin-dependent and -independent mechanisms”. *Nat Commun*, 4:1635.

Pacary E, Heng J, Azzarelli R, Riou P, Castro D, Lebel-Potter M, ParrasC, Bell DM, Ridley AJ, Parsons M, Guillemot F (2011). “Proneural transcription factors regulate different steps of cortical neuron migration through Rnd-mediated inhibition of RhoA signaling”. *Neuron*, 69: 1069-1084.

Pagliara, S., Franze, K., McClain, C. R., Wylde, G., Fisher, C. L., Franklin, R. J. M., ... Chalut, K. J. (2014). “Transition from pluripotency in embryonic stem cells distinguished by an auxetic nucleus”. *Nature Materials*, 13(6);638–644.

Pellegrini G, Dellambra E, Golisano O, Martinelli E, Fantozzi I, Bondanza S *et al* (2001). “p63 identifies keratinocyte stem cell”. *PNAS* 98: 3156–3161.

Pertz O (2010). “Spatio-temporal Rho GTPase signaling - where are we now?” *Journal of Cell Sci*, 123,1841-50.

Raymond K, Kreft M, Janssen H, Calafat J, Sonnenberg A. (2005). “Keratinocytes display normal proliferation, survival and differentiation in conditional beta4-integrin knockout mice”. *J Cell Sci*, 118:1045–1060.

Reagan-Shaw S, Nihal M, Ahmad N. (2008) Dose translation from animal to human studies revisited. *FASEB J* 22:659–661.

Riento, K., Guasch, R. M., Garg, R., Jin, B. and Ridley, A. J (2003). “RhoE binds toROCK I and inhibits downstream signaling”. *Mol. Cell. Biol.* 23: 4219-4229.

Riou P, Kjaer S, Garg R, Purkiss A, George R, Cain RJ, Bineva G, Reymond N, McColl B, Thompson AJ, O’Reilly N, McDonald NQ, Parker PJ, Ridley AJ (2013). “14-3-3 proteins interact with a hybrid prenyl-phosphorylation motif to inhibit g proteins”. *Cell*;153:640–653.

Romano RA, Ortt K, Birkaya B, Smalley K, Sinha S (2009). “An active role of the DeltaN isoform of p63 in regulating basal keratin genes K5 and K14 and directing epidermal cell fate”. *PLoS One.* 20;4(5):e5623.

Ryan, KR, Lock. FE, Heath. JK, Hotchin NA (2012). “Plakoglobin-dependent regulation of keratinocyte apoptosis by Rnd3”. *J Cell Sci*, (13):3202-3209

Sampath P, Pritchard DK, Pabon L, Reinecke H, Schwartz SM, Morris DR, Murry CE. (2008). “A hierarchical network controls protein translation during murine embryonic stem cell self-renewal and differentiation”. *Cell Stem Cell* 8;2(5).

Savill.N.J, Sherrat.J.A (2002). “Control of epidermal stem cell clusters by Notch-mediated lateral induction” *Developmental Biology* 258: 141–153.

Segre. JA (2006). “Epidermal barrier formation and recovery in skin disorders”. *Journal of Clinical Investigation*, 116: 1150–1158.

Senoo M, Pinto F, Crum CP, McKeon F (2007). “p63 Is essential for the proliferative potential of stem cells in stratified epithelia”. *Cell*; 129:523-36.

Shi X, Garry DJ (2012). “Foxk1 recruits the Sds3 complex and represses gene expression in myogenic progenitors.” *J Biochem*, (1-2): 251-8.

Shin JS, Ha JH, Lee DH, Ryu KS, Bae KH, Park BC, Park SG, Yi GS, Chi SW (2015). “Structural convergence of unstructured p53 family transactivation domains in MDM2 recognition.” *Cell Cycle*, 14(4):533-43.

Simpson. CL, Patel.DM & Green.KJ (2011). “Deconstructing the skin: cytoarchitectural determinants of epidermal morphogenesis”. *Nature Reviews Molecular Cell Biology*, 12, 565-580.

Snyder JT, Worthylake DK, Rossman KL, Betts L, Pruitt WM, Siderovski DP, Der CJ, Sondek J (2002). “Structural basis for the selective activation of Rho GTPases by Dbl exchange factors”. *Nature Structural Biology*; 9, 468-75.

Szklarczyk D, Franceschini A, Wyder S, Forslund K, Heller D, Huerta-Cepas J, Simonovic M, Roth A, Santos A, Tsafou KP, Kuhn M, Bork P, Jensen LJ, von Mering C (2015). “STRING v10: protein-protein interaction networks, integrated over the tree of life”. *Nucleic Acids Res*; 43:D447-52.

Tan, D. W. M., Jensen, K. B., Trotter, M. W. B., Connelly, J. T., Broad, S., & Watt, F. M. (2013). “Single-cell gene expression profiling reveals functional heterogeneity of undifferentiated human epidermal cells”. *Development (Cambridge, England)*, 140(7), 1433–1444.

Tang Y, Hu C, Yang H, Cao L, Li Y, Deng P, Huang L. Rnd3 regulates lung cancer cell proliferation through notch signaling. *PLoS One*. 2014;9:e111897.

Trojan L, Schaaf A, Steidler A, Haak M, Thalmann G, Knoll T, Gretz, Tumber.T, Guasch.G, Greco.V, Blanpain.C, Lowry.WE, Rendl.M, and Fuchs.E (2004). “Defining the Epithelial Stem Cell Niche in Skin”. *Science*; 303: 359-363.

Trojan L, Schaaf A, Steidler A, Haak M, Thalmann G, Knoll T, Gretz N, Alken P, Michel MS (2005). "Identification of metastasis-associated genes in prostate cancer by genetic profiling of human prostate cancer cell lines". *Anticancer Res* 25: 183-191, (2005)

Truong AB, Khavari PA. (2007). "Control of keratinocyte proliferation and differentiation by p63." *CelEpub* 2007 Feb 28.1 *Cycle* (3):295-9.

Vanbokhoven.H, Melino.G, Candi.E and Declercq.W (2011). "p63, a Story of Mice and Men". *Journal of Investigative Dermatology* 131, 1196-1207.

Viganò,M.A, Mantovani.R (2007). Hitting the numbers: the emerging network of p63 targets". *Cell Cycle*, (3): 233-239.

Villalonga P, Fernandez de Mattos S, Ridley AJ (2009). "RhoE inhibits 4E-BP1 phosphorylation and eIF4E function impairing cap-dependent translation". *J Biol Chem* 284: 35287-35296.

Villalonga P, Guasch RM, Riento K, Ridley AJ (2004). "RhoE inhibits cell cycle progression and Ras-induced transformation". *Mol Cell Biol* 24: 7829-7840.

Walko. G, Castañón MJ and Wiche.M (2015). "Molecular architecture and function of the hemidesmosome as revealed by super-resolution microscopy, *J Cell Sci*, (20): 3714-3719

Wan H, South AP, Hart IR. 2007. Increased keratinocyte proliferation initiated through downregulation of desmoplakin by RNA interference. *Exp Cell Res* 313: 2336–2344

Watt.FM (2001). "Stem cell fate and patterning in mammalian epidermis". *Current Opinion in Genetics & Development*; 11: 410–417.

Watt.FM (2002). "Role of integrins in regulating epidermal adhesion, growth and differentiation". *The EMBO Journal* 21, 3919 – 3926.

Watt.FM, Celso.CL, Silva-Vargas.V (2006). “ Epidermal stem cells: an update”. *Current Opinion in Genetics & Development*; 16: 518–524.

Wennerberg K, Rossman KL, Der CJ (2005). “The Ras superfamily at a glance”. *J Cell Sci* 118:843-6.

Westfall MD, Joyner AS, Barbieri CE, Livingstone M, Pietenpol JA (2005). “Ultraviolet radiation induces phosphorylation and ubiquitin-mediated degradation of DeltaNp63alpha”. *Cell Cycle*, (5) 710-716.

Williams SE, Beronja S, Pasolli HA, Fuchs E. (2011) “Asymmetric cell divisions promote Notch-dependent epidermal differentiation”. *Nature* 470, 353 – 358.

Wittinghofer A, Vetter IR (2011). “Structure-function relationships of the G domain, a canonical switch motif”. *Annu Rev Biochem*; 80,943-71.

Xie T, Spradling AC (2000). “ A niche maintaining germ line stem cells in the *Drosophila* ovary”. *Science*; 13;290 (5490):328-30.

Yang A., Kaghad M., Wang Y., Gillett E., Fleming M.D., Dotsch V., Andrews N.C., Caput D., McKeon F (1998). “p63, a p53 homolog at 3q27–29, encodes multiple products with transactivating, death-inducing, and dominant-negative activities”. *Mol. Cell*. 2:305–316.

Yang, A., Schweitzer, R., Sun, D., Kaghad, M., Walker, N., Bronson, R.T., Tabin, C., Sharpe, A., Caput, D., Crum, C., *et al* (1999). “p63 is essential for regenerative proliferation in limb, craniofacial and epithelial development”. *Nature* 398: 714–718.

Zhang J. G., Wang J. J., Zhao F., Liu Q., Jiang K., Yang G. H. (2010). “MicroRNA-21 (miR-21) represses tumor suppressor PTEN and promotes growth and invasion in non-small cell lung cancer (NSCLC)”. *Clin. Chim. Acta* 411, 846-852

Zhu Y, Zhou J, Xia H, Chen X, Qiu M, Huang J, Liu S, Tang Q, Lang N, Liu Z, Liu M, Zheng Y, Bi F (2014). "The Rho GTPase RhoE is a p53-regulated candidate tumor suppressor in cancer cells". *Int J Oncol* 44: 896-904.

Zhu Z, Todorova K, Lee KK, Wang J, Kwon E, Kehayov I, Kim HG, Kolev V, Dotto GP, Lee SW, Mandinova A (2014). "Small GTPase RhoE/Rnd3 is a critical regulator of Notch1 signaling". *Cancer Res* 74: 2082-2093.